

REPORT NO.  
UCB/EERC-78/25  
DECEMBER 1978

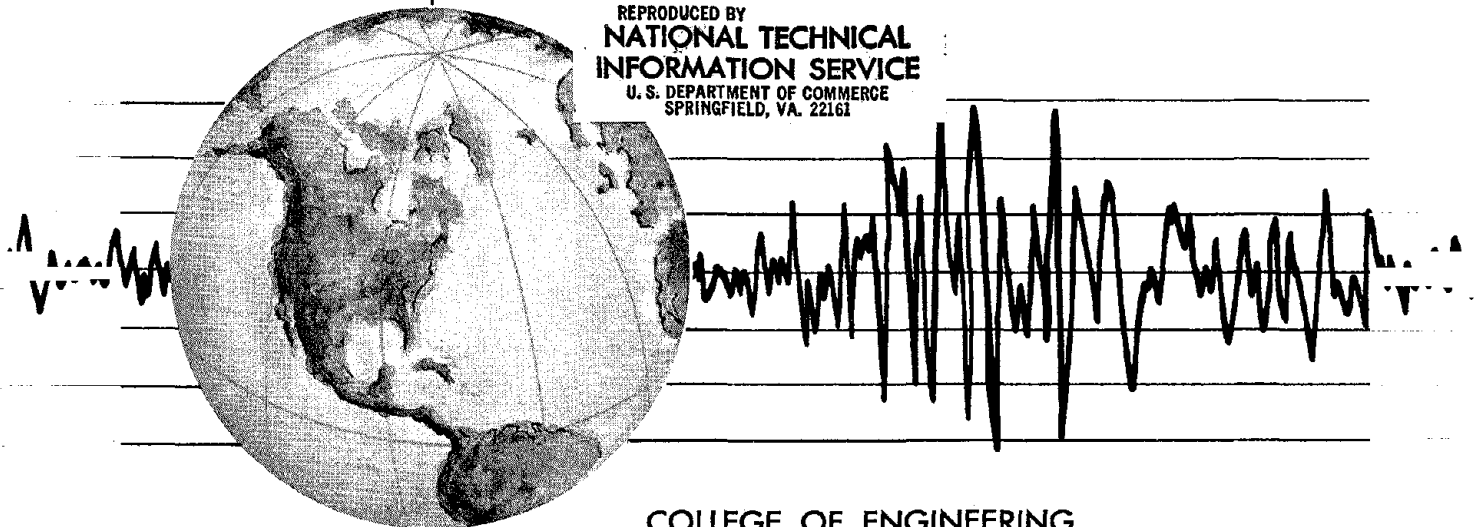
EARTHQUAKE ENGINEERING RESEARCH CENTER

# INVESTIGATION OF THE NONLINEAR CHARACTERISTICS OF A THREE STORY STEEL FRAME USING SYSTEM IDENTIFICATION

by  
IZAK KAYA  
and  
HUGH D. McNIVEN

*Report to the National Science Foundation*

REPRODUCED BY  
**NATIONAL TECHNICAL  
INFORMATION SERVICE**  
U. S. DEPARTMENT OF COMMERCE  
SPRINGFIELD, VA. 22161



COLLEGE OF ENGINEERING

UNIVERSITY OF CALIFORNIA · Berkeley, California

For sale by the National Technical Information Service, U. S. Department of Commerce, Springfield, Virginia 22161.

See back of report for up to date listing of EERC reports.

BIBLIOGRAPHIC DATA SHEET	1. Report No. NSF/RA-780681	2.	3. Recipient's Accession No. 02301363
4. Title and Subtitle Investigation of the Nonlinear Characteristics of a Three Story Steel Frame using System Identification		5. Report Date December 1978	6.
7. Author(s) Izak Kaya and Hugh D. McNiven		8. Performing Organization Rept. No. UCB/EERC-78/25	
9. Performing Organization Name and Address Earthquake Engineering Research Center University of California - Richmond Field Station 47th. & Hoffman Blvd. Richmond, CA 94804		10. Project/Task/Work Unit No.	
12. Sponsoring Organization Name and Address National Science Foundation 1800 G Street, N.W. Washington, D.C. 20550		11. Contract/Grant No. ENV76-04262	
15. Supplementary Notes		13. Type of Report & Period Covered	
		14.	
<p>16. Abstract: In the study reported here we construct two mathematical models of a three-story steel frame that are meant to predict its responses to seismic disturbances. This is an extension of work previously reported, devoted to the construction of mathematical models of the same frame to predict its linear response. This study benefits from the previous study to such an extent that here we have to consider only how to extend the previous models to accommodate nonlinear responses.</p> <p>This extension consists of accounting both for changes in the damping coefficients when the amplitudes of motion are large, and for yielding by including the hysteretic behavior of the ends of the members. Perhaps the most important decision in this extension has been the choice to model the hysteretic relationship between the bending moments and rotations at the ends of the members. After some consideration we chose to let the relationship be bilinear. This choice was made partly because we have not used this form before and partly because we considered it to be the simplest. Whereas it did prove to be simple, the bilinear form introduced a complication that we had not encountered previously, but which we have been able to surmount.</p> <p>With the introduction of hysteretic material behavior, three parameters are added to the eight which are a carry-over from the linear model, so that the new nonlinear models contain eleven parameters. For economy, we chose to fix two of the parameters in each model leaving the remaining nine to be determined from optimization. The difference between the two models that we construct is in the choice of which two of the parameters we fix. In the first we fix the values of the damping parameters giving them the values which we found after optimization for the linear model. In the second model we fix the parameters representing the yield moments in the bilinear model, one each for the columns and girders, and allow the damping parameters to be found from optimization.</p> <p>Both of the models predict the experimental time histories of the floor translations and joint rotations extremely accurately, with the advantage going slightly to the first model. As the two models represent different mechanisms which the frame exhibits to account for its nonlinear response, we were tempted to draw physical conclusions from the predictive abilities of the models. We decided against doing so because the responses recorded experimentally represent only a mildly nonlinear behavior of the frame.</p>			
17. COSATI Field/Group		19. Security Class (This Report) UNCLASSIFIED	
18. Availability Statement Release Unlimited		21. No. of Pages 97	
		20. Security Class (This Page) UNCLASSIFIED	
		22. Price PCAO5/A01	



INVESTIGATION OF THE NONLINEAR CHARACTERISTICS  
OF A THREE-STORY STEEL FRAME  
USING SYSTEM IDENTIFICATION

by

IZAK KAYA

and

HUGH D. McNIVEN

Report to the  
National Science Foundation

Report No. UCB/EERC-78/25

Earthquake Engineering Research Center  
College of Engineering  
University of California  
Berkeley, California  
December 1978



## ABSTRACT

In the study reported here we construct two mathematical models of a three-story steel frame that are meant to predict its responses to seismic disturbances. This is an extension of work previously reported, devoted to the construction of mathematical models of the same frame to predict its linear response. This study benefits from the previous study to such an extent that here we have to consider only how to extend the previous models to accommodate nonlinear responses.

This extension consists of accounting both for changes in the damping coefficients when the amplitudes of motion are large, and for yielding by including the hysteretic behavior of the ends of the members. Perhaps the most important decision in this extension has been the choice to model the hysteretic relationship between the bending moments and rotations at the ends of the members. After some consideration we chose to let the relationship be bilinear. This choice was made partly because we have not used this form before and partly because we considered it to be the simplest. Whereas it did prove to be simple, the bilinear form introduced a complication that we had not encountered previously, but which we have been able to surmount.

With the introduction of hysteretic material behavior, three parameters are added to the eight which are a carry-over from the linear model, so that the new nonlinear models contain eleven parameters. For economy, we chose to fix two of the parameters in each model leaving the remaining nine to be determined from optimization. The difference between the two models that we construct is in the choice of which two of the parameters we fix. In the first we fix the values of the damping

parameters giving them the values which we found after optimization for the linear model. In the second model we fix the parameters representing the yield moments in the bilinear model, one each for the columns and girders, and allow the damping parameters to be found from optimization.

Both of the models predict the experimental time histories of the floor translations and joint rotations extremely accurately, with the advantage going slightly to the first model. As the two models represent different mechanisms which the frame exhibits to account for its nonlinear response, we were tempted to draw physical conclusions from the predictive abilities of the models. We decided against doing so because the responses recorded experimentally represent only a mildly nonlinear behavior of the frame.



ACKNOWLEDGMENTS

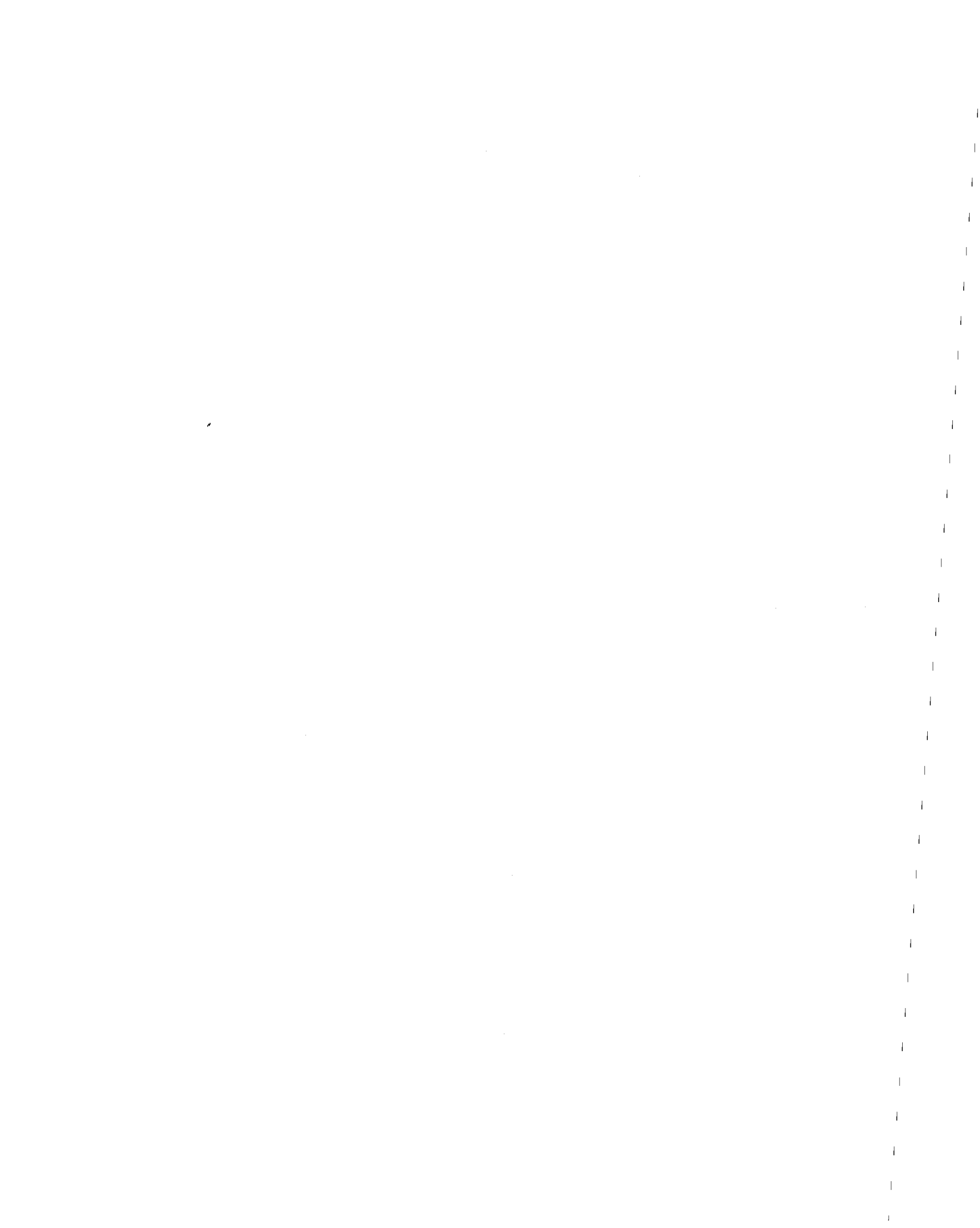
The research reported here was sponsored by the National Science Foundation under Grant No. ENV76-04262. The computing and plotting facilities were provided by the University of California Computer Center at Berkeley.

Al Klash and his associates are responsible for the drafting and Ellen McCutcheon did paste-ups and typed the manuscript.



TABLE OF CONTENTS

	<u>Page</u>
ABSTRACT . . . . .	i
ACKNOWLEDGMENTS . . . . .	iii
TABLE OF CONTENTS . . . . .	v
LIST OF TABLES . . . . .	vii
LIST OF FIGURES . . . . .	ix
1. INTRODUCTION . . . . .	1
2. THE EXPERIMENTAL PROGRAM . . . . .	6
2.1 The Test Structure . . . . .	6
2.2 Instrumentation . . . . .	11
2.3 The Forcing Functions . . . . .	11
3. BACKGROUND FOR FORMULATING THE MODELS . . . . .	13
3.1 System Identification as Used in the Study . . . . .	13
3.2 Bilinear Model for Structural Members . . . . .	21
3.3 Rotations of the Joints . . . . .	29
3.4 The Computer Program . . . . .	32
4. FORMULATION OF THE MODELS . . . . .	37
4.1 The First Nine Parameter Model . . . . .	39
4.2 The Second Nine Parameter Model . . . . .	43
5. COMPLETION AND PERFORMANCES OF THE MATHEMATICAL MODELS . . . . .	45
5.1 Model No. 1: EC-900II . . . . .	46
5.2 Model No. 1: MEC-600II . . . . .	52
5.3 Model No. 2: EC-900II . . . . .	58
5.4 Model No. 2: MEC-600II . . . . .	64
6. COMMENTS ON THE MODELS . . . . .	70
REFERENCES . . . . .	76



## LIST OF TABLES

<u>Table</u>		<u>Page</u>
1	Section and Material Properties of Test Frame . . . . .	10
2	Weight of Structural Components and Concrete Blocks . . . . .	10
3	Change in Parameters and Reduction in Error During a Typical Run Model No. 1: EC-900II . . . . .	46
4	Comparison of Initial Versus Final Parameters Model No. 1: EC-900II . . . . .	47
5	Change in Parameters and Reduction in Error During a Typical Run Model No. 1: MEC-600II . . . . .	52
6	Comparison of Initial Versus Final Parameters Model No. 1: MEC-600II . . . . .	53
7	Change in Parameters and Reduction in Error During a Typical Run Model No. 2: EC-900II . . . . .	58
8	Comparison of Initial Versus Final Parameters Model No. 2: EC-900II . . . . .	59
9	Change in Parameters and Reduction in Error During a Typical Run Model No. 2: MEC-600II . . . . .	64
10	Comparison of Initial Versus Final Parameters Model No. 2: MEC-600II . . . . .	65
11	Final Values of Parameters for Both Models EC-900II . . . . .	70
12	Comparison of Stiffness Parameters EC-900II . . . . .	71
13	Final Values of Parameters for Both Models MEC-600II . . . . .	74



LIST OF FIGURES

<u>Figure</u>	<u>Page</u>
1 Test Structure on the Shaking Table . . . . .	7
2 Plan and Elevations of the Test Structure . . . . .	8
3 Details of Girder to Column Connection Under-Designed . . . . .	9
4 Details of Girder to Column Connection Reinforced . . . . .	9
5 Typical Error Surface Profile, Bilinear Model . . . . .	18
6 Typical Error Surface Profile, Refined Bilinear Model . . . . .	20
7 Model of a Nonlinear Beam . . . . .	21
8 Bilinear Bending Moment-Rotation Relationship . . . . .	23
9 Definition of the "p" Parameter . . . . .	29
10 Rotation Calculation of Joints (Linear Case) . . . . .	31
11 Rotation Calculation of Joint B (Nonlinear Case) . . . . .	31
12 Flow Chart of the Identification Program . . . . .	36
13 Effective Length Parameters . . . . .	38
14 Correlation of Measured Versus Predicted Responses Model No. 1: EC-900II . . . . .	48
15 Correlation of Measured Versus Predicted Responses Model No. 1: EC-900II . . . . .	49
16 Correlation of Measured Versus Predicted Responses Model No. 1: EC-900II . . . . .	50
17 Measured and Predicted Hysteretic Behaviors Model No. 1: EC-900II . . . . .	51
18 Correlation of Measured Versus Predicted Responses Model No. 1: MEC-600II . . . . .	54
19 Correlation of Measured Versus Predicted Responses Model No. 1: MEC-600II . . . . .	55
20 Correlation of Measured Versus Predicted Responses Model No. 1: MEC-600II . . . . .	56
21 Measured and Predicted Hysteretic Behaviors Model No. 1: MEC-600II . . . . .	57

## LIST OF FIGURES (cont'd.)

<u>Figure</u>		<u>Page</u>
22	Correlation of Measured Versus Predicted Responses Model No. 2: EC-900II . . . . .	60
23	Correlation of Measured Versus Predicted Responses Model No. 2: EC-900II . . . . .	61
24	Correlation of Measured Versus Predicted Responses Model No. 2: EC-900II . . . . .	62
25	Measured and Predicted Hysteretic Behaviors Model No. 2: EC-900II . . . . .	63
26	Correlation of Measured Versus Predicted Response Model No. 2: MEC-600II . . . . .	66
27	Correlation of Measured Versus Predicted Response Model No. 2: MEC-600II . . . . .	67
28	Correlation of Measured Versus Predicted Response Model No. 2: MEC-600II . . . . .	68
29	Measured and Predicted Hysteretic Behaviors . . . . .	69



CHAPTER 1  
INTRODUCTION

This report is the second of two devoted to constructing mathematical models to predict the seismic response of a three-story steel frame. The first, by the same authors [1], presents a number of models to predict linear response whereas the models constructed in this work are meant to predict nonlinear response.

In this study we benefit enormously from the knowledge we gained in the previous investigation. We learned, for the particular frame that we are modeling, that a model can predict the seismic responses accurately only if it accommodates both floor translations and joint rotations. This enables us here to choose the order of the models that can be expected to predict accurately the nonlinear responses. We learned, having assumed a model form of this appropriate order, what response quantities from experiments to include in our error function so that convergence of the optimization algorithm is ensured. We also found how to introduce parameters into the model in such a way that they give physical insight into the behavior of the frame. This knowledge left us with the single additional problem here of extending the models to accommodate nonlinear responses.

In a three-story steel frame a nonlinear response derives from changes in the damping which the frame exhibits when the amplitudes of motions are large, and from the hysteretic material behavior resulting when material at the ends of the members suffers some yielding. In the models constructed here we consider only viscous damping and let it be of the Rayleigh type as we did in the linear models, but here we allow the values of the parameters thus introduced to change with

changes in the amplitude of the response.

We choose to let the hysteretic material behavior influence the model by accounting for the nonlinear relationship between the bending moments and the rotations at the ends of the members. There are several ways to model this nonlinear, global relationship. The Ramberg-Osgood formulation was used successfully by McNiven and Matzen [2] in constructing a model to predict the nonlinear response of a single-story steel frame. Equations somewhat the same as Ramberg-Osgood, but exhibiting certain properties of advantage to system identification, have been presented by Menegotto and Pinto [3]. A modified version of the Menegotto and Pinto equations that allows the parameters to be strain dependent was used by Stanton and McNiven [4] to mimic extremely complicated stress-strain relations for steel reinforcing bars. In spite of this previous experience and success with these models, in this study we choose a bilinear model to reflect the relationship between moment and rotation for the members. In making this choice, we were attracted by the simplicity of the formulation, predicting that computer time in solving the equations and converging on a set of parameters by optimization would be less than other formulations. This proved to be only partly true. The solution of the nonlinear equations was simple, but because the bilinear shape of the moment-rotation relationship is a crude approximation of the continuous true form, the surface representing the error function in parametric space displayed a large array of inundations, encumbering the search for a global minimum. We explain in the report how we adjusted our algorithm to overcome this difficulty. The predictions of the nonlinear responses derived from the resulting models seem to support this choice of the bilinear model of material behavior. We construct in the report two different models.

The total number of parameters existing in the model form is eleven. Eight, which are a carry-over from the linear model, consist of two damping parameters and six stiffness parameters representing effective length factors for the members. Three new ones are introduced here to account for hysteretic material behavior. They are a parameter representing the ratio of slopes of the bilinear model, and two representing the yield moment, one for the columns and one for the girders, possible because each class of member has the same cross section. As computer costs and storage requirements grow rapidly as the number of parameters increases, we decide that each of the two models will have only nine free parameters. The difference in the two models is in the choice of which two of the eleven parameters we fix before optimization.

In the first model we fix the values of the damping coefficients to the values we found after optimization for the linear model. It follows that with this model all of the nonlinear behavior is accounted for by the three hysteretic parameters.

In the second model we fix the two yield moments to the final values they attained in the first model. This was the choice because these two parameters varied little during optimization. The upshot of this choice is that in the second model the nonlinear behavior is shared by the damping parameters and the material behavior.

To construct mathematical models one needs accurate records of both the input to the frame and the responses. We are fortunate in having an excellent set of data from experiments performed in 1975 on the shaking table at the Earthquake Engineering Research Center of the University of California, Berkeley, reported by Clough and Tang [5]. In 1975 the system for stabilizing the table had not as yet been completed. This restricted the intensity of seismic input that could be

imposed on the frame, with the result that the responses recorded represent only mildly nonlinear behavior.

This study is the third that we know of which uses the data from the Clough and Tang experiments to construct mathematical models. The first was conducted by Tang himself [6] in 1975. Tang used the same model form as we do. He formulated his best model using physical intuition and trial and error and arrived at a very credible model. Distefano and Peña-Pardo [7] used system identification, but introduced a new form for the equations. Their model is fairly successful.

Both of the models presented in this study predict the time histories of both the floor accelerations and joint rotations very accurately, with slight advantage going to the first model. It is tempting to draw conclusions about what mechanisms account for the nonlinear behavior by comparing the quality of the predictions, but we hesitate to do so with the models constructed from responses that are so mildly nonlinear.

In the second chapter we describe the physical frame, the instrumentation of the frame giving the response data that we used and the earthquake force time histories that created the disturbances.

In Chapter 3 we lay the preparations for constructing the models. We describe briefly system identification as we use it here, how we construct a bilinear model for each member, how we calculate joint rotations from recorded data and finally we discuss the computer program.

In Chapter 4 we construct the two models, that is we choose which parameters will be free, with reasons for the choices. Chapter 5 presents the results of the computer program which is a set of parameter values completing each model. Each of the two models is constructed first using data from the El Centro earthquake and then from a modified version of the El Centro time history. A large variety of time histories

are displayed comparing the experimental and predicted responses. The last chapter contains a discussion of the parameters in each of the four models, how they compare and what similarities and differences mean. The four consist of two using Model No. 1 in which the values of the parameters are derived from two different forcing functions, and a comparable pair for Model No. 2. We comment on the invariance of the model to changes in the forcing function giving data from which the model is constructed.

## CHAPTER 2

### THE EXPERIMENTAL PROGRAM

The experiments performed on the three-story steel frame, the results of which are used in the formulation of the models, will be discussed here briefly. A detailed account of the program is contained in a report by Clough and Tang [5]. In this chapter we describe the physical frame, the instrumentation giving the response data that we actually use, and the forcing functions imposed by the shaking table which generated these responses.

#### 2.1 The Test Structure

The test structure shown on the shaking table in Fig. 1 is fabricated from rolled shapes of ASTM A-36 grade steel. Typical floor plans as well as front and side elevations of the structure are shown in Fig. 2. The two frames designated A and B are separated by a distance of 6'-0". They are connected at floor levels by removable cross beams and bracing angles. Thus the effect of a floor diaphragm rigid in its own plane is obtained.

The total height of the structure is 17'-4", the story heights are 6'-8", 5'-4" and 5'-4". The bay width is 12'-0". Sections W5-16 and W6-12 are used for column and girder members, respectively.

The fully penetrated welded girder to column connections are used for the test structure. Figures 3 and 4 depict the details of these connections; the panel zone thickness is 1/4" (i.e. the column web thickness) for Phase I of the experiments, and 1" (column web reinforced by 3/8" doubler plates on both sides) for Phase II. Because of the different strengths of these two types of connections, the test structure is expected to yield primarily in the panel zone in Phase I of the study and exclusively in the girder and column ends in the Phase II tests.

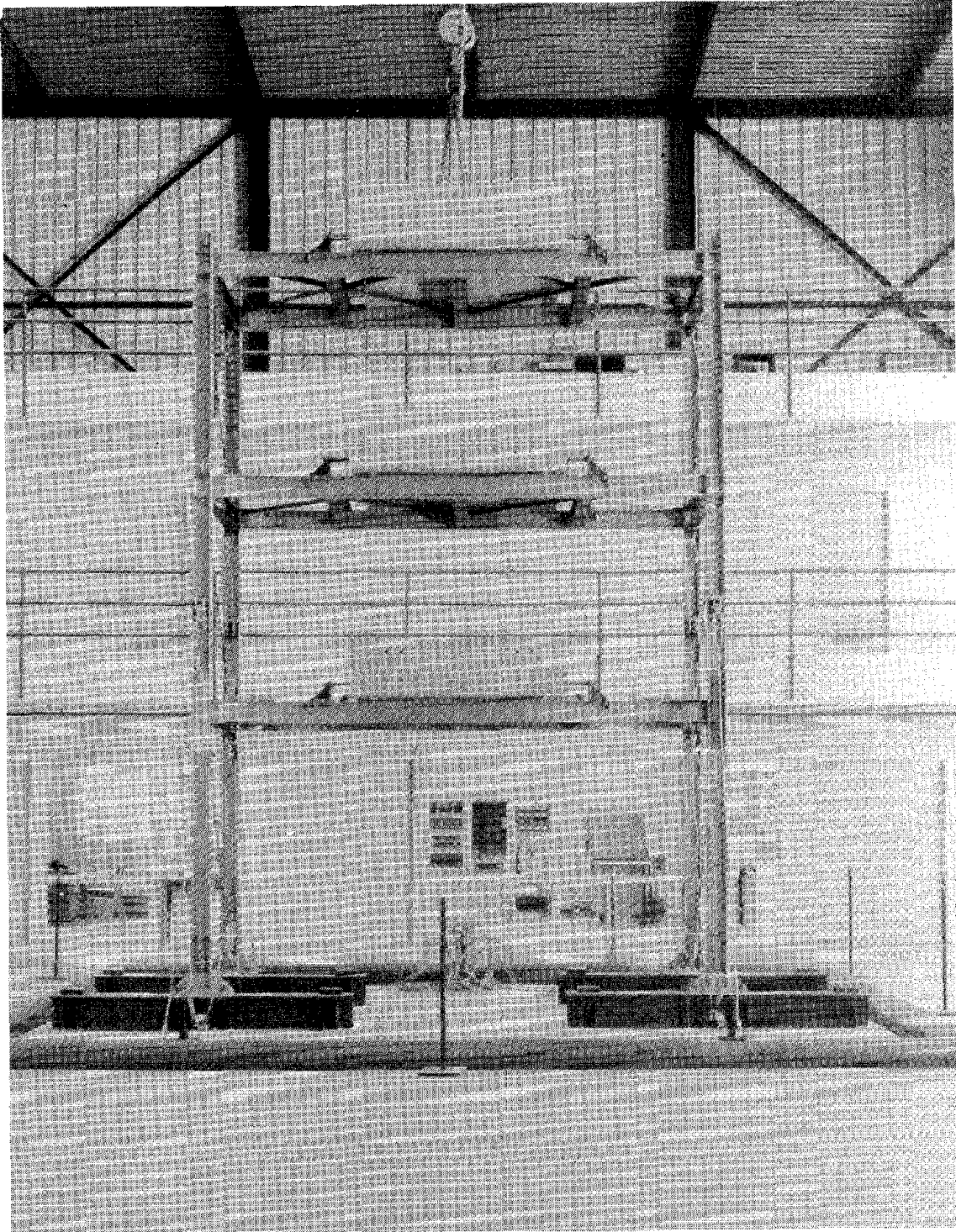


FIGURE 1 TEST STRUCTURE ON THE SHAKING TABLE

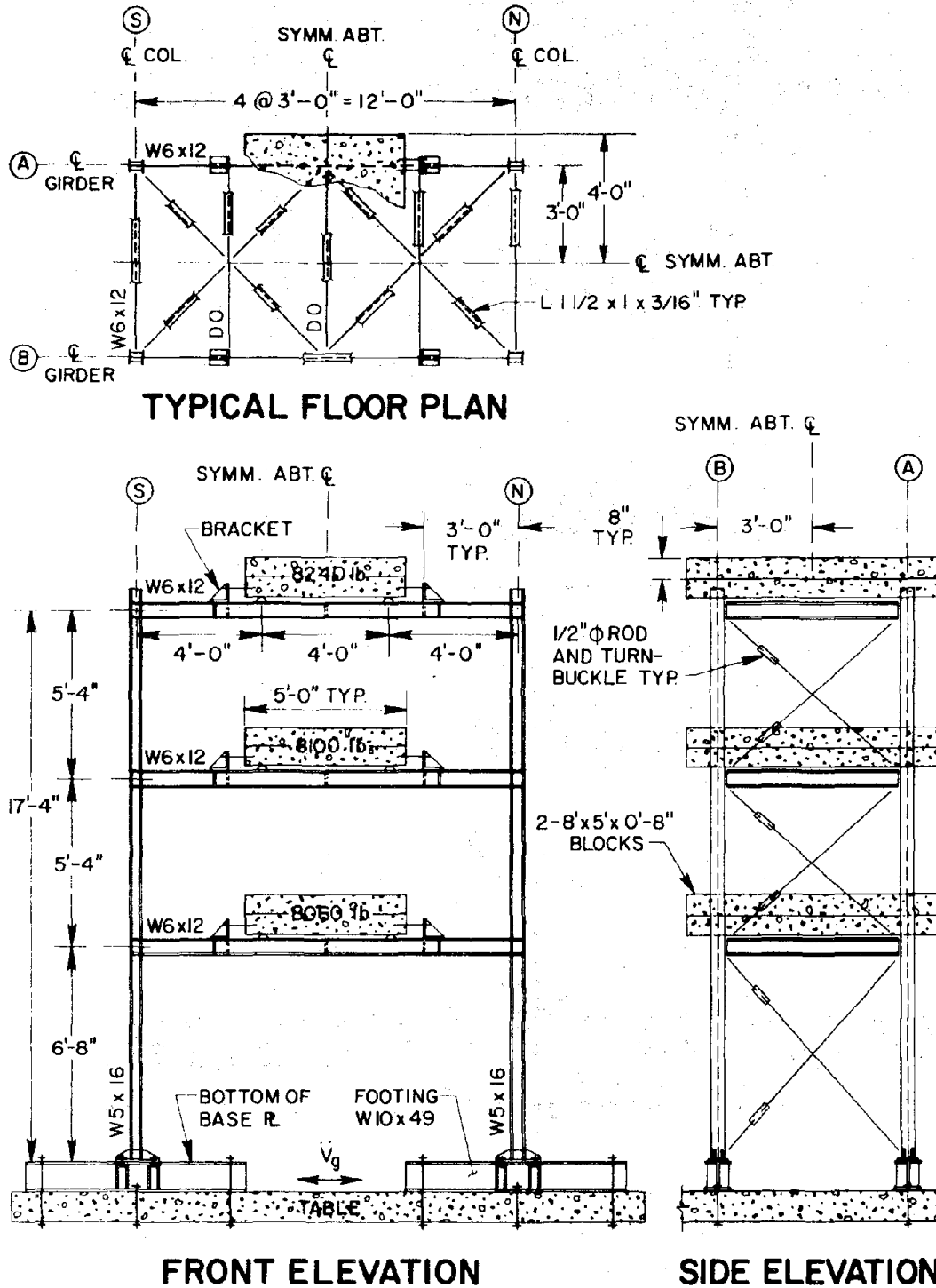
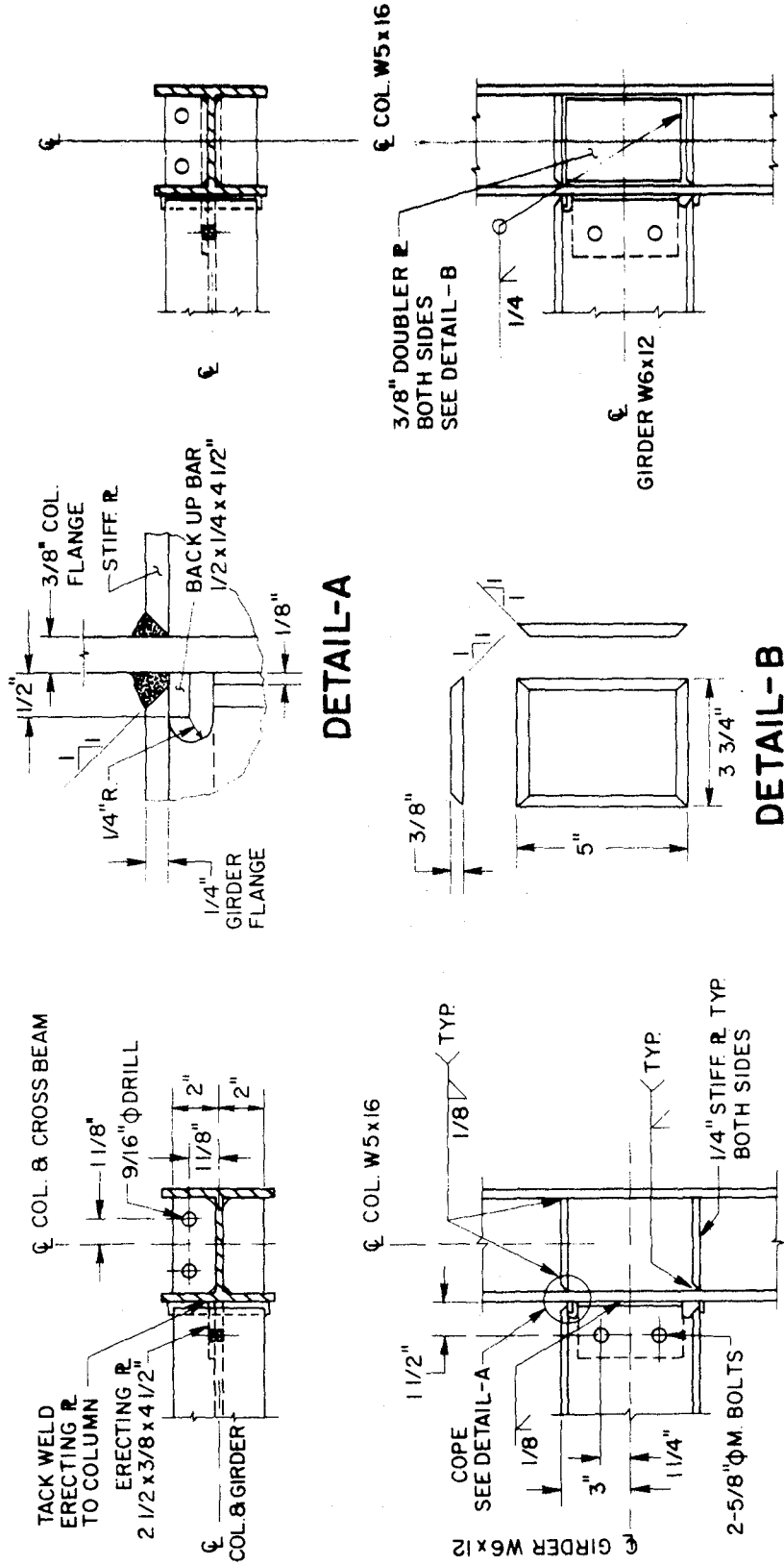


FIGURE 2 PLAN AND ELEVATIONS OF THE TEST STRUCTURE





TYPICAL CONNECTION REINFORCED

FIGURE 4 DETAILS OF GIRDER TO COLUMN CONNECTION REINFORCED

TYPICAL CONNECTION AS BUILT

FIGURE 3 DETAILS OF GIRDER TO COLUMN CONNECTION UNDER-DESIGNED

	Girder W6x12	Column W5x16
	Nominal*	Nominal*
b(in)	4.00	5.00
d(in)	6.00	5.00
t <sub>w</sub> (in)	0.230	0.240
t <sub>f</sub> (in)	0.279	0.360
A (in <sup>2</sup> )	3.54	4.70
I <sub>x</sub> (in <sup>4</sup> )	21.7	21.3
S <sub>x</sub> (in <sup>3</sup> )	7.25	8.53
Z <sub>x</sub> (in <sup>3</sup> )	8.23	9.61
σ <sub>y</sub> (ksi)	45.9	45.9
τ <sub>y</sub> (ksi)	26.5	26.5
P <sub>y</sub> (kip)	126	216
M <sub>y</sub> (kip-in)	333	392
M <sub>p</sub> (kip-in)	378	441

\*Material properties are based on mill test report

TABLE 1 SECTION AND MATERIAL PROPERTIES OF TEST FRAME

	Conc. Blocks**	Column†	Girder	Cross Beams	Brac'gs	Misc.	Total
3rd Floor (lb)	8240	214	274	402	50	120	9300
2nd Floor (lb)	8100	342	274	402	50	120	9288
1st Floor (lb)	8060	384	274	402	50	120	9290

\* Frame A and Frame B

\*\* Center of gravity at 9 1/4" above girder top flange

† Half column heights

TABLE 2 WEIGHT OF STRUCTURAL COMPONENTS  
AND CONCRETE BLOCKS

Blocks of concrete weighing about 8,000 lb per floor are added to the structure to provide a period of vibration in the range appropriate to actual steel buildings and to apply a gravity load to the girders. The use of this particular weight at each floor gives a rather small gravity load stress in the structure, so that the test structure exhibits unusually high capacity in resisting lateral loads.

Table 1 lists the nominal section properties and force capacities of the structure while Table 2 summarizes the estimated weights of the structure.

## 2.2 Instrumentation

The response data that we use in our model formulation are only part of the data recorded. The data that we do use were acquired from accelerometers, strain gages and LVDT's. The linear accelerations at all floor levels were recorded by accelerometers. The joint rotations are calculated using both strain gage readings and measurements from an LVDT. The foil strain gages are situated on opposite outside surfaces of the columns at each joint, one pair nine inches below the bottom of the beam, and other nine inches above the top of the beam. The center line of the LVDT was situated eleven inches above the base plate at the lower end of the column.

The data used in the construction of the models were those acquired from testing the reinforced frame, denoted as Phase II.

## 2.3 The Forcing Functions

The forcing functions are imposed by the shaking table and can vary both in character and intensity. The character of the excitation can be derived from an historical earthquake or can be artificial. The intensity of the excitation is reflected in the "span" number. Clough

and Tang subjected the Phase II frame to the 1940 El Centro N-S earthquake, a modified version of the same and to a narrow band artificial earthquake. The word "modified" in this context denotes the process of scaling the "time" of an earthquake record.

The scale number is indicative of what part of the displacement capacity (1,000) is being used. For a particular earthquake doubling the span number will roughly double the input peak acceleration. In the designation used in the report the code EC900-II has the meaning "El Centro earthquake, span or intensity number 900, imposed on Phase II frame." We use the response data generated by the El Centro and Modified El Centro excitations.

At the time of the experiments the intensity of shaking was limited by overturning moment imposed by the structure on the table, and whereas nonlinear response was realized, it could be termed mildly nonlinear.

## CHAPTER 3

### BACKGROUND FOR FORMULATING THE MODELS

In this chapter the background for formulating the mathematical models is presented. The general method is system identification, and the way in which this method is applied here is discussed first. This part benefits enormously from insight which we gained in an earlier study [1] for modeling the linear response of the same frame. The details we leave for a study of this reference and discuss system identification here as briefly as possible.

There are problems introduced by the nonlinearity of the model formulated in this report, and these are discussed in some detail. The nonlinear response of the frame is accommodated in the model by the hysteretic material behavior of the steel. For this we use a bilinear model and problems are introduced that were not encountered with the linear model. In the third section, the computer program describing the numerical analysis for the first two sections is presented.

#### 3.1 System Identification as Used in the Study

The first part of system identification is the form of the equations which constitute the model.

For a multistory structure subjected to rigid base motion, the following set of second order differential equations in incremental form apply.

$$[M] \{\Delta\ddot{u}\} + [C] \{\Delta\dot{u}\} + [K] \{\Delta u\} = -[M] \{I\} \Delta\ddot{u}_g \quad (1)$$

In this equation  $[M]$  is the mass matrix taken to be constant,  $[C]$  and  $[K]$  are the instantaneous damping and stiffness matrices valid within the time interval  $t$  to  $t+\Delta t$ ,  $\{I\}$  is the identity vector and  $\{\Delta u\}$ ,  $\{\Delta\dot{u}\}$  and  $\{\Delta\ddot{u}\}$  are the vectors for the instantaneous changes in the relative

nodal displacement, velocity and acceleration, respectively, and  $\Delta\ddot{u}_g$  is the change of the base motion  $\ddot{u}_g$  for the same time interval.

From our study of the linear model we learned that accurate predictions for the response of the frame are possible only if it accommodates both floor translation and joint rotations. This influences the form of the elements appearing in the  $[K]$  matrix. The major difference between this model and the linear one formulated in Reference [1] is in the material properties of the steel which is also reflected in the elements of the  $[K]$  matrix. This is treated at some length in the next section.

If the matrices  $[C]$  and  $[K]$  can be defined within each time step and taken constant within that interval, the solution of Eq. 1 at each time step  $\Delta t$ , from  $t=0$  to  $t=T$ , yields the nodal displacement, velocity and acceleration time histories. This is done using cumulative results as

$$\begin{aligned}\{u\}_t &= \{u\}_{t-\Delta t} + \{\Delta u\}_t \\ \{\dot{u}\}_t &= \{\dot{u}\}_{t-\Delta t} + \{\Delta \dot{u}\}_t \\ \{\ddot{u}\}_t &= \{\ddot{u}\}_{t-\Delta t} + \{\Delta \ddot{u}\}_t\end{aligned}\tag{2}$$

The solution of Eq. 1 is obtained assuming the acceleration for each degree of freedom to vary linearly within the time increment  $\Delta t$ . The integration technique used is one presented by Wilson and Clough [8] and is similar to the Newmark  $\beta$ -method [9] with  $\beta=1/6$ .

The second part of system identification is the criterion or error function. This function reflects what it is that we want the model to do. For this study we want the model to predict as accurately as possible particular response quantities recorded by the physical frame. Here again we benefit from our linear study where we learned that the response quantities that lead to a unique model are the floor

acceleration and joint rotation time histories. It is these quantities, therefore, that appear in the error function. Specifically the cost function is the integral squared error of these quantities accumulated over some specified time interval  $T$ . In addition to being functions of time the predicted response quantities will depend on the set of model parameters  $\bar{\beta}$ . The error function, therefore, is

$$J(\bar{\beta}, T) = \sum_{j=1}^n \int_0^T \{[\ddot{x}_j(\bar{\beta}, t) - \ddot{y}_j(t)]^2 + [E.\omega_j(\bar{\beta}, t) - E.\theta_j(t)]^2\} dt \quad (3)$$

where  $\ddot{y}_j(t)$  and  $\theta_j(t)$  are the measured accelerations and rotations of the joints and  $\ddot{x}_j(\bar{\beta}, t)$  and  $\omega_j(\bar{\beta}, t)$  are their predicted counterparts. Note that the rotations have been multiplied by the modulus of elasticity,  $E$ , so that the two different sets of quantities within the error function are of the same order of magnitude.

The final part of system identification is the selection of an algorithm to systematically adjust the parameters in the mathematical model until the error is minimized. Defining by  $\bar{\beta}_i$  the vector of parameters,  $\bar{\beta}_{i+1}$  will denote an improved version of the parameters which gives a smaller value of  $J$ . The Gauss-Newton method used here is generated in the following way. The fundamental equation is

$$\bar{\beta}_{i+1} = \bar{\beta}_i + \alpha \bar{d}_i \quad (4)$$

where  $\bar{d}_i$  is a direction vector and  $\alpha$  a step size.

Expanding the error function in a Taylor series about the initial point  $\bar{\beta}_i$ , retaining only the first three terms and setting the gradient of the error with respect to  $\beta_{i+1}$  equal to zero, we get

$$\bar{\beta}_{i+1} = \bar{\beta}_i - [\bar{\nabla}^2 J(\bar{\beta}_i, T)]^{-1} \bar{\nabla} J(\bar{\beta}_i, T) \quad (5)$$

where  $\bar{\nabla}^2 J(\bar{\beta}_i, T)$  is the Hessian matrix and  $\bar{\nabla} J(\bar{\beta}_i, T)$  is the gradient vector. The  $p^{\text{th}}$  component of the gradient is

$$\frac{\partial}{\partial \beta_p} J(\bar{\beta}, T) = 2 \sum_{j=1}^n \int_0^T \{ [\ddot{x}_j(\bar{\beta}, t) - \ddot{y}_j(t)] \frac{\partial \ddot{x}_j(\bar{\beta}, t)}{\partial \beta_p} + [E\omega_j(\bar{\beta}, t) - E\theta_j(t)] \frac{\partial (E\omega_j(\bar{\beta}, t))}{\partial \beta_p} \} dt \quad (6)$$

and the ps<sup>th</sup> component of the Hessian is

$$\begin{aligned} \frac{\partial^2}{\partial \beta_p \partial \beta_s} J(\bar{\beta}, T) = & 2 \sum_{j=1}^n \int_0^T \left[ \frac{\partial \ddot{x}_j(\bar{\beta}, t)}{\partial \beta_p} \cdot \frac{\partial \ddot{x}_j(\bar{\beta}, t)}{\partial \beta_s} + \frac{\partial}{\partial \beta_p} (E\omega_j(\bar{\beta}, t)) \cdot \frac{\partial}{\partial \beta_s} (E\omega_j(\bar{\beta}, t)) \right] dt \\ & + \int_0^T \left[ (\ddot{x}_j(\bar{\beta}, t) - \ddot{y}_j(t)) \frac{\partial^2 \ddot{x}_j(\bar{\beta}, t)}{\partial \beta_p \partial \beta_s} + (E\omega_j(\bar{\beta}, t) - E\theta_j(t)) \frac{\partial^2 (E\omega_j(\bar{\beta}, t))}{\partial \beta_p \partial \beta_s} \right] dt \end{aligned} \quad (7)$$

Assuming that the errors go to zero and the second partial derivatives do not increase faster than the errors are decreasing, the second integral in the right hand side of Eq.(7) can be dropped, thus a typical component of the approximate Hessian matrix will then be

$$\frac{\partial^2 J(\bar{\beta}, T)}{\partial \beta_p \partial \beta_s} = 2 \sum_{j=1}^n \int_0^T \left[ \frac{\partial \ddot{x}_j(\bar{\beta}, t)}{\partial \beta_p} \cdot \frac{\partial \ddot{x}_j(\bar{\beta}, t)}{\partial \beta_s} + \frac{\partial}{\partial \beta_p} (E\omega_j(\bar{\beta}, t)) \cdot \frac{\partial}{\partial \beta_s} (E\omega_j(\bar{\beta}, t)) \right] dt \quad (8)$$

Thus the direction vector in Eq.(4) can now be defined as

$$\bar{d}_i = - [\overline{AH}(\bar{\beta}_i, T)]^{-1} \nabla J(\bar{\beta}_i, T) \quad (9)$$

where  $\overline{AH}(\bar{\beta}_i, T)$  stands for the approximate Hessian.

Eq. 5 is re-written as

$$\bar{\beta}_{i+1} = \bar{\beta}_i - \alpha [\overline{AH}(\bar{\beta}_i, T)]^{-1} \nabla J(\bar{\beta}_i, T) \quad (10)$$

where  $\alpha$  is a step size introduced which may be different from 1.0 if the error surface is not quadratic and will be defined within each error surface profile such that the error within that profile is minimized. It is the replacement of the Hessian matrix by the approximate Hessian that



introduces the term "modified". The optimization algorithm therefore takes the title modified Gauss-Newton.

The terms in Eq.(8) which involve the derivatives of the response quantities with respect to the  $\bar{\beta}_i$  parameters and which are called sensitivity coefficients will be evaluated using finite differences such that

$$\frac{\Delta \dot{x}(\bar{\beta}, t)}{\Delta \beta_p} = \frac{\dot{x}_j(\bar{\beta}, t) \Big|_{\beta_p + \Delta \beta_p} - \dot{x}_j(\bar{\beta}, t) \Big|_{\beta_p}}{\Delta \beta_p} \quad (11)$$

To obtain an improved version of the parameters in Eq.(10), means of obtaining a proper step size  $\alpha$  should be defined. This is established by systematically searching the error surface in the direction defined by Eq.(9) until a point is found on this error surface profile where the error is minimum.

This step was previously performed by writing the error function in terms of  $\alpha$  and then differentiating with respect to  $\alpha$  and setting the resulting slope equal to zero.

$$J(\bar{\beta}_{i+1}, T) = J \left[ \bar{\beta}_i - \alpha [\overline{AH}(\bar{\beta}_i, T)]^{-1} \overline{\nabla J}(\bar{\beta}_i, T) \right] \quad (12)$$

$$\frac{\partial}{\partial \alpha} J(\bar{\beta}_{i+1}, T) = -\overline{\nabla J}(\bar{\beta}_{i+1}, T) [\overline{AH}(\bar{\beta}_i, T)]^{-1} \overline{\nabla J}(\bar{\beta}_i, T) \quad (13)$$

Using the values of the error function and its slope at  $\alpha=0$  and  $\alpha=1$  a cubic polynomial is fitted between those two points, whose minimum point defines a new  $\alpha$ . The minimum of the error profile and of the polynomial do not necessarily match at this value of  $\alpha$ . The procedure is continued using this newly defined point until a point is found on the error profile where the slope is practically zero.

This curve fitting technique which worked extremely well for the linear case is found to be ineffective for the nonlinear case. In the

present work the error surface is far from being close to a quadratic surface. This is due to the discontinuity in the slope of the bilinear model at the yield point. The error surface is quite complicated as a typical error profile in Fig. 5 indicates. This is understandable when we realize the sudden change in slope as we go from the linear to the nonlinear range which is reflected in the possible change of the stiffness matrix  $[K]$  from one time step to the next.

Therefore obtaining the minimum point of an error profile by fitting a cubic or quadratic polynomial, as was done in the linear case, appears impractical here.

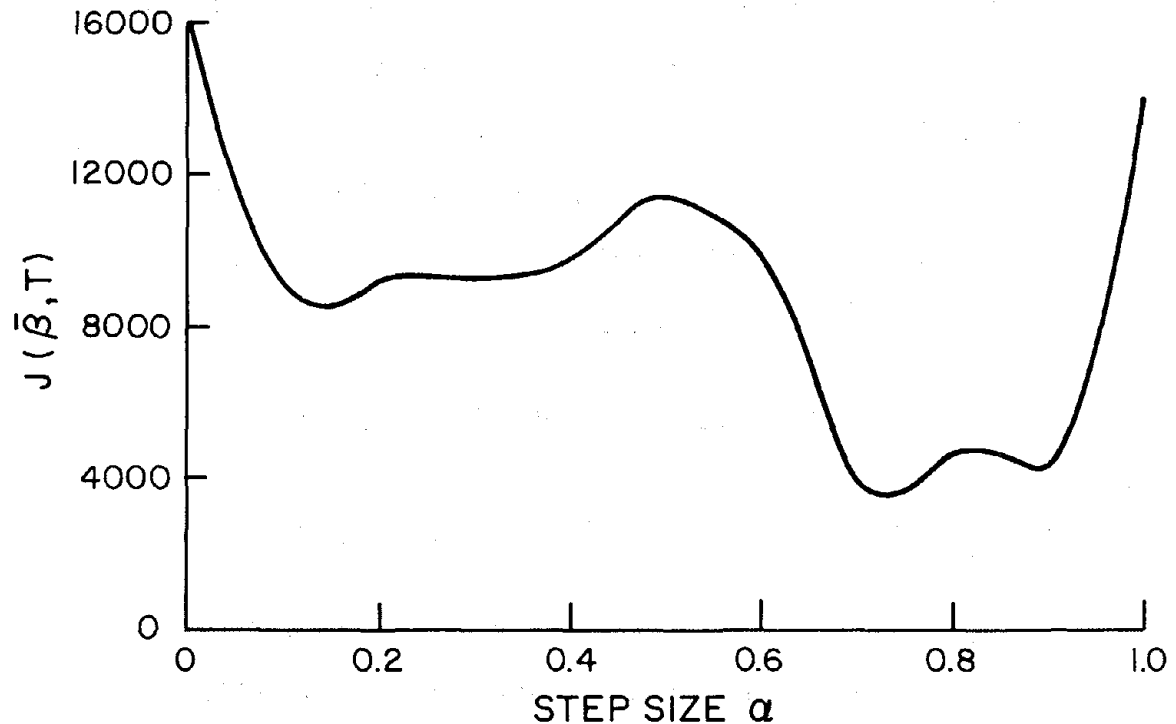


FIGURE 5 TYPICAL ERROR SURFACE PROFILE  
BILINEAR MODEL

This is the first complication introduced when we replace a linear model by a bilinear, which we do in the next section.

The minimum of an error profile is obtained in this study by subdividing the Error vs Step Size diagram into a number of intervals

between 0 and 1.0 and evaluating the error at each of these points. The point with the minimum value of the error (even though this is not the true minimum) is chosen as the initial starting point for the next cycle of the iteration.

The larger the number of subdivisions, the more accurately is the minimum of the error profile located. In our work, ten subdivisions between  $\alpha=0$  and  $\alpha=1$  is usually found to be satisfactory.

A second problem which did not occur in the linear case and which is closely related to this problem, is the inability of the method to reduce the slope of the error surface to very small values. In the linear case, due to the well behaved error profiles, the slope of the error surface could be reduced to small values and the minimum accurately located. In the present case, as we come closer and closer to the minimum, the error profile becomes flat, but with occasional bumps along the profile. This circumstance made it difficult to locate a point on the profile where the slope is less than some stopping tolerance. We were forced to use as our minimum a point representing an error that could not be reduced by further search.

This problem did not turn out to be critical since the components of the direction vector were by this time very small indicating that we were close to the minimum. The problem could probably be remedied by taking a much larger number of intervals.

The fact that these problems did not occur in the linear problem or in Matzen and McNiven's work [ 2 ] where the Ramberg-Osgood model was used in which the force-deflection relationship is a continuously differentiable function, seems to indicate that the behavior is due to the sharp discontinuity in the slope of the bending moment-rotation relationship.

To pinpoint this as the cause, we study a "refined bilinear model. To avoid the sudden change from the linear to nonlinear behaviors, we introduce a parabola that will make the transition gradual. The parabola is fitted to the two straight lines by matching the slopes of the lines and the parabola at the end of the linear and the beginning of the non-linear phases. The interval over which this is done is chosen arbitrarily.

The error surface for this refined model is much more suitably behaved. A typical error surface profile shown in Fig. 6, when compared to the profile of Fig. 5, shows this. This supports the discontinuity of the slope in the bilinear model as the cause of the problems.

However, we also learned that the set of parameters identified by the coordinates of the global minimum, established using the refined model are close to those established with the bilinear model. As the refined model is more difficult to use and has little influence on the final values of the parameters, we decided to return to the bilinear material model in the remainder of the work.

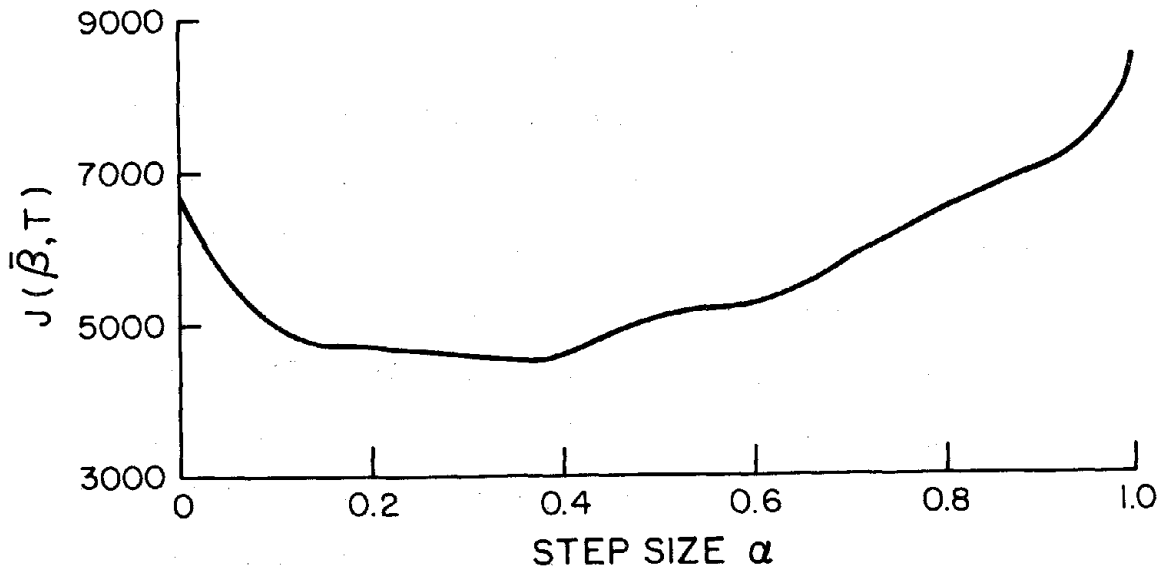


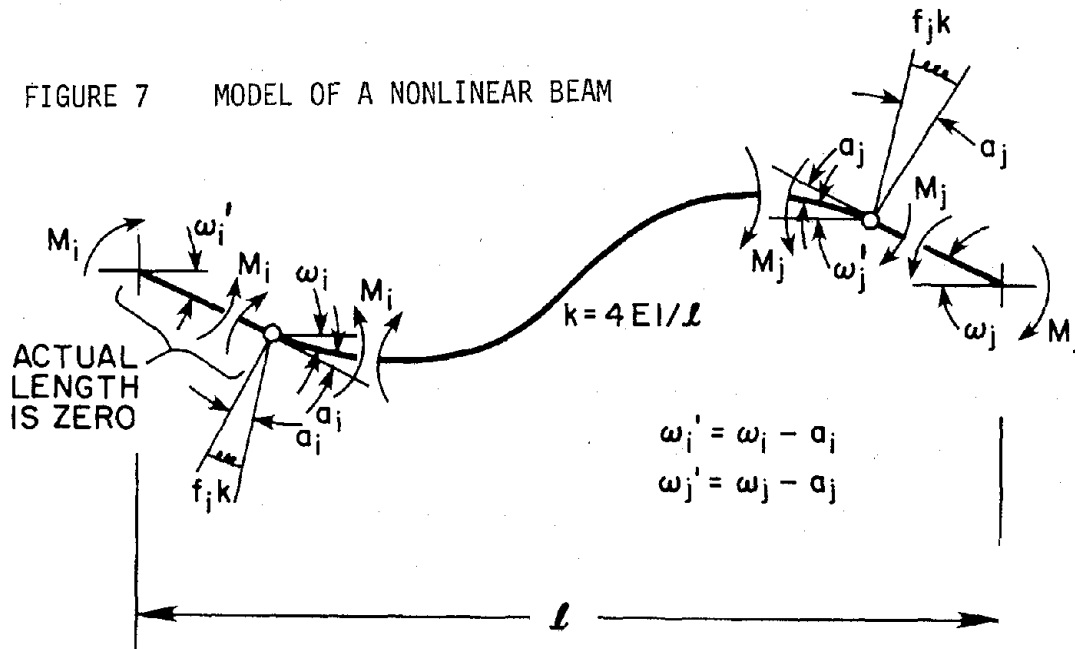
FIGURE 6 TYPICAL ERROR SURFACE PROFILE  
REFINED BILINEAR MODEL

### 3.2 Bilinear Model for Structural Members

Bilinear material properties are well known, but what we require in our modeling here is a bilinear model to represent the global behavior of the members of the frame, both beams and columns. We choose to have the behavior reflected in the relationship between the bending moment and the angle of rotation. In what follows we develop a general relationship and then exploit the symmetry of the frame and symmetry of the deformed shape due to the seismic disturbance. We will find that in extending our model from linear to nonlinear we introduce, or can introduce, three additional parameters.

Detailed information on two beam models developed and used by different investigators is given in Giberson [10]. One of the models is able to handle only bilinear hysteresis loops while the other one can handle both bilinear and curvilinear, the only restriction being that the initial slopes of the hysteresis loops at both ends of the same beam must be the same. We make the choice of the second model, starting with the bilinear knowing that if this proves to be inadequate we can resort to a curvilinear model.

We begin with a study of Fig. 7 which shows a member deformed antisymmetrically so that yielding has taken place at both ends.



In the linear state the beam has a stiffness

$$k = 4EI/L \quad (14)$$

where E is Young's modulus, I is the moment of inertia and L is the length of the beam. In Fig. 7, the symbols have the following meanings:

- $M_i, M_j$       bending moments at the ends (i) and (j)
- $\omega_i, \omega_j$       end rotations
- $\omega_i', \omega_j'$     end rotations of central beam
- $\alpha_i, \alpha_j$       incurred plastic angles at the ends (i) and (j).

For the central beam

$$\begin{aligned} M_i &= k(\omega_i' + \frac{1}{2}\omega_j') \\ M_j &= k(\frac{1}{2}\omega_i' + \omega_j'). \end{aligned} \quad (15)$$

Introducing

$$\omega_i' = \omega_i - \alpha_i \quad \text{and} \quad \omega_j' = \omega_j - \alpha_j$$

into Eq. 15, the fundamental bending moment-end rotation equations become

$$\begin{aligned} M_i &= k [(\omega_i - \alpha_i) + \frac{1}{2}(\omega_j - \alpha_j)] \\ M_j &= k [\frac{1}{2}(\omega_i - \alpha_i) + (\omega_j - \alpha_j)] \end{aligned} \quad (16)$$

or in incremental form

$$\begin{aligned} M_i &= k [(\Delta\omega_i - \Delta\alpha_i) + \frac{1}{2}(\Delta\omega_j - \Delta\alpha_j)] \\ M_j &= k [\frac{1}{2}(\Delta\omega_i - \Delta\alpha_i) + (\Delta\omega_j - \Delta\alpha_j)] \end{aligned} \quad (17)$$

The purpose of writing these equations in incremental form is that in this form it is possible to solve the equations of motion using finite integration techniques assuming that the state of yield remains constant throughout each time increment.

As seen in Eqs. (16) and (17), the incremental bending moments,

$\Delta M$ , are related to both the incremental rotations,  $\Delta\omega$ , and incremental plastic angles,  $\Delta\alpha$ . Now if the state of yield is known at the beginning of the time increment, it is possible to establish beforehand an equation of the form

$$\Delta\alpha = \Delta\alpha(\Delta\omega_i, \Delta\omega_j) \quad (18)$$

relating the incremental plastic angles to the end rotations. Using these equations it is possible to eliminate the incremental plastic angles from the incremental moment-rotation equations resulting in equations of the form

$$\Delta M = \Delta M(\Delta\omega_i, \Delta\omega_j) \quad (19)$$

which are valid for each time increment.

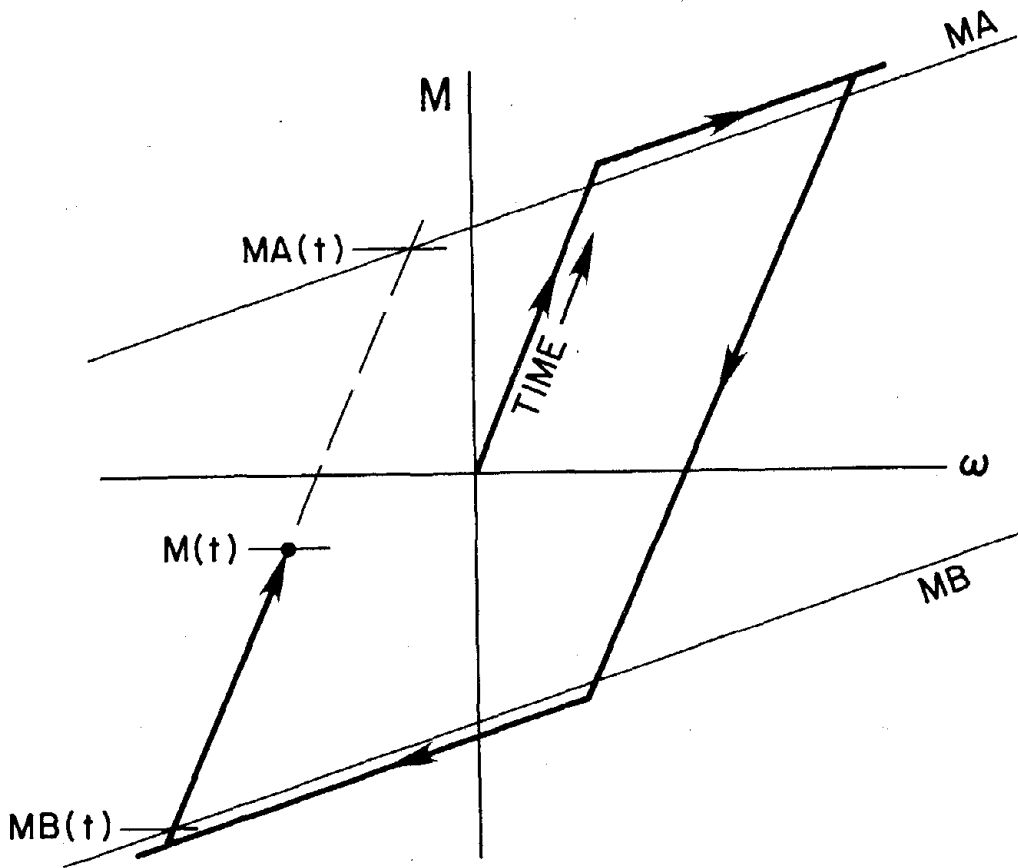


FIGURE 8 BILINEAR BENDING MOMENT-ROTATION RELATIONSHIP

The criteria for establishing the state of yield at the time  $t$  (at the beginning of a time increment) are based upon the bending moment at time  $t$  and the last incremental bending moment prior to time  $t$ . These criteria are the following: (see Fig. 8)

If  $MB(t) < M(t) < MA(t)$  the relationship is elastic

if {or 
$$\begin{array}{l} M(t) \geq MA(t) \text{ and } \Delta M(t) > 0 \\ M(t) \leq MA(t) \text{ and } \Delta M(t) < 0 \end{array} \} \text{ then the relationship is plastic}$$
 (20)

where

- $M(t)$  : total bending moment at time  $t$
- $MA(t)$  : upper yield bending moment at time  $t$
- $MB(t)$  : lower yield bending moment at time  $t$ , and
- $\Delta M(t)$  : the last incremental bending moment prior to time  $t$ .

Inherent in this procedure are the phenomena of "overshooting" the yield limit upon entering the nonlinear state and "backtracking" upon returning to the linear state. This results from the demand that the state of stress remain constant throughout the time increment.

When the relationship is elastic at end (i) and/or end (j) the corresponding incremental plastic angle must be zero

at end (i),  $\Delta\alpha_i = 0$

and/or at end (j),  $\Delta\alpha_j = 0$ . (21)

When the relationship is plastic at end (i) and/or end (j) the corresponding incremental bending moment is proportional to the incremental plastic angle

at end (i)  $\Delta M_i = f_i k \Delta\alpha_i$

and/or at end (j)  $\Delta M_j = f_j k \Delta\alpha_j$  (22)

where  $f_i$  and  $f_j$  are independent.



Since  $f_i$  and  $f_j$  are independent, it is possible to use a curvilinear hysteresis loop with this model.

Since a linear or nonlinear state can exist for each joint, there are four possible combinations for each member. These states, denoted by (a), (b), (c) and (d) are described below:

State (a): Elastic at (i) and (j)

$$\Delta\alpha_i = 0 \quad \Delta\alpha_j = 0 \quad (23)$$

State (b): Plastic at (i) elastic at (j)

$$\begin{aligned} \Delta M_i &= f_i k \Delta\alpha_i \\ \Delta\alpha_j &= 0 \end{aligned} \quad (24)$$

State (c): Elastic at (i) plastic at (j)

$$\begin{aligned} \Delta\alpha_i &= 0 \\ \Delta M_j &= f_j k \Delta\alpha_j \end{aligned} \quad (25)$$

State (d): Plastic at (i) and (j)

$$\begin{aligned} \Delta M_i &= f_i k \Delta\alpha_i \\ \Delta M_j &= f_j k \Delta\alpha_j \end{aligned} \quad (26)$$

The functional dependencies of the incremental plastic angles on rotations are as follows:

$$\text{State (a): } \Delta\alpha_i = 0 \quad \Delta\alpha_j = 0 \quad (27)$$

$$\text{State (b): } k[(\Delta\omega_i - \Delta\alpha_i) + \frac{1}{2}\Delta\omega_j] = f_i k \Delta\alpha_i$$

Hence

$$\begin{aligned} \Delta\alpha_i &= \left(\frac{1}{1+f_i}\right) (\Delta\omega_i + \frac{1}{2}\Delta\omega_j) \\ \Delta\alpha_j &= 0 \end{aligned} \quad (28)$$

State (c): replacing i and j

$$\Delta\alpha_i = 0 \quad (29)$$

$$\Delta\alpha_j = \frac{1}{1+f_j} \left( \frac{1}{2}\Delta\omega_i + \Delta\omega_j \right)$$

$$\text{State (d): } k[(\Delta\omega_i - \Delta\alpha_i) + \frac{1}{2}(\Delta\omega_j - \Delta\alpha_j)] = f_i k \Delta\alpha_j$$

$$k\left[\frac{1}{2}(\Delta\omega_i - \Delta\alpha_i) + (\Delta\omega_j - \Delta\alpha_j)\right] = f_j k \Delta\alpha_j$$

Rearranging and solving for  $\Delta\alpha_i$  and  $\Delta\alpha_j$

$$\Delta\alpha_i = \frac{(1 + \frac{4}{3}f_j)\Delta\omega_i + \frac{2}{3}f_j\Delta\omega_j}{1 + 4/3(f_i + f_j + f_i f_j)} \quad (30)$$

$$\Delta\alpha_j = \frac{2/3 f_i \Delta\omega_i + (1 + \frac{4}{3} f_i) \Delta\omega_j}{1 + 4/3(f_i + f_j + f_i f_j)}$$

By substitution the  $\Delta\alpha$ 's can be eliminated from the incremental moment-rotation equations

$$\begin{aligned} \text{State (a): } \Delta M_i &= k[\Delta\omega_i + \frac{1}{2}\Delta\omega_j] \\ \Delta M_j &= k[\frac{1}{2}\Delta\omega_i + \Delta\omega_j] \end{aligned} \quad (31)$$

$$\begin{aligned} \text{State (b): } \Delta M_i &= \left(\frac{f_i}{1+f_i}\right)k(\Delta\omega_i + \frac{1}{2}\Delta\omega_j) \\ \Delta M_j &= k\left[\frac{1}{2}\left(\frac{f_i}{1+f_i}\right)\Delta\omega_i + \frac{3+4f_i}{4(1+f_i)}\Delta\omega_j\right] \end{aligned} \quad (32)$$

$$\begin{aligned} \text{State (c): } \Delta M_i &= k\left[\frac{3+4f_j}{4(1+f_j)}\Delta\omega_i + \frac{1}{2}\left(\frac{f_j}{1+f_j}\right)\Delta\omega_j\right] \\ \Delta M_j &= \left(\frac{f_j}{1+f_j}\right)k\left[\frac{1}{2}\Delta\omega_i + \Delta\omega_j\right] \end{aligned} \quad (33)$$

$$\begin{aligned} \text{State (d): } \Delta M_i &= \frac{f_i k [1 + \frac{4}{3} f_j] \Delta \omega_i + \frac{2}{3} f_j \Delta \omega_j}{1 + \frac{4}{3} (f_i + f_j + f_i f_j)} \\ \Delta M_j &= \frac{f_j k [\frac{2}{3} f_i \Delta \omega_i + (1 + \frac{4}{3} f_i) \Delta \omega_j]}{1 + \frac{4}{3} (f_i + f_j + f_i f_j)} \end{aligned} \quad (34)$$

Since the incremental bending moment-end rotation equations have a regular pattern for all four states, the following matrix equations using "effective stiffness" parameters  $S_A$ ,  $S_B$  and  $S_C$  can be established

$$\begin{Bmatrix} \Delta M_i \\ \Delta M_j \end{Bmatrix} = \begin{bmatrix} S_A & S_B \\ S_B & S_C \end{bmatrix} \begin{Bmatrix} \Delta \omega_i \\ \Delta \omega_j \end{Bmatrix} \quad (35)$$

where

	$S_A$	$S_B$	$S_C$
State (a)	$k$	$\frac{1}{2} k$	$k$
State (b)	$\frac{f_i}{1+f_i} k$	$\frac{1}{2} \frac{f_i}{1+f_i} k$	$\frac{3+4f_i}{4(1+f_i)} k$
State (c)	$\frac{3+4f_j}{4(1+f_j)} k$	$\frac{1}{2} \frac{f_j}{1+f_j} k$	$\frac{f_j}{1+f_j} k$
State (d)	$\frac{f_i (1 + \frac{4}{3} f_j)}{D} k$	$\frac{\frac{2}{3} f_i f_j}{D} k$	$\frac{f_j (1 + \frac{4}{3} f_i)}{D} k$

where  $D = 1 + \frac{4}{3} (f_i + f_j + f_i f_j)$

For the bilinear hysteresis loops, which are used here,  $f_i = f_j = f$ . As a result the effective stiffnesses can be simplified as

	$S_A$	$S_B$	$S_C$
State a	$k$	$\frac{1}{2} k$	$k$
State b	$\frac{f}{1+f} k$	$\frac{1}{2} \frac{f}{1+f} k$	$\frac{3+4f}{4(1+f)} k$

$$\begin{array}{l}
 \text{State c} \quad \frac{3+4f}{4(1+f)} k \quad \frac{1}{2} \frac{f}{1+f} k \quad \frac{f}{1+f} k \\
 \text{State d} \quad \frac{f(1+\frac{4}{3}f)}{D} k \quad \frac{\frac{2}{3}f^2}{D} k \quad \frac{f(1+\frac{4}{3}f)}{D} k
 \end{array}$$

where  $D = 1 + \frac{4}{3} f(2+f)$

To draw an exact two-dimensional hysteresis loop, for either end of a beam, it is necessary to have the same functional relationship between the bending moment and the curvature for all states.

Taking one typical member of the frame under consideration, and taking into account that, due to symmetry, either state (a) or state (d) exists, we can write

$$\text{State (a)} \quad \Delta M_i = \Delta M_j = \Delta M = \frac{3}{2} k \Delta \omega \quad (36)$$

$$\begin{aligned}
 \text{State (d)} \quad \Delta M_i = \Delta M_j = \Delta M &= \frac{f(1+2f)k\Delta\omega}{1 + \frac{4}{3} f(2+f)} \\
 &= \Delta M = \frac{f}{(1 + \frac{2}{3}f)} k\Delta\omega \quad (37)
 \end{aligned}$$

$$= 3/2(\frac{f}{f+3/2}) k\Delta\omega$$

If we let  $\frac{f}{f+1.5} = p$  we can rewrite the above two equations as

$$\text{State (a)} \quad \Delta M = \frac{3}{2} k\Delta\omega \quad (38)$$

$$\text{State (d)} \quad \Delta M = \frac{3}{2} p k\Delta\omega$$

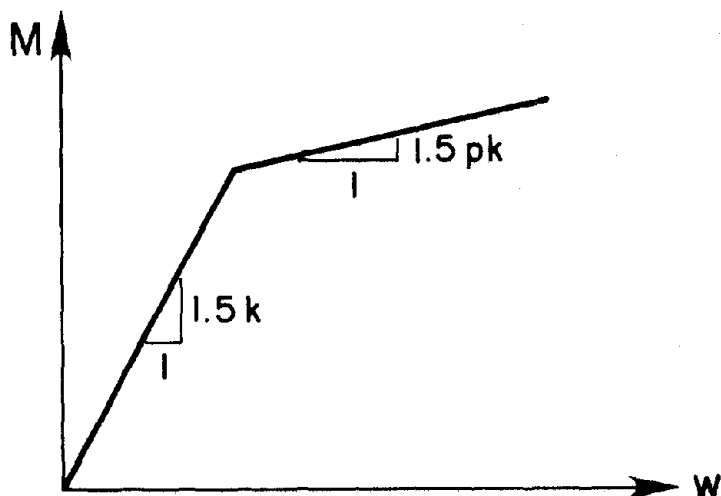


FIGURE 9 DEFINITION OF THE "p" PARAMETER

Thus  $p$  can be considered as the ratio of the plastic slope of the  $M$ - $\omega$  diagram to its elastic slope (Fig. 9).

### 3.3 Rotations of the Joints

One of the significant findings of our study involving the formulation of linear models, Ref. [1], was the determination of the response data that are effective in formulating a model which accommodates both floor translations and joint rotations. We found that the most effective set of responses consisted of the floor acceleration and joint rotation time histories. It follows that the same set of response quantities should be used here in formulating the nonlinear models. The problem for constructing both types of models is that, whereas the acceleration time histories were recorded directly, the joint rotation time histories have to be calculated from other response data. For the linear response this was not particularly difficult. We were able to take the strain readings at the stations where they were recorded, calculate the  $M/EI$  (or  $1/\rho$ ) at that station and extrapolate linearly to the base of the lower

column and to the center of a joint, see Fig. (10). The areas of these diagrams represent the change in rotation between the ends of a column and, assuming the rotation of the column at the base to be zero, we moved upward column by column calculating the rotations of each of the joints. The only error that we felt could be introduced would be in not accounting for the change in the moment of inertia of the column at the base due to the gusset plates. We felt that this would have an insignificant effect and so we had confidence in the joint rotations that we used as response quantities.

We are on shakier ground in calculating the rotations with the response quantities available for the nonlinear response. To understand the problem we must recall the instrumentation of the columns. In Fig. (11) we see that at the base there is an LVDT at A" and strain gages at A', B', B'', etc. (see Fig. (10)). If yielding occurs, it will be first at the base and then at the joints both above and below, with diminishing possibility as we move upward.

We will illustrate the difficulty for the nonlinear response by finding the rotation of the joint at B by studying the column AB. We assume that the bottom of the column at A does not rotate, so that the rotation of joint B is its rotation relative to A.

Of prime importance is the fact that we have the LVDT reading at A" which gives the relative rotation of A" to that of A. All we need in addition then are the relative rotations of the column at B and A". To complete this accurately we would need the M/EI diagram from B to A". We do not have all of it, but we have the major part.

Strain readings at B' and A' show that the moments at these points correspond to a linear state of stress, so that the linear distribution

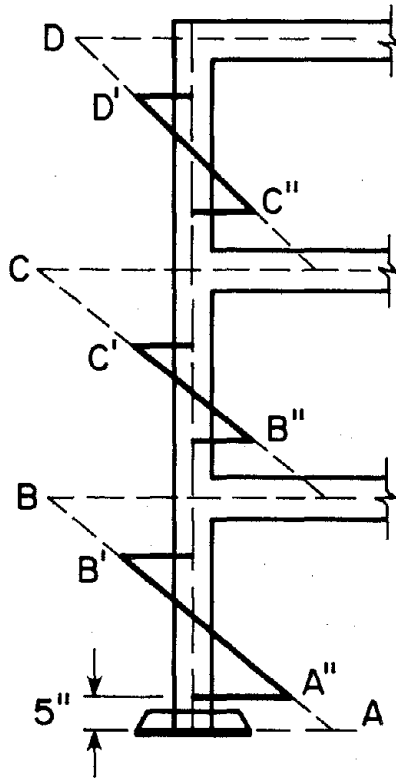


FIGURE 10 ROTATION CALCULATION OF JOINTS (LINEAR CASE)

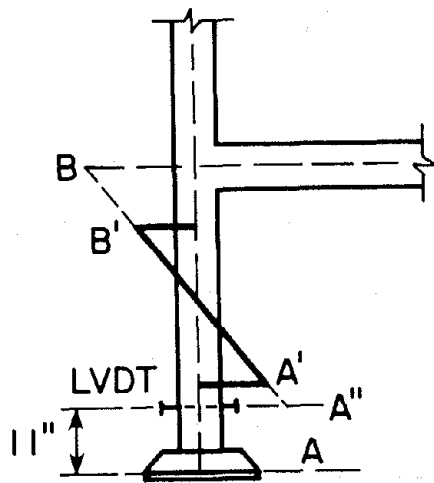


FIGURE 11 ROTATION OF CALCULATION OF JOINT B (NONLINEAR CASE)

of bending moment between A' and B' shown in Fig. 11 is correct. We are left with two missing pieces of the moment diagram to complete our calculation of the relative rotations at B and A". The part from B' to B and the part from A' to A". We must extrapolate the moment diagram in some way to cover these two pieces. As the response of the frame was only mildly nonlinear, and because in a region of nonlinearity we do not know the extent of yielding and how to extrapolate accurately, we decided to calculate the rotations by extrapolating linearly as indicated in Fig. 11. The same method was used for the upper columns. We do not think that the error thus introduced is serious.

The resulting joint rotation time histories were used in the error function in formulating the model. The model derived should then predict the calculated rotation time histories (as we shall find that it does). The rub comes when we try to interpret the parameters of the model physically. Six of the parameters introduced into the stiffness matrix are the effective length factors associated with each of the three columns and the three beams. We will, in fact, find that they differ from those found for the linear model. Because of the analysis which we have just presented, we place more credence on the physical interpretation of the effective length factors associated with the linear model than those derived here.

If we were to design and perform the experiments again we could arrange to place an array of strain gages above the LVDT and above and below each girder. Better still would be gages placed at the juncture of beams and columns that would directly record rotation time histories.



### 3.4 The Computer Program

In this section the computer program used to implement the programs outlined in the previous sections is described. Much of the program is the same as was used for the linear model and so will be described only briefly. The part that is new, involving the complications due to the nonlinear behavior, is dealt with in more detail. The description ends with a complete flow chart for the program (Fig. 12).

The program consists of the program OPTIM and eleven subroutines. Control always returns to OPTIM at which time numerous checks are performed and decisions made as to whether to continue or stop a process.

Subroutine ONE reads in all of the input data, which consists of the ground acceleration time histories  $\ddot{u}_g(t)$ , the nodal masses, the measured quantities which enter into the error function i.e. relative floor accelerations  $\ddot{y}_j(t)$  and nodal rotations  $\theta_j(t)$ , the initial set of parameters  $\bar{\beta}_1$ , the duration of the excitation or a portion of it denoted by T, the maximum number of iterations in a given line search,  $k_{max}$ , the maximum number of cycles allowed in the program,  $i_{max}$ , and the program stopping tolerance (PST).

Subroutine TWO sets up at each time increment the nxn translational stiffness matrix [K] and forms the damping matrix. While setting up [K], this subroutine is in direct communication with another subroutine (CHECKM), which checks the values of the moments at the ends of all members, decides on the state of yield for each particular member using the criteria defined in Eq.(20) and accordingly chooses the proper values for  $S_A$ ,  $S_B$  and  $S_C$  in Eq.(35) for each member. With this information provided by CHECKM, subroutine TWO sets up the translational stiffness matrix [K] by the usual procedure of setting up the total stiffness matrix and then condensing it according to the classical

structural analysis approach.

Subroutine THREE includes the solution of Eq.(1), for the particular time step  $n$ , and the given set of parameters  $\bar{\beta}$  by the linear acceleration method, and yields the incremental and cumulative values of all quantities such as displacements, velocities, accelerations, rotations and moments at all floor levels and at the ends of all members.

From THREE control returns to TWO with  $n=n+1$  and the same procedure is continued until  $n$  reaches  $n_{\max}$  the maximum number of time steps to be considered between  $t=0$  and  $t=T$ .

Subroutine FOUR evaluates the error function  $J(\bar{\beta}_i, T)$  while routines FIVE and SIX evaluate the terms in the gradient vector  $\nabla J(\bar{\beta}_i, T)$  and the approximate Hessian matrix  $\overline{AH}(\bar{\beta}_i, T)$ , respectively. These terms are evaluated using finite differences calling upon subroutines TWO and THREE for the solution of Eq.(1) with all coefficients kept constant except for  $\beta_p$  which is increased by  $\Delta\beta_p$ .

Subroutine SEVEN evaluates the inverse of the approximate Hessian  $\overline{AH}(\bar{\beta}_i, T)^{-1}$ , while EIGHT evaluates the direction vector

$$\bar{d}_i = - \left[ \overline{AH}(\bar{\beta}_i, T) \right]^{-1} \nabla J(\bar{\beta}_i, T)$$

and the initial slope

$$J'(\alpha, T) \Big|_{\alpha=0} = \nabla J(\bar{\beta}_i, T) \bar{d}_i$$

At this stage OPTIM checks the value of  $J'(\alpha, T) \Big|_{\alpha=0}$  against the program stopping tolerance. If the slope is too large, routine NINE is called to perform the line search. With  $k=1$  and  $\alpha_k=0.1$  it evaluates

$$\bar{\beta}_{i+1} = \bar{\beta}_i + \alpha_k \bar{d}_i$$

and

$$J(\bar{\beta}_{i+1}, T)$$

The procedure is repeated until  $k=10$  and  $\alpha_k=1.0$ . The value for  $\alpha_k$  which yields the smallest value for the error function  $J$ , is considered to be the proper step size within this particular line search, and the corresponding  $\bar{\beta}_{i+1}$  set of coefficients is taken as the initial set of values for the next cycle of the process.

The process is repeated for a number of cycles until within OPTIM the requirement

$$\left. \frac{dJ(\alpha, T)}{d\alpha} \right|_{\alpha=0} < \text{program stopping tolerance is met.}$$

If the program stopping tolerance is set to a very small value it may very well be that, due to the particular conditions of the model used and for reasons previously discussed in detail, for the new cycle the error is not smaller than the error for the previous cycle. This is checked within subroutine TEN.

If either one of the conditions above occur, subroutine ELEVEN is called to print as output the final value of the error, the final set of coefficients  $\bar{\beta}$ , the final predicted displacements, accelerations, rotations and moments and also the corresponding measured input quantities.

A flow chart of the identification program is given in Fig. 12.

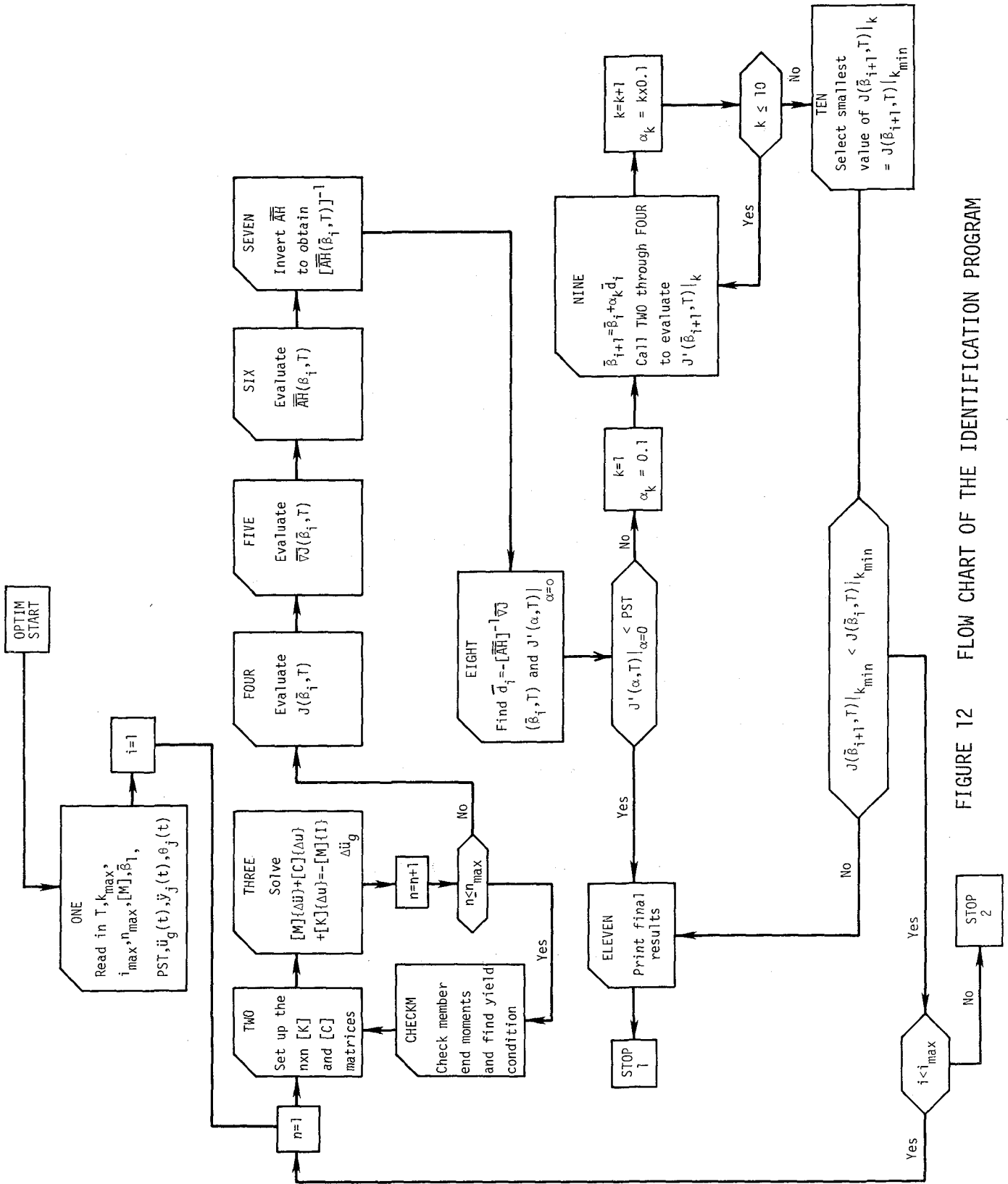


FIGURE 12 FLOW CHART OF THE IDENTIFICATION PROGRAM

CHAPTER 4  
FORMULATION OF MODELS

When the form of the equations has been chosen, as it was in Chapter 3, there still remain many decisions that have to be made before the formulation is complete. In the form there are damping and stiffness matrices, but their details have not been studied. By this we mean that it remains for us to decide how many parameters should be introduced into each matrix, what will be their method of introduction and finally, of the array of parameters, how many will be assigned fixed sensible values, and how many will be free to change and be established by the optimization algorithm. These decisions are made twice in this chapter, as we formulate two separate models. The reasons for the different choices will be presented when the choices are made.

We benefit enormously in this chapter from our formulation of the linear models. Most of the decisions that we make are derived from our previous study. First, we found that for damping, Rayleigh type viscous damping is appropriate, which introduces two parameters into the system according to  $[C] = a_0 [M] + a_1 [K]$ . We found that response predictions are accurate only when the model accommodates both floor translations and joint rotations. We also found that the best way of introducing the parameters for the linear case was to associate a parameter with the stiffness of each of the members of the frame. Because the frame is symmetrical, there are only six independent stiffnesses resulting in the introduction of six parameters. We made the discovery that these parameters gave physical insight into the behavior of the frame when each parameter was associated in the expression for

stiffness  $EI/L$  with the  $L$ , so that the parameters become effective length coefficients. The physical insight gained by this arrangement is not as effective as it was for the linear case, which was explained in Section 3.3, but it will be used again here as it is still effective. The assignment of these six parameters is clarified by an examination of Fig. (13).

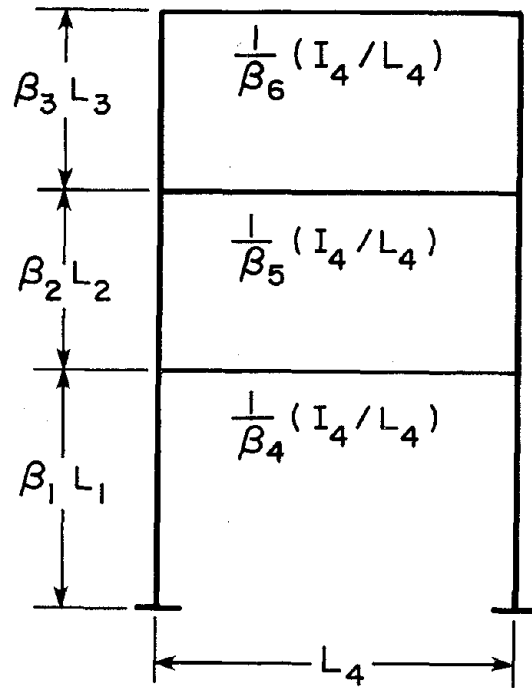


FIGURE 13 EFFECTIVE LENGTH PARAMETERS

With this type of introduction of the parameters a 6x6 matrix is formed and then condensed into a 3x3 matrix by the usual practice. The individual stiffnesses appear in the 3x3 matrix in each of the elements in a somewhat complicated way.

It still remains to extend the linear model to the nonlinear for our bilinear formulation. To gain physical insight into the structure we formulate two separate models. As we handle the nonlinear parameters somewhat differently for each of the two models, we leave a discussion of their introduction to the sections devoted to the models.

#### 4.1 The First Nine Parameter Model

At this point in the development we have introduced eight parameters, two in the damping matrix, and six in the stiffness matrix. We now turn our attention to the additional parameters needed to accommodate the nonlinear relationship between bending moment and rotation for each of the members. For this refer again to Fig. (9). To completely identify the  $M-\omega$  relationship we need two additional parameters for each member. First is the ratio of the slope after yield to the slope before yield which involves "p", or "f" when we recall that  $p = f/(f+1.5)$ . We expect that the parameter "f" will be significant in the accuracy of the model.

The second is the yield moment. We recognize that for the global behavior of the member, the bilinear model is not accurate in that the true hysteretic behavior would appear with a rounded "knee" extending from the beginning of yield  $M_A$  to  $M_B$  where it meets the yield slope. A single yield moment indigenous to the bilinear global model can be thought of as the average of these two moments.

Another factor that would modify those values is the presence of dead load moments. Those moments, which are constant and can accurately be computed, are always of the same sign thus implying that if only lateral loads are to be considered,  $M_A$  and  $M_B$  should be taken differently. Although it has been stated previously that the dead load stresses are kept small in the test frame, it is hard to make any precise statement as to the values that  $M_A$  and  $M_B$  should take for each member.

Thus it is decided to set  $M_A$  equal to  $M_B$  (now called  $M_A$ ) and also to assume, since the section properties for all columns are identical, that one additional parameter in the identification process can define a proper value for the yield moment of the columns. The same applies

for the girders and a ninth parameter is introduced to define the yield moment value for the girders.

To keep the values of all  $\bar{\beta}$  parameters of the same order of magnitude the three nonlinear parameters are taken as

$$f = 0.166 \times \beta_7 ; \quad MA|_{col} = 325 \times \beta_8 \text{ k.in} ; \quad MA|_{gir} = 275 \times \beta_9 \text{ k.in}$$

Thus with  $\beta_7$  equal to 1,  $f$  becomes 0.166, corresponding to a ratio of 0.1 of the second to the first slope of the  $M-\omega$  relationship for the girders. With  $\beta_8$  and  $\beta_9$  equal to 1, the upper yield moment values for columns and girders are 325 k.in and 275 k.in, respectively, which correspond to the yield moment values computed on the basis of section properties minus the dead load moments.

We now have introduced eleven parameters. Undoubtedly the best model would be the one for which we allow all eleven parameters to vary and be established by optimization. However, the computer costs and memory requirements needed for optimization rise quickly as the number of parameters increases. For this reason we decide here to fix two of the parameters before optimization allowing only nine of the eleven to be free to change.

In this first model we decide to fix  $a_0$  and  $a_1$ , the damping parameters, giving them the values that we found for them after optimization in the linear, eight parameter model. This decision is based on the experience gained by McNiven and Matzen [2] in formulating a nonlinear model for the behavior of a single-story steel frame. In that study it was found that the hysteretic material behavior accounted for the major part of the nonlinear response, with the damping parameter changing little during optimization from the value it assumed for the linear model. This characteristic is confirmed by preliminary study of this model where



we found that changing the values of  $a_0$  and  $a_1$  by as much as 15% changes the final model very little.

With the selection of the form for the model, the parameters contained in the model and the way in which they are introduced into it, and the values for two of the parameters, it only remains to establish values for the other nine parameters to complete the model.

We review here, very briefly, the identification process along with some of the problems we found which might not be anticipated. First, the governing set of differential equations must be solved, Eq. (1), and to this end we write in the incremental form:

$$[M] \{\Delta\ddot{u}\} + [C] \{\Delta\dot{u}\} + [K] \{\Delta u\} = - [M] \{I\} \Delta\ddot{u}_g$$

The matrix M is known as is the C matrix. The formulation of the K matrix begins by assigning beginning values to the parameters  $\beta_1$ - $\beta_6$ , the effective length parameters. Having expressions for the stiffness of each of the members we construct the six by six stiffness matrix and condense it into a three by three translational matrix. Each of the elements of this matrix can change according to whether a member is in an elastic state, or a yield state. For this step of the integration we assume an elastic state so that we derive  $\{\Delta u\}$ ,  $\{\Delta\dot{u}\}$  and  $\{\Delta\ddot{u}\}$  from the solution. Having these, the incremental rotations and consequently the incremental end moments are obtained, completing the first step. From then on, having the defined values for the upper and lower yield moments of the columns and girders and also the coefficient f, subroutine CHECKM checks the values of the moments at the ends of all members and decides on the state of stress of each member at the beginning of the next time step of integration.  $S_A$ ,  $S_B$  and  $S_C$  from Eq.(35) are accordingly identified for each member and the procedure continues up to time step  $n_{\max}$  which corresponds to the upper limit of integration T. At the end of each time

step the incremental values obtained for each quantity are superimposed to their previous values to obtain the cumulative values of the same quantities as given by Eq. (2).

We found a minor problem in optimization. It is necessary to calculate the inverted approximate Hessian matrix. Without caution this can be singular or near singular causing problems. The sensitivity coefficients for the member end moments are found using finite differences. These involve the sensitivity of parameters  $\beta_8$  and  $\beta_9$  and these can be zero, or close to it due to overshooting the yield moment upon entering the nonlinear state and backtracking to return to the elastic state. This situation is aggravated when the number of excursions into the yield state is small, which is the situation we have here. We were forced to make numerous trials to ascertain appropriate increments to use for  $\beta_8$  and  $\beta_9$  to avoid a singular matrix and found that an increment in the range of 0.05 which corresponds to a change in the moment of approximately 15 k.in is a good choice. The increments for the other parameters are kept to much smaller values of the order of 0.001.

We also noticed that  $\beta_7$  tends towards much larger values than expected. Consistently  $f$  tends towards a value of approximately 3 which corresponds to a ratio of second to first slope in the  $M-\omega$  diagram for the members of the order of 0.5. An investigation of the true hysteresis loops proves this to be reasonable. We concluded that the excitations we are dealing with are mildly nonlinear and a ratio of second to first slope of the order of 0.5 does make sense. Unfortunately even with the excitations which are known to be the strongest in Clough and Tang's work [ 5 ], the situation remains practically unchanged meaning that only mildly nonlinear data are available.  $f$  was then

changed to  $f=1.666x\beta_7$  for more consistent results.

The values of the parameters that result for this program and the assessment of the resulting nonlinear model are presented in the next chapter.

#### 4.2 The Second Nine-Parameter Model

As we will find in the next chapter, the first nine-parameter model predicts very accurately the nonlinear response of the frame, and to two different seismic disturbances. The need for an additional model seems open to question. The purpose of mathematical modeling, however, is not only that of predicting response but of helping to gain insight into the characteristics of the physical system. It is to this second end that this additional model is constructed.

For the first model we decided to fix the values of the damping parameters. Though there is evidence to support this decision, it is by no means conclusive and there is in fact evidence in opposition. From a study of the response of the single story steel frame, Rea, Clough and Bouwkamp [11] report that they found the viscous damping is amplitude dependent. In this second model we free the damping parameters from their linear model values and let them change to values established by optimization. Comparison of the effectiveness of the two models should help us to ascertain the influence that these two parameters exert in describing the response.

As first suggested, the damping matrix has the form

$$[C] = a_0 [M] + a_1 [K]$$

By retaining this form and by using the fixed values of Model 1 as the starting values we can trace the changes during identification.

We are now in the same position as we were in completing the formulation of the first model. We could include  $a_0$  and  $a_1$  in the array of

parameters simply by increasing the number from nine to eleven. Increasing the number of parameters will improve the model but not always dramatically while the computer time required and the memory requirements increase considerably. From a preliminary study, we can state with confidence that introduction of  $a_0$  and  $a_1$  as parameters will affect the optimum values of the yield moments obtained in Model 1 very little. Thus instead of changing to an eleven parameter model we decide to keep the number of parameters at nine. The yield moment values for columns and girders will be kept constant while  $a_0$  and  $a_1$  will be taken as the new eighth and ninth parameters of the system. This requires very simple modifications of the computer program.

Thus in Model No. 2, parameters  $\beta_1$  through  $\beta_7$  have the same meaning as before while  $\beta_8$  and  $\beta_9$  are now defined to be

$$a_0 = 0.2340 \times \beta_8 \text{ and } a_1 = 0.0003 \times \beta_9.$$

The values for the constant terms in  $a_0$  and  $a_1$  are taken to be those assigned in the first model.

## CHAPTER 5

### COMPLETION AND PERFORMANCES OF THE MATHEMATICAL MODELS

This Chapter is divided into four parts. It is first divided in two in which each half is devoted to each of the two nine parameter models denoted in the chapter as Models No. 1 and 2. Each type of model is further divided by developing models generated by the data from two separate seismic disturbances. The first is the actual historical El Centro earthquake (EC-900II), and the second, the modified El Centro (MEC-600II).

In each of the four parts we first present results of the numerical program. This ends with values of the nine parameters. These values, combined with the two fixed parametric values, completes each model. These values are presented in tables, and study of the tables shows that the final acceptable set (representing the global minimum on the error surface) requires very few steps in the search. This circumstance resulted, not because the surface representing the error function is particularly well behaved, but because we started each search with an accurate set. For this we credit the study already completed in constructing the linear model.

The expression for the error function reveals that the error depends on the upper limit of the integral "T". This can represent the full duration of the excitation or some fraction of it. For the sake of economy we choose to establish our parameters using only the first six seconds of each excitation. The implications of this are discussed in the next chapter.

The second part of this chapter consists of presenting evidence which displays the performance of each mathematical model. This

evidence is in the form of the time histories of various response quantities. We present a sufficient number of these to assess the quality of each model. In each time history the physical response is represented by a solid line, whereas the comparable response predicted by the model is shown dashed.

5.1 MODEL NO. 1: EC-900II

	Starting Values of Parameters*	End of First Cycle	End of Second Cycle	End of Third Cycle	End of Fourth Cycle	End of Fifth Cycle
$\beta_1$	0.956	1.035	1.077	1.084	1.084	1.084
$\beta_2$	0.971	0.985	1.004	1.050	0.044	1.034
$\beta_3$	0.891	0.889	0.886	0.872	0.875	0.877
$\beta_4$	1.242	1.184	1.085	1.096	0.096	1.127
$\beta_5$	1.274	1.216	1.078	1.055	1.057	1.058
$\beta_6$	1.322	1.121	1.078	1.103	1.106	1.107
$\beta_7$	1.000	1.197	1.242	1.231	1.224	1.223
$\beta_8$	1.000	1.041	1.049	1.050	1.051	1.052
$\beta_9$	1.000	1.103	1.122	1.127	1.130	1.133
Error	225606	73163	32367	23561	20097	18081
Extrapolated Error to T=10 sec.						52078
*From the eight parameter linear model derived from EC400-II						

TABLE 3 CHANGE IN PARAMETERS AND REDUCTION IN ERROR DURING A TYPICAL RUN

	Initial Values		Final Values	
	$\beta$	$\beta \times \text{Constant}$	$\beta$	$\beta \times \text{Constant}$
$\beta_1$ vs. $\beta_1 L_1$	0.956	76.48 in	1.084	86.72 in
$\beta_2$ vs. $\beta_2 L_2$	0.971	62.15 in	1.034	66.17 in
$\beta_3$ vs. $\beta_3 L_3$	0.891	57.85 in	0.877	56.13 in
$\beta_4$ vs. $\beta_4 L_4$	1.242	178.85 in	1.127	162.29 in
$\beta_5$ vs. $\beta_5 L_5$	1.274	183.46 in	1.058	152.35 in
$\beta_6$ vs. $\beta_6 L_6$	1.322	190.37 in	1.107	159.41 in
$\beta_7$ vs. f	1.000	1.66	1.223	2.04
$\beta_8$ vs. $MA _{col.}$	1.000	325 k.in	1.052	341.90 k.in
$\beta_9$ vs. $MA _{gir.}$	1.000	275 k.in	1.133	311.57 k.in
$a_0$ (kept constant)	0.574 x 0.2340 = 0.134			
$a_1$ (kept constant)	0.612 x 0.0003 = 0.00018			

TABLE 4 COMPARISON OF INITIAL VERSUS FINAL PARAMETERS

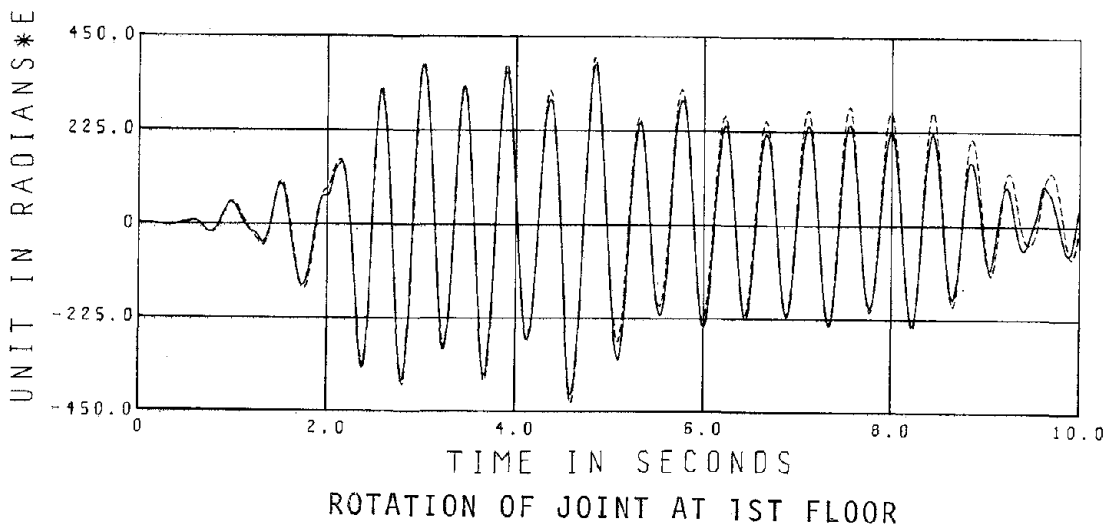
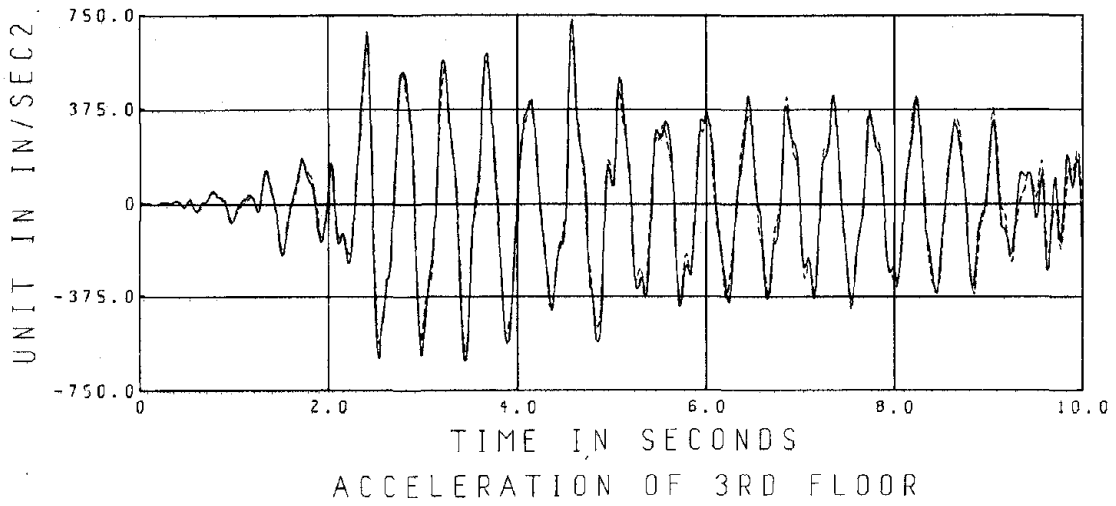
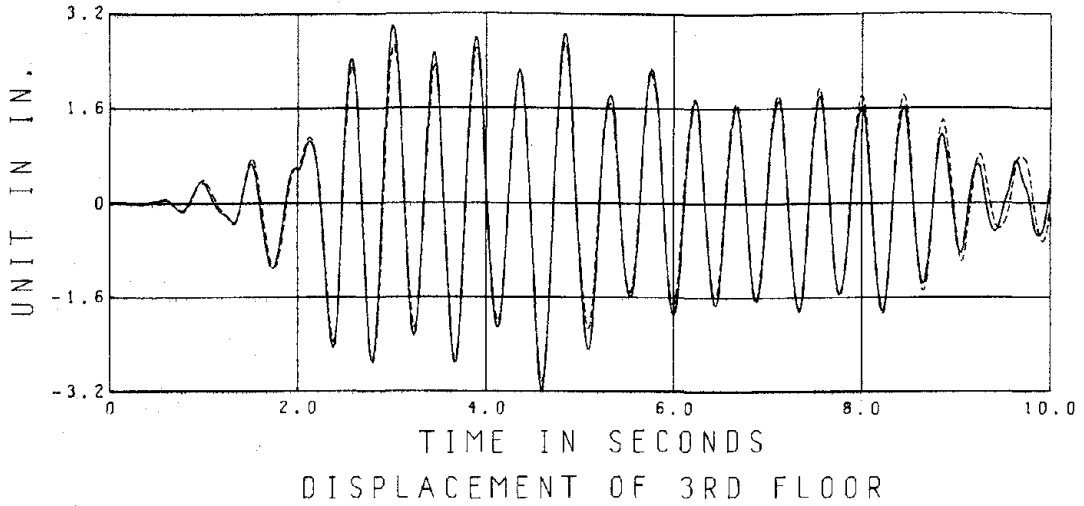


FIGURE 14 CORRELATION OF MEASURED VERSUS PREDICTED RESPONSES



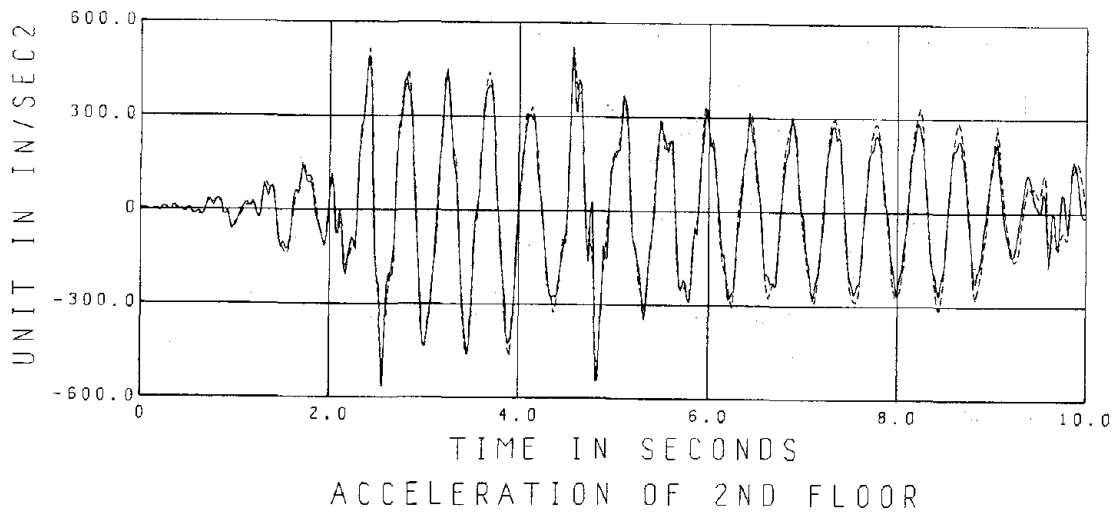
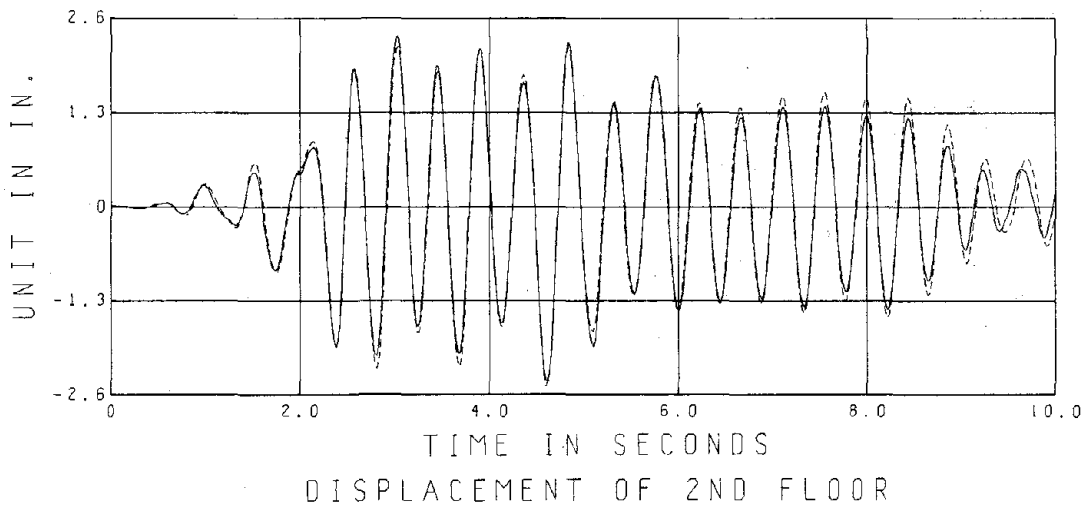
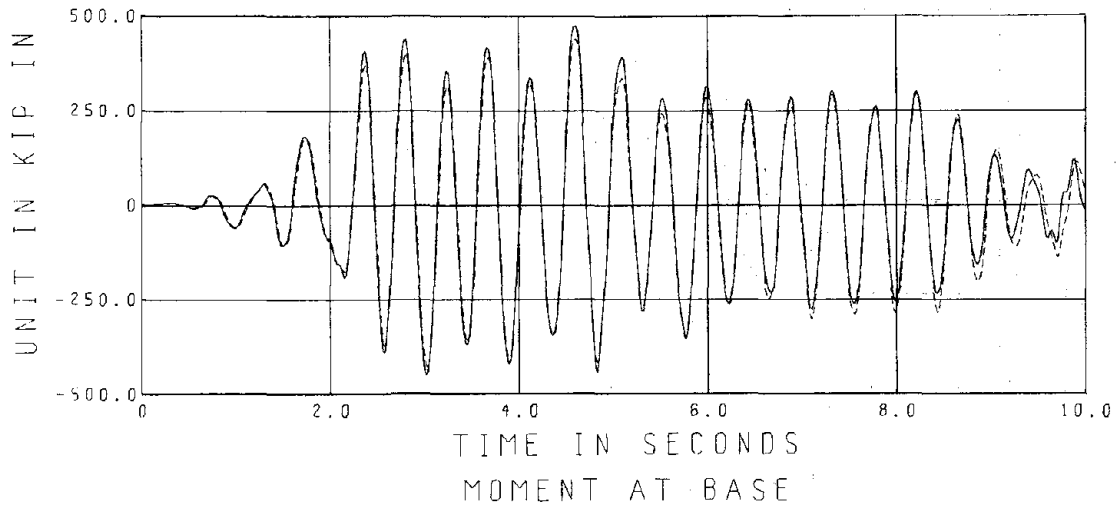


FIGURE 15 CORRELATION OF MEASURED VERSUS PREDICTED RESPONSES

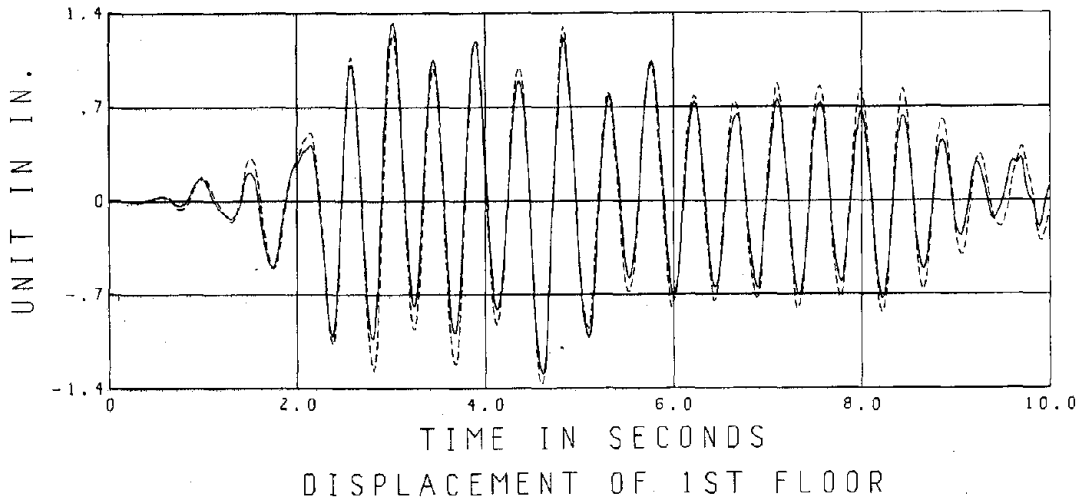
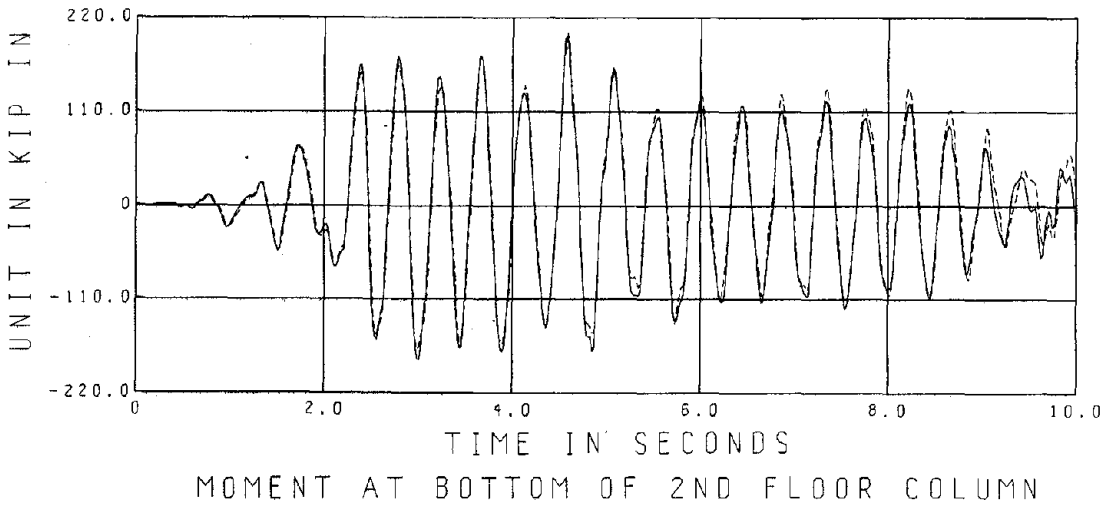
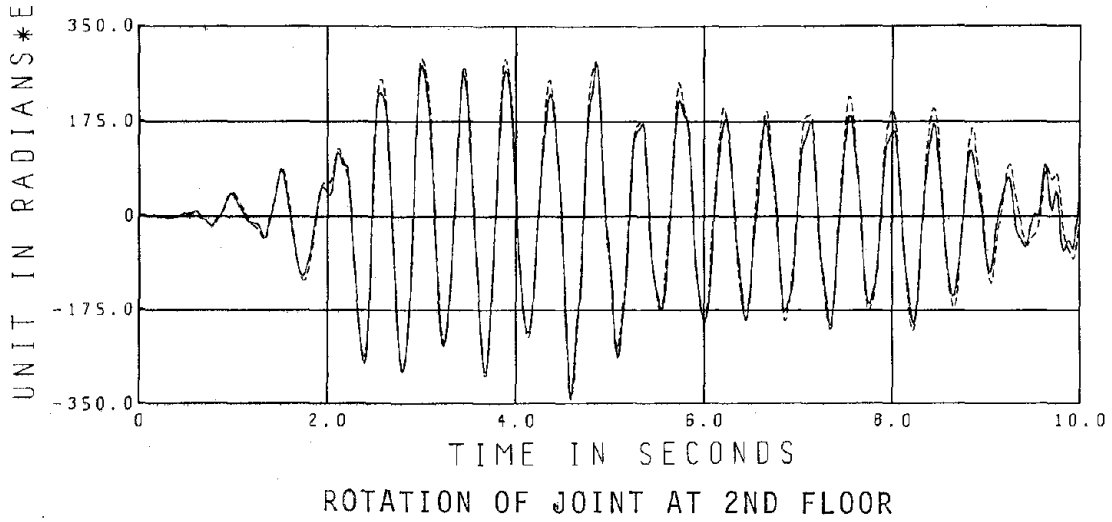


FIGURE 16 CORRELATION OF MEASURED VERSUS PREDICTED RESPONSES

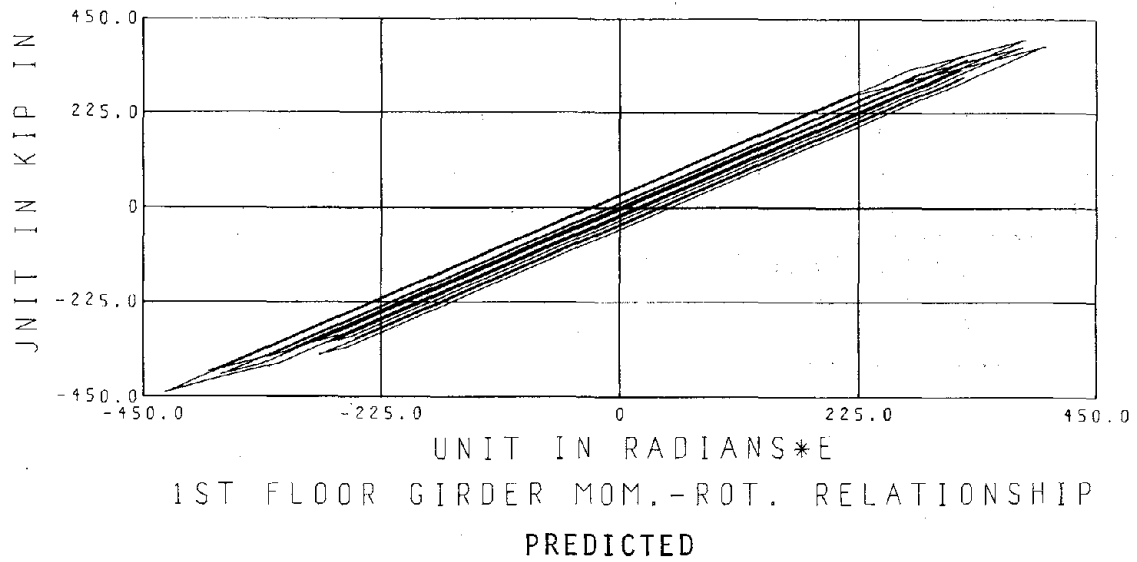
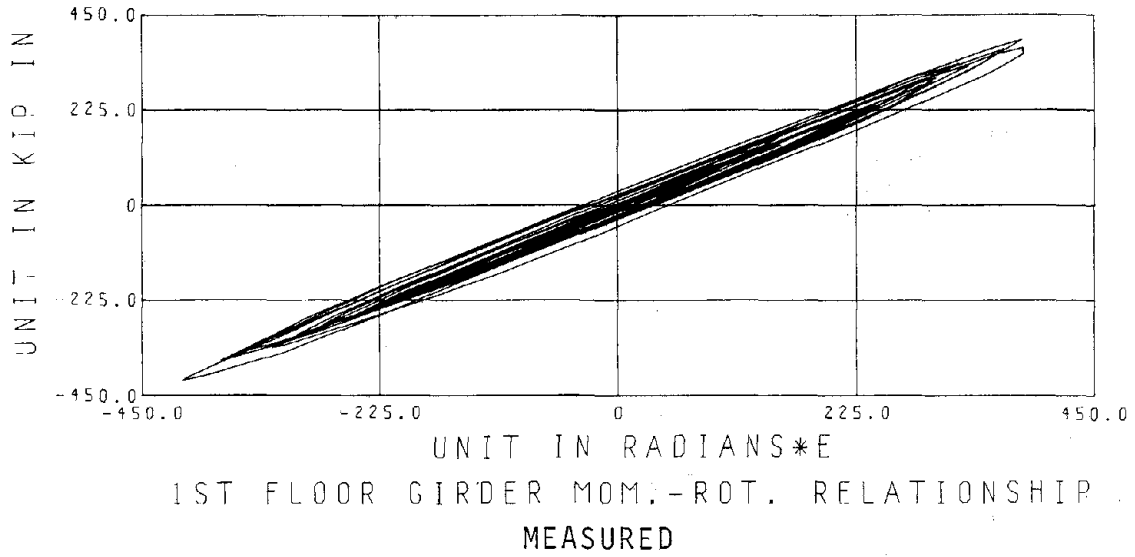


FIGURE 17 MEASURED AND PREDICTED HYSTERETIC BEHAVIORS

5.2 MODEL NO. 1: MEC-600II

	Starting Values of Parameters*	End of First Cycle	End of Second Cycle	End of Third Cycle	End of Fourth Cycle
$\beta_1$	1.084	1.050	1.047	1.048	1.048
$\beta_2$	1.034	1.047	1.053	1.056	1.058
$\beta_3$	0.877	0.893	0.899	0.903	0.902
$\beta_4$	1.127	1.143	1.150	1.155	1.157
$\beta_5$	1.058	1.079	1.088	1.092	1.094
$\beta_6$	1.107	1.092	1.083	1.086	1.087
$\beta_7$	1.223	1.097	1.052	1.050	1.049
$\beta_8$	1.052	1.040	1.032	1.028	1.027
$\beta_9$	1.133	1.162	1.171	1.178	1.176
Error	48423	32517	30243	28212	26923
Extrapolated Error to T=10 sec.					72096
*From the Final Values in Table 3					

TABLE 5 CHANGE IN PARAMETERS AND REDUCTION IN ERROR DURING A TYPICAL RUN

	Initial Values		Final Values	
	$\beta$	$\beta \times \text{Constant}$	$\beta$	$\beta \times \text{Constant}$
$\beta_1$ vs. $\beta_1 L_1$	1.084	86.72 in	1.048	83.84
$\beta_2$ vs. $2L_3$	1.034	66.17 in	1.058	67.71
$\beta_3$ vs. $3L_3$	0.877	56.13 in	0.902	57.73
$\beta_4$ vs. $4L_4$	1.127	162.29 in	1.157	166.61
$\beta_5$ vs. $4L_4$	1.058	152.35 in	1.094	157.54
$\beta_6$ vs. $6L_4$	1.107	159.41 in	1.087	156.53
$\beta_7$ vs. $f$	1.223	2.04	1.049	1.75
$\beta_8$ vs. $MA_{col.}$	1.052	341.90 k.in	1.027	333.78
$\beta_9$ vs. $MA_{gir.}$	1.133	311.57 k.in	1.176	323.40
$a_0$ (kept constant)	0.134			0.134
$a_1$ (kept constant)	0.00018			0.00018

TABLE 6 COMPARISON OF INITIAL VERSUS FINAL PARAMETERS

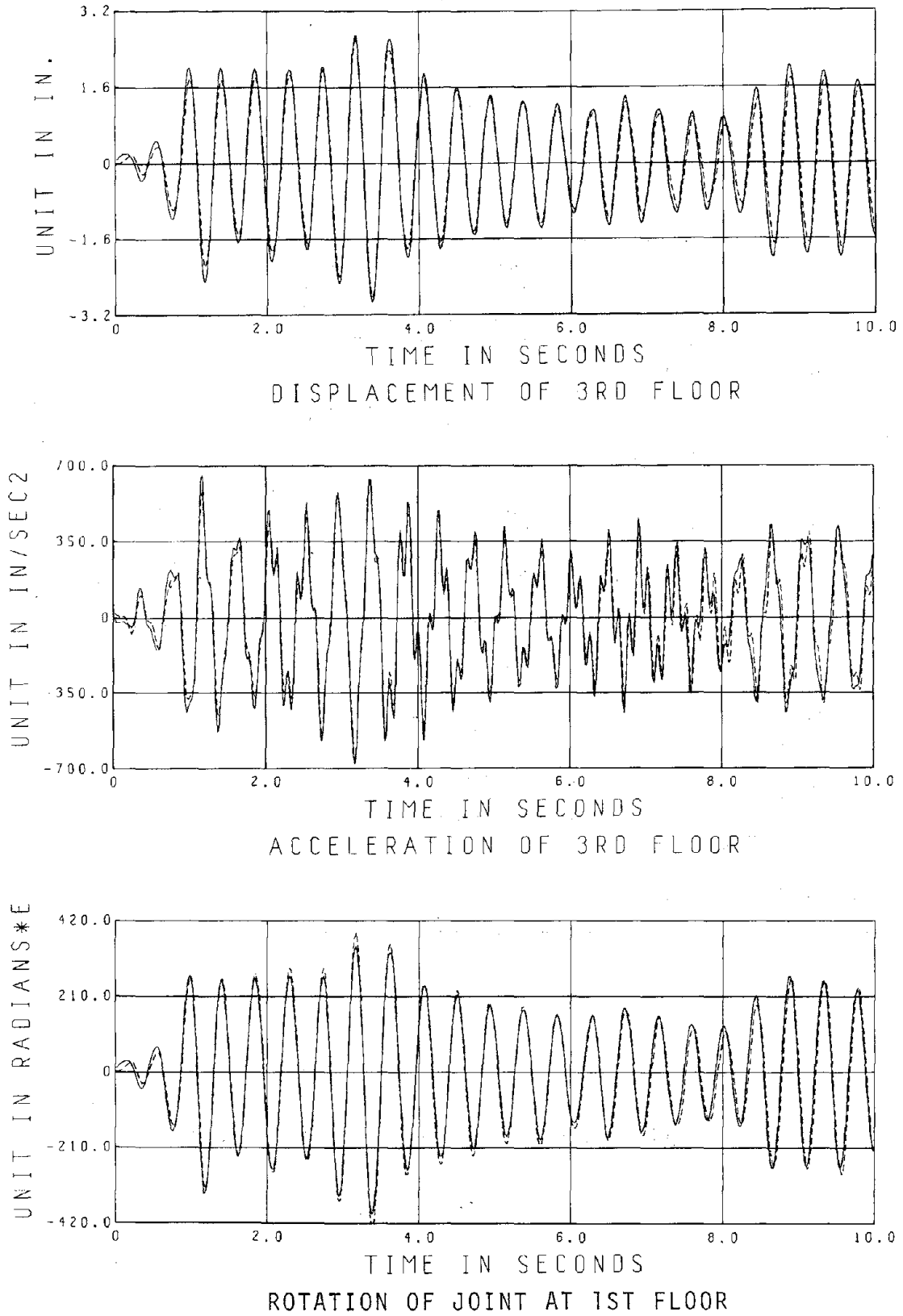


FIGURE 18 CORRELATION OF MEASURED VERSUS PREDICTED RESPONSES

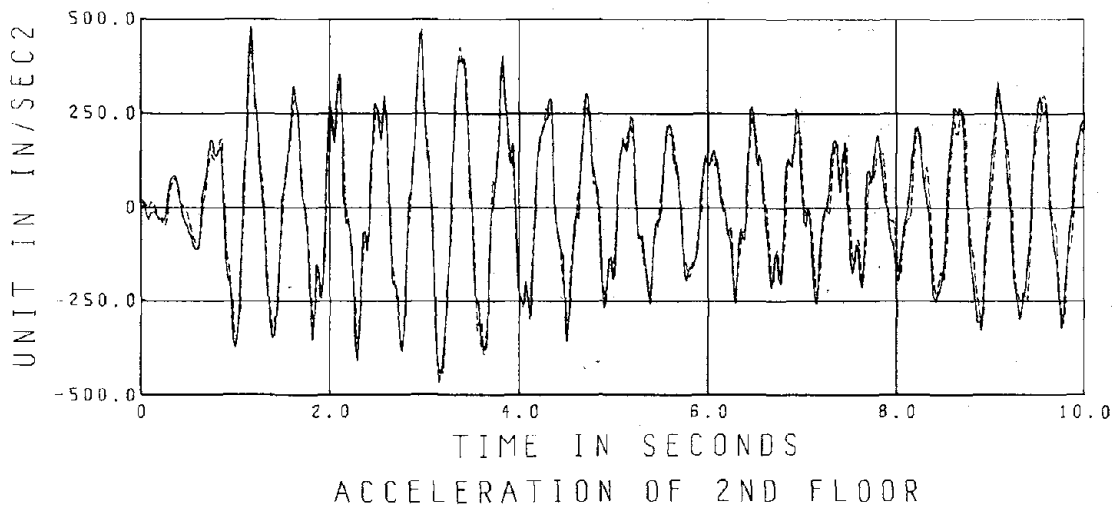
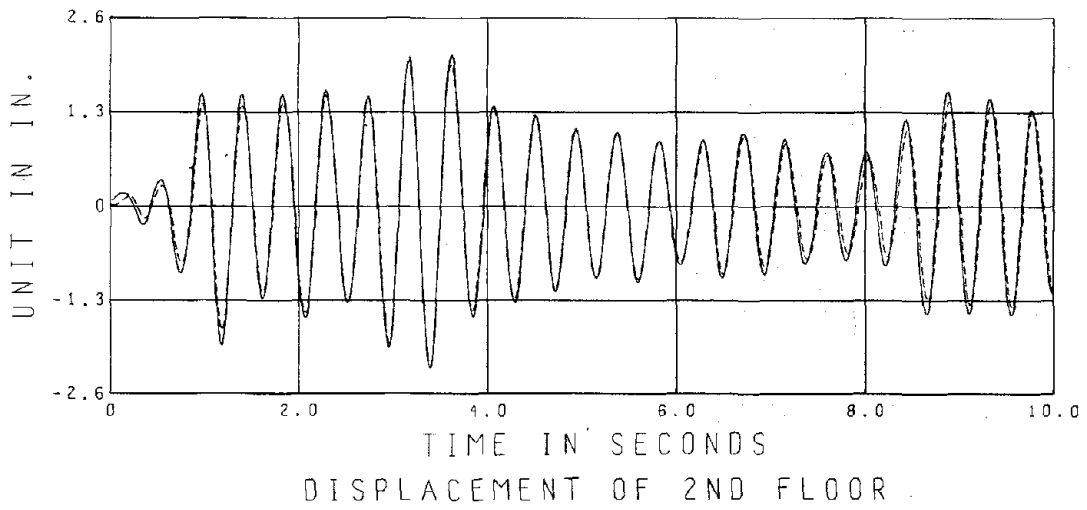
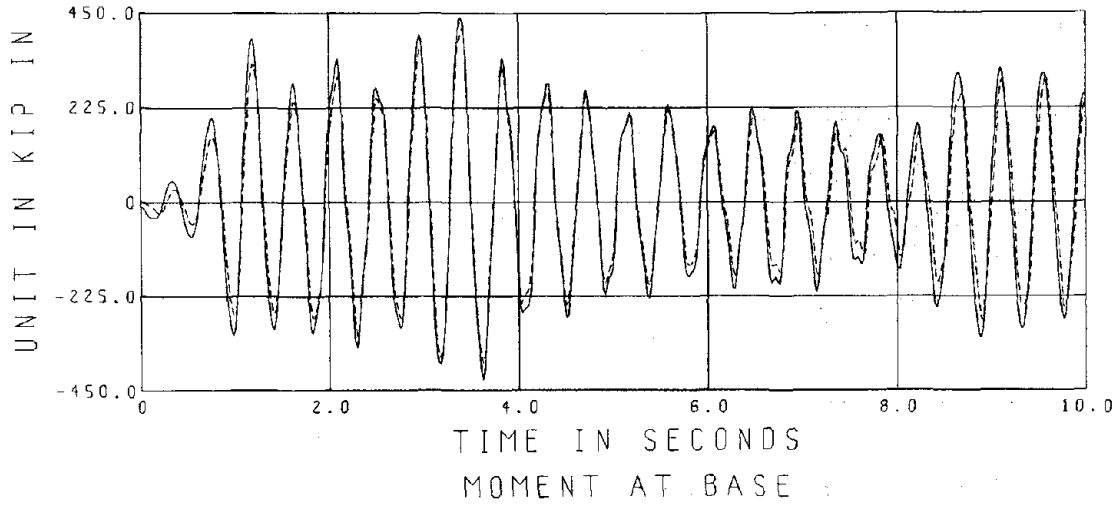


FIGURE 19 CORRELATION OF MEASURED VERSUS PREDICTED RESPONSES

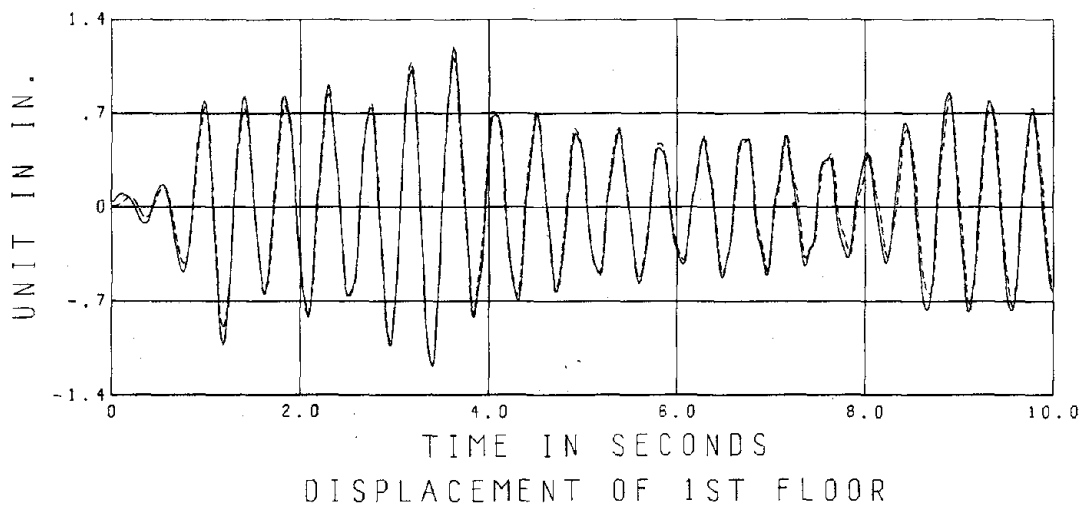
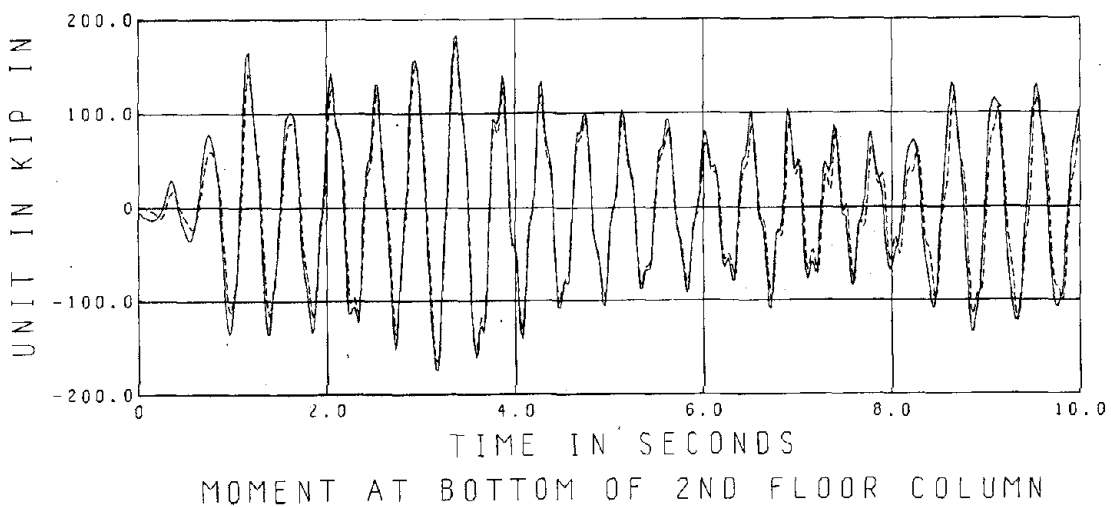
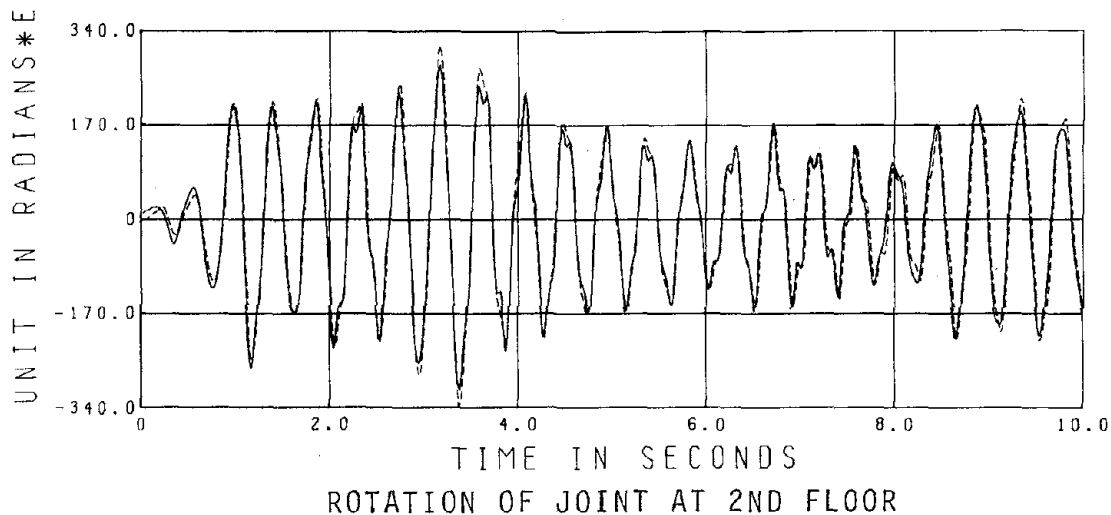


FIGURE 20 CORRELATION OF MEASURED VERSUS PREDICTED RESPONSES



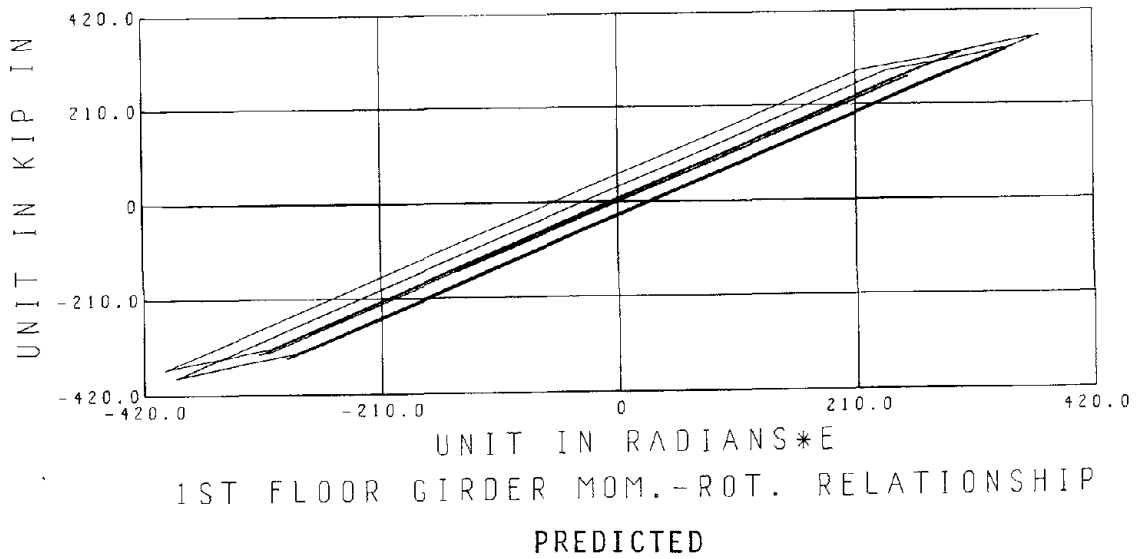
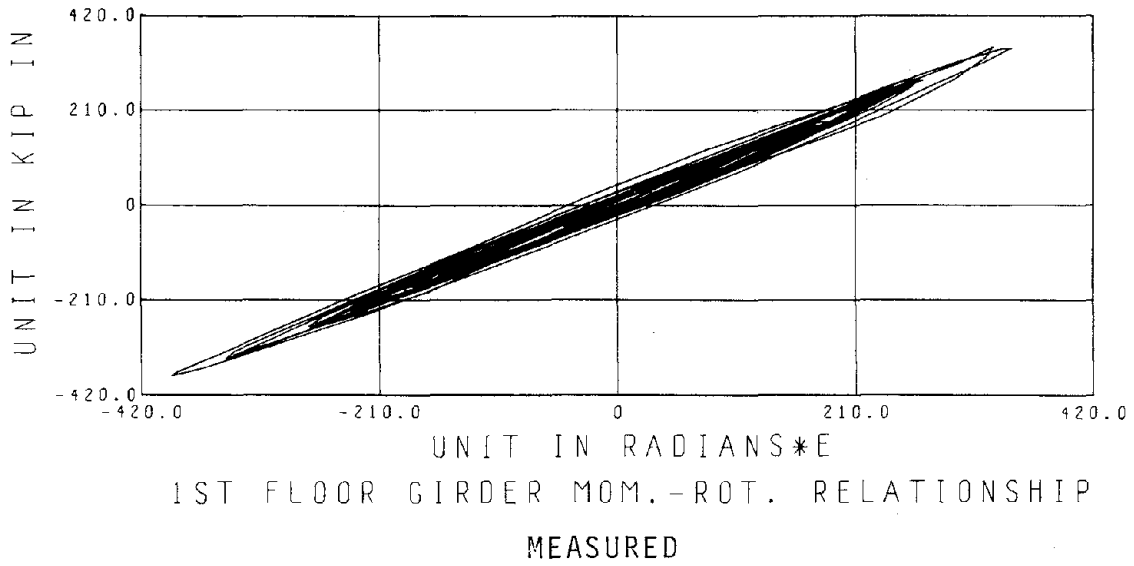


FIGURE 21 MEASURED AND PREDICTED HYSTERETIC BEHAVIORS

5.3 MODEL NO. 2: EC-900II

	Starting Values of Parameters*	End of First Cycle	End of Second Cycle	End of Third Cycle	End of Fourth Cycle
$\beta_1$	1.084	1.069	1.076	1.077	1.077
$\beta_2$	1.034	1.019	1.022	1.014	1.013
$\beta_3$	0.877	0.902	0.920	0.914	0.912
$\beta_4$	1.127	1.101	1.096	1.097	1.097
$\beta_5$	1.058	1.077	1.085	1.084	1.082
$\beta_6$	1.107	1.104	1.102	1.101	1.100
$\beta_7$	1.223	2.174	2.280	2.321	2.315
$\beta_8$	0.574	1.963	1.849	1.837	1.830
$\beta_9$	0.612	0.648	0.739	0.726	0.724
Error	28177	15026	12950	12632	12574
Extrapolated Error to T=10 sec.					54535
*From Final Values in Table 4 (except for $\beta_8$ and $\beta_9$ )					

TABLE 7 CHANGE IN PARAMETERS AND REDUCTION IN ERROR DURING A TYPICAL RUN

	Initial Values		Final Values	
	$\beta$	$\beta \times \text{Constant}$	$\beta$	$\beta \times \text{Constant}$
$\beta_1$ vs. $\beta_1 L_1$	1.084	86.72 in	1.077	86.16 in
$\beta_2$ vs. $\beta_2 L_2$	1.034	66.17 in	1.013	64.83 in
$\beta_3$ vs. $\beta_2 L_3$	0.877	56.13 in	0.912	58.37 in
$\beta_4$ vs. $\beta_4 L_4$	1.127	162.29 in	1.097	157.97 in
$\beta_5$ vs. $\beta_5 L_4$	1.058	152.35 in	1.082	155.81 in
$\beta_6$ vs. $\beta_6 L_4$	1.107	159.41 in	1.100	158.40 in
$\beta_7$ vs. $f$	1.223	2.038	2.315	3.857
$\beta_8$ vs. $a_0$	0.574	0.134	1.830	0.428
$\beta_9$ vs. $a_1$	0.612	0.00018	0.724	0.00022
$MA _{\text{column}}$ (kept constant)	1.052 x 325 =		341.90 k.in	
$MA _{\text{girder}}$ (kept constant)	1.133 x 275 =		311.57 k.in	

TABLE 8 COMPARISON OF INITIAL VERSUS FINAL PARAMETERS

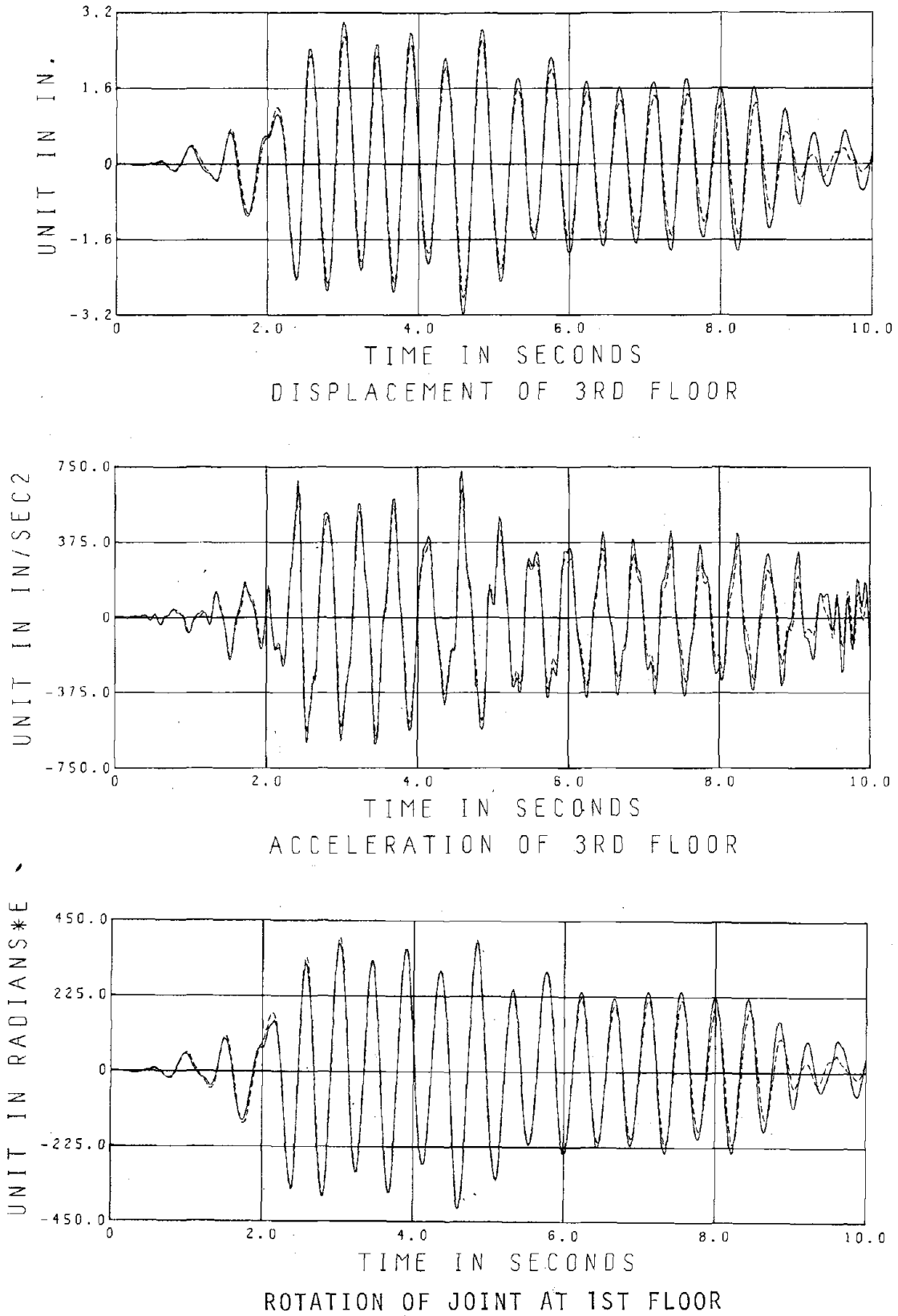


FIGURE 22 CORRELATION OF MEASURED VERSUS PREDICTED RESPONSES

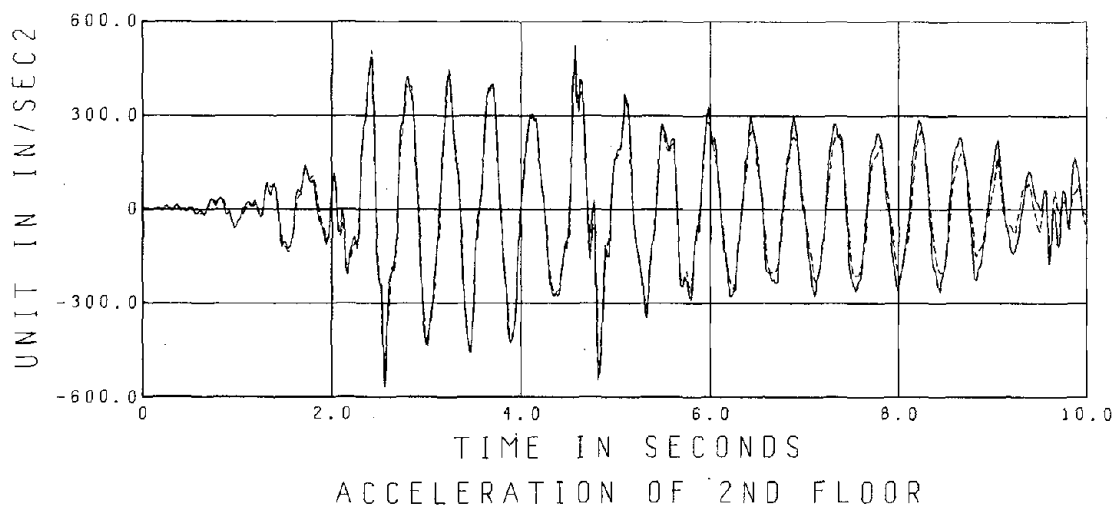
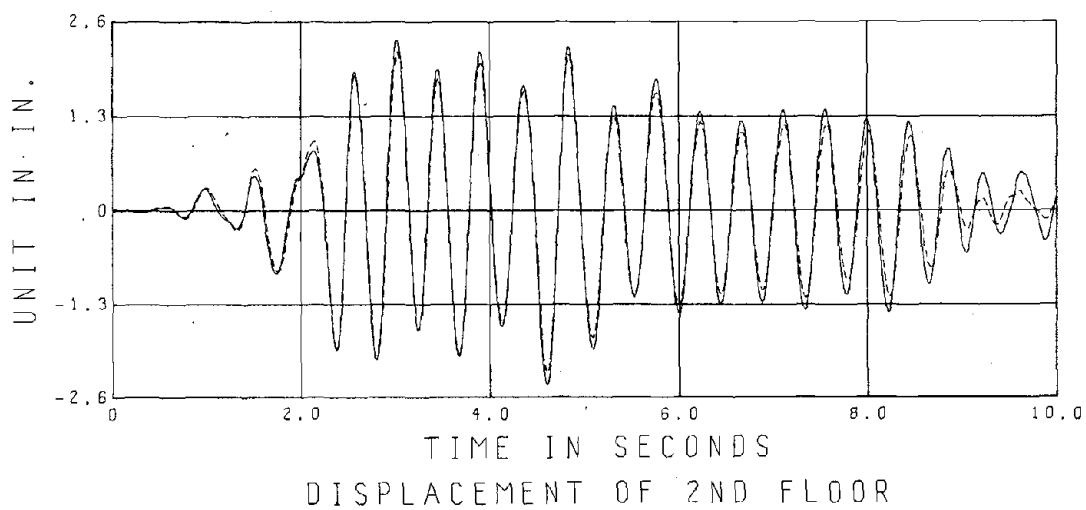
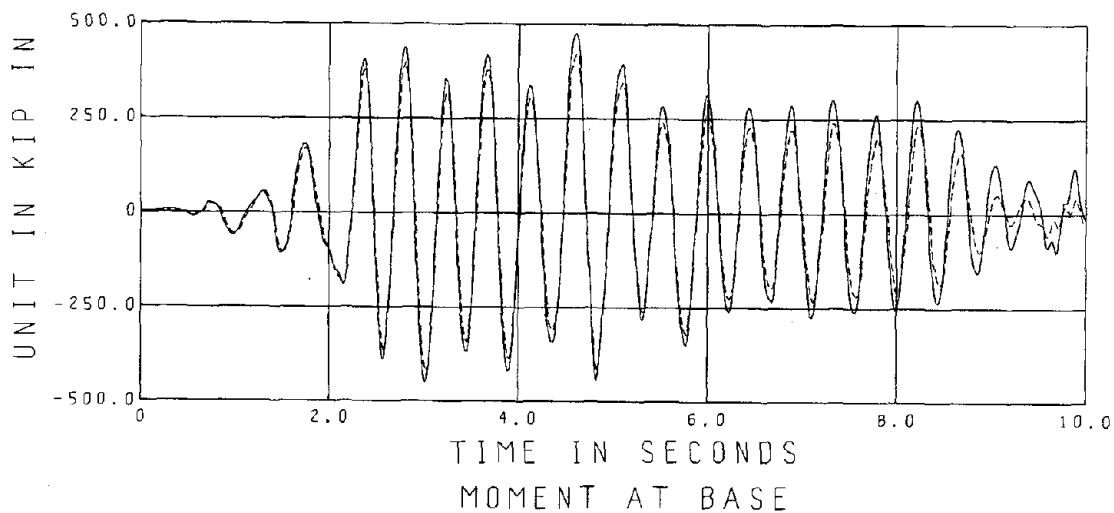


FIGURE 23 CORRELATION OF MEASURED VERSUS PREDICTED RESPONSES

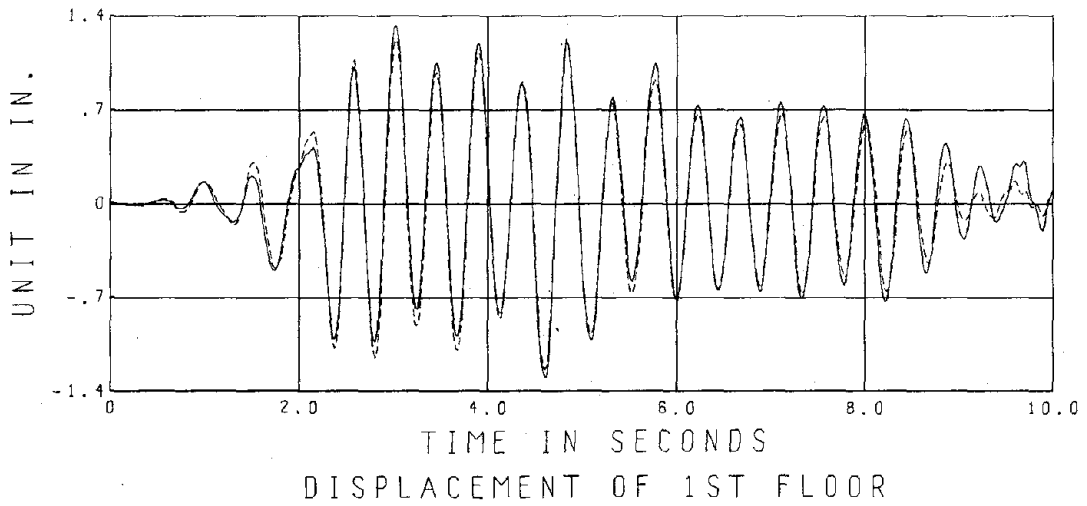
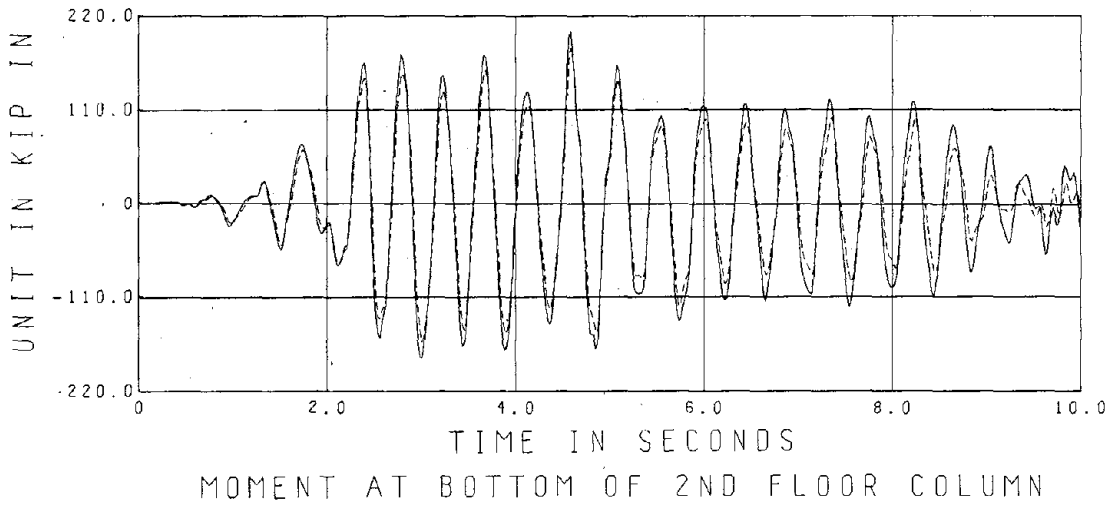
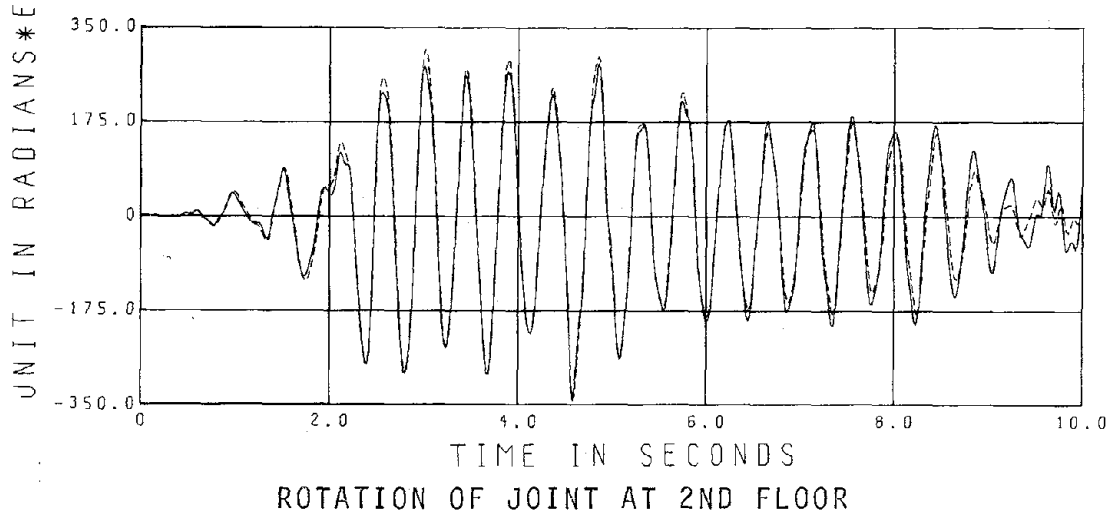


FIGURE 24 CORRELATION OF MEASURED VERSUS PREDICTED RESPONSES

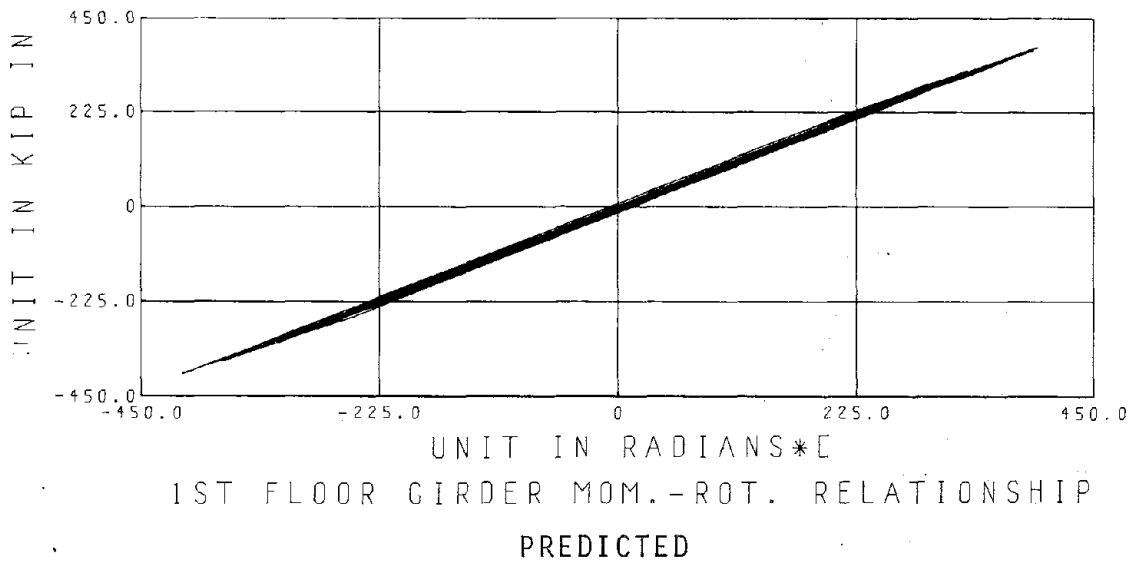
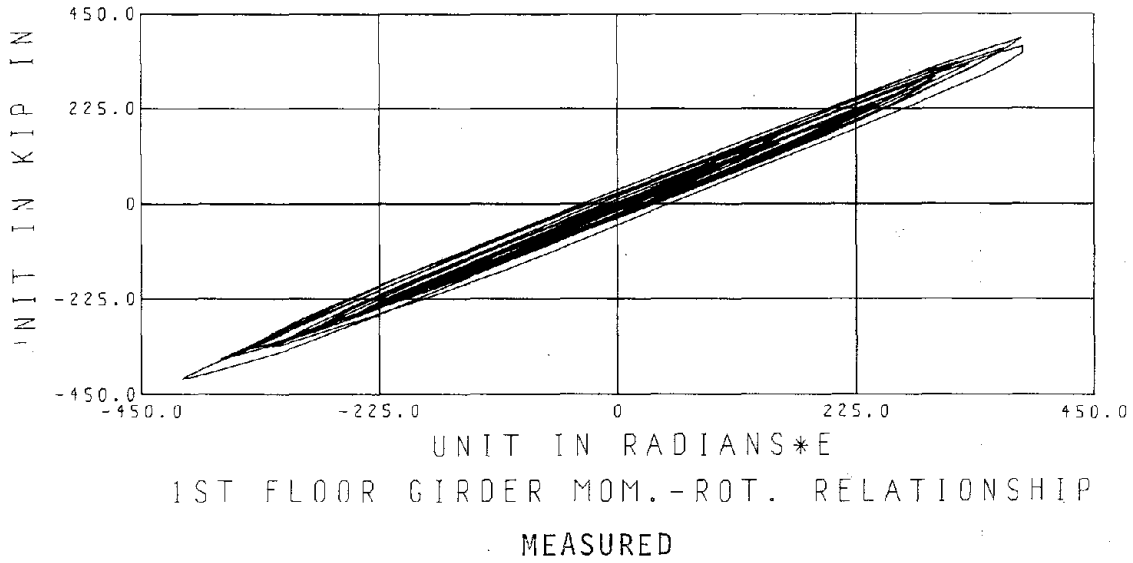


FIGURE 25 MEASURED AND PREDICTED HYSTERETIC BEHAVIORS

5.4 MODEL NO. 2: MEC-600II

	Starting Values of Parameters*	End of First Cycle	End of Second Cycle	End of Fourth Cycle
$\beta_1$	1.077	1.045	1.041	1.039
$\beta_2$	1.013	1.043	1.042	1.042
$\beta_3$	0.912	0.924	0.927	0.926
$\beta_4$	1.097	1.130	1.141	1.148
$\beta_5$	1.082	1.073	1.075	1.077
$\beta_6$	1.100	1.090	1.082	1.084
$\beta_7$	2.315	2.017	1.959	1.947
$\beta_8$	1.830	1.641	1.550	1.524
$\beta_9$	0.724	0.672	0.681	0.684
Error	39728	25214	22318	21935
Extrapolated Error to T=10 sec.				76982
*From Final Values in Table 7				

TABLE 9 CHANGE IN PARAMETERS AND REDUCTION IN ERROR DURING A TYPICAL RUN



	Initial Values		Final Values	
	$\beta$	$\beta \times \text{Constant}$	$\beta$	$\beta \times \text{Constant}$
$\beta_1$ vs. $\beta_1 L_1$	1.077	86.16 in	1.039	83.12 in
$\beta_2$ vs. $\beta_2 L_2$	1.013	64.83 in	1.042	66.69 in
$\beta_3$ vs. $\beta_3 L_3$	0.912	58.37 in	0.926	59.26 in
$\beta_4$ vs. $\beta_4 L_4$	1.097	157.97 in	1.148	165.31 in
$\beta_5$ vs. $\beta_5 L_4$	1.082	155.81 in	1.077	155.09 in
$\beta_6$ vs. $\beta_6 L_4$	1.100	158.40 in	1.084	156.10
$\beta_7$ vs. $f$	2.315	3.857	1.947	3.244
$\beta_8$ vs. $a_0$	1.830	0.428	1.524	0.357
$\beta_9$ vs. $a_1$	0.724	0.00022	0.684	0.00021
$MA _{\text{column}} (\text{kept constant}) = 1.027 \times 325 = 333.78 \text{ k.in}$ $MA _{\text{girder}} (\text{kept constant}) = 1.176 \times 275 = 311.57 \text{ k.in}$				

TABLE 10 COMPARISON OF INITIAL VERSUS FINAL PARAMETERS

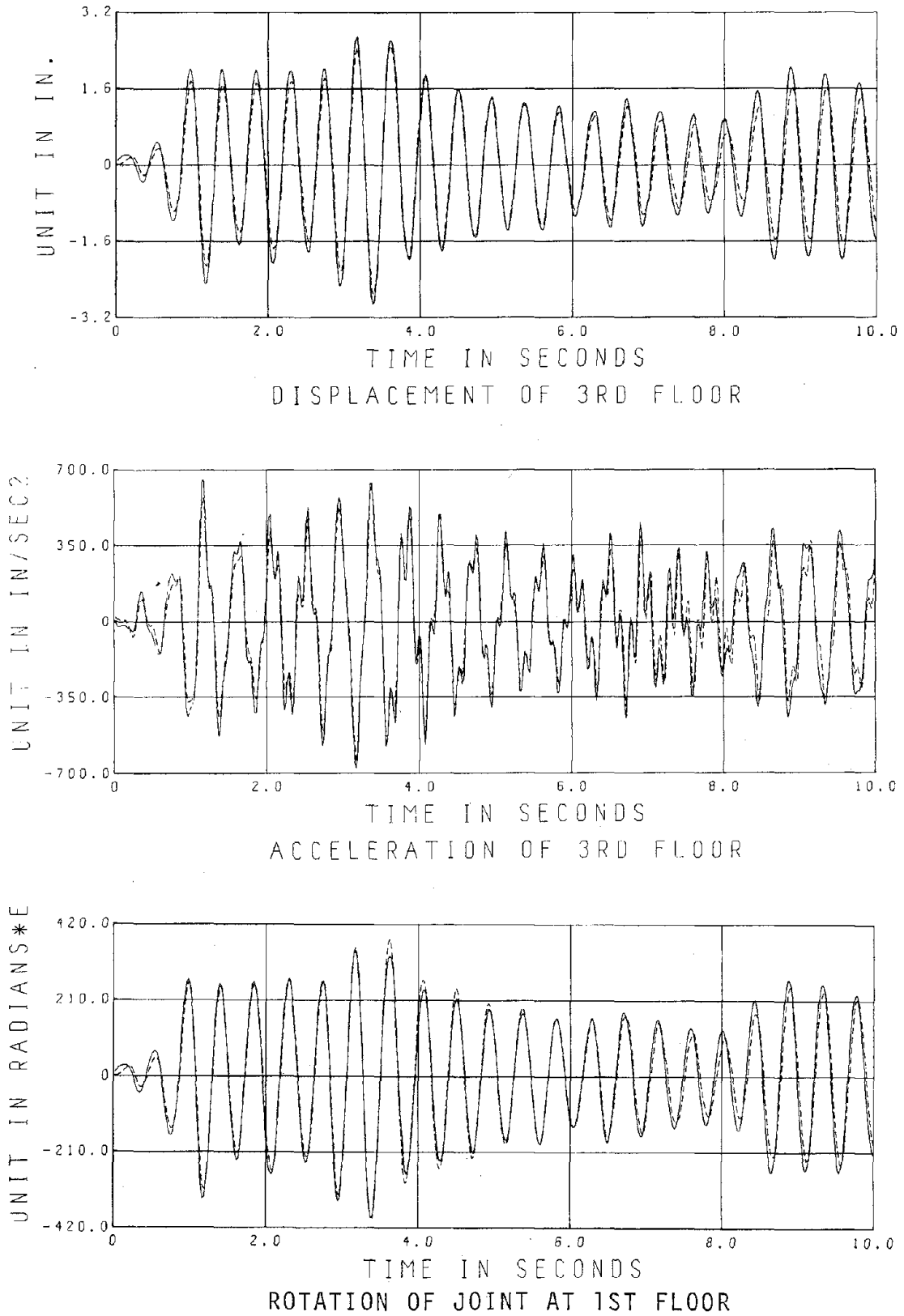


FIGURE 26 CORRELATION OF MEASURED VERSUS PREDICTED RESPONSES

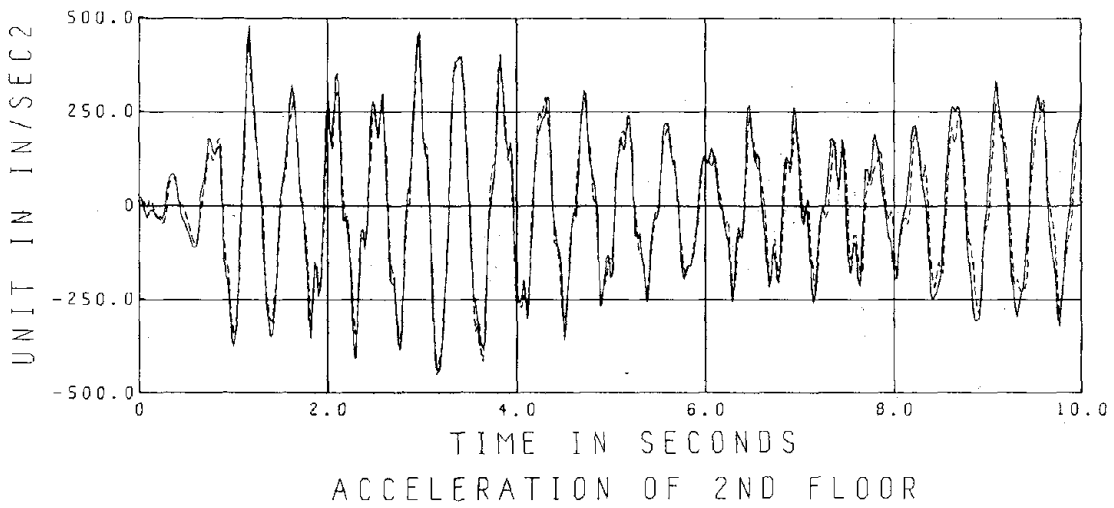
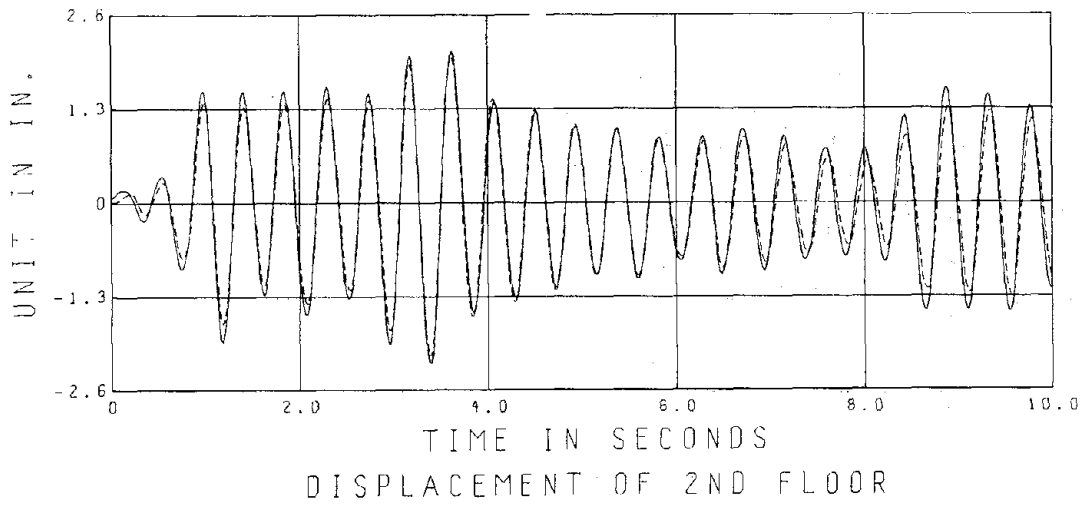
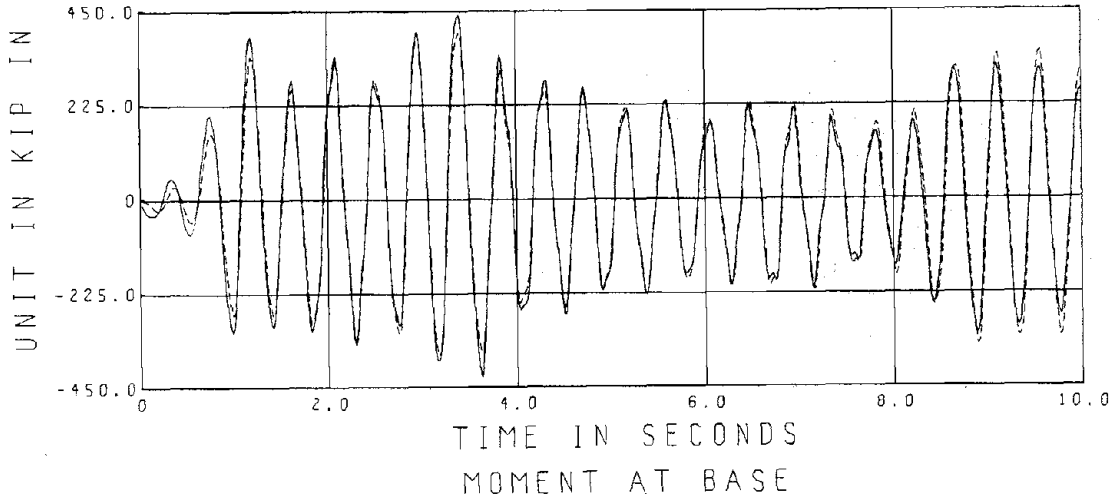
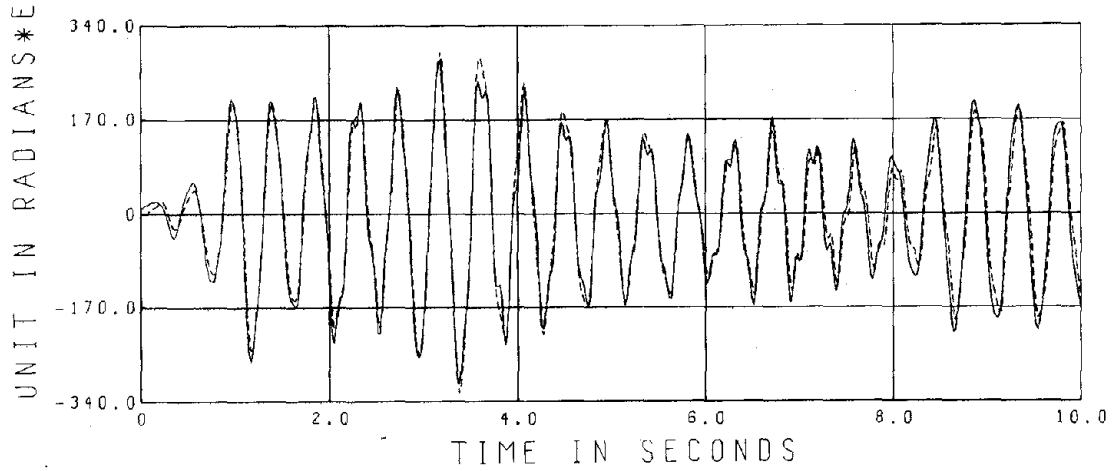
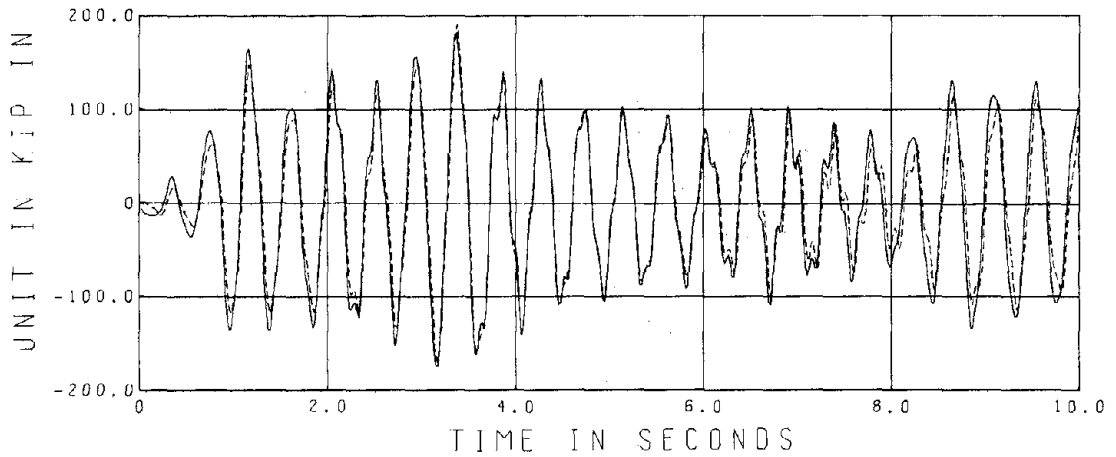


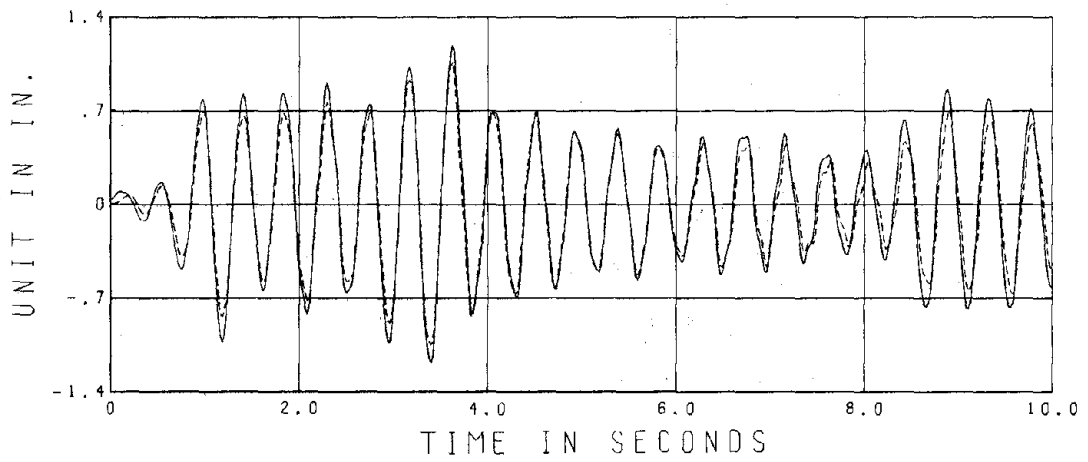
FIGURE 27 CORRELATION OF MEASURED VERSUS PREDICTED RESPONSES



ROTATION OF JOINT AT 2ND FLOOR



MOMENT AT BOTTOM OF 2ND FLOOR COLUMN



DISPLACEMENT OF 1ST FLOOR

FIGURE 28 CORRELATION OF MEASURED VERSUS PREDICTED RESPONSES

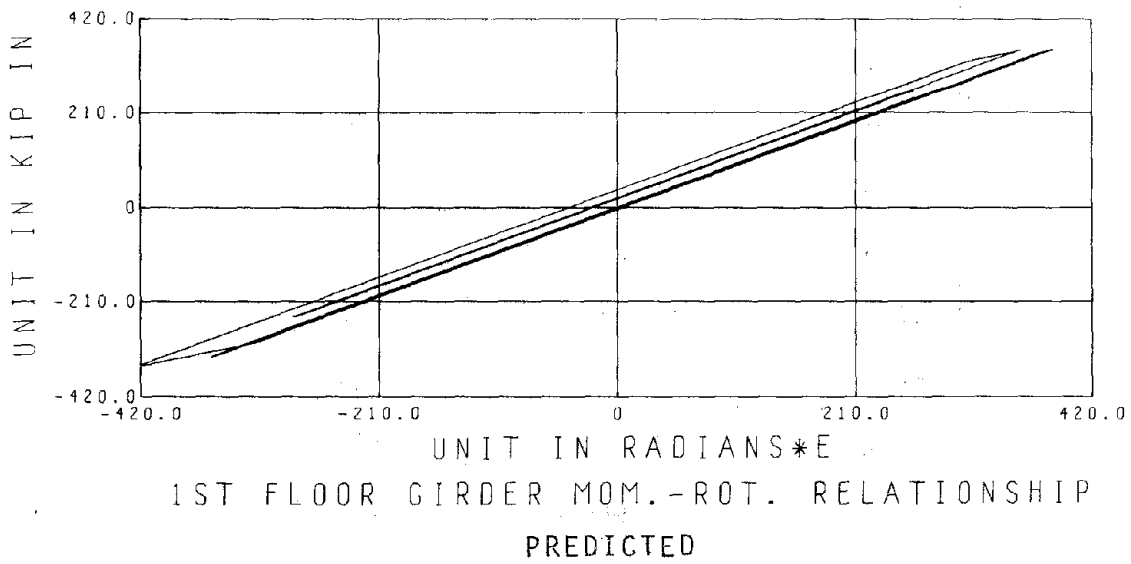
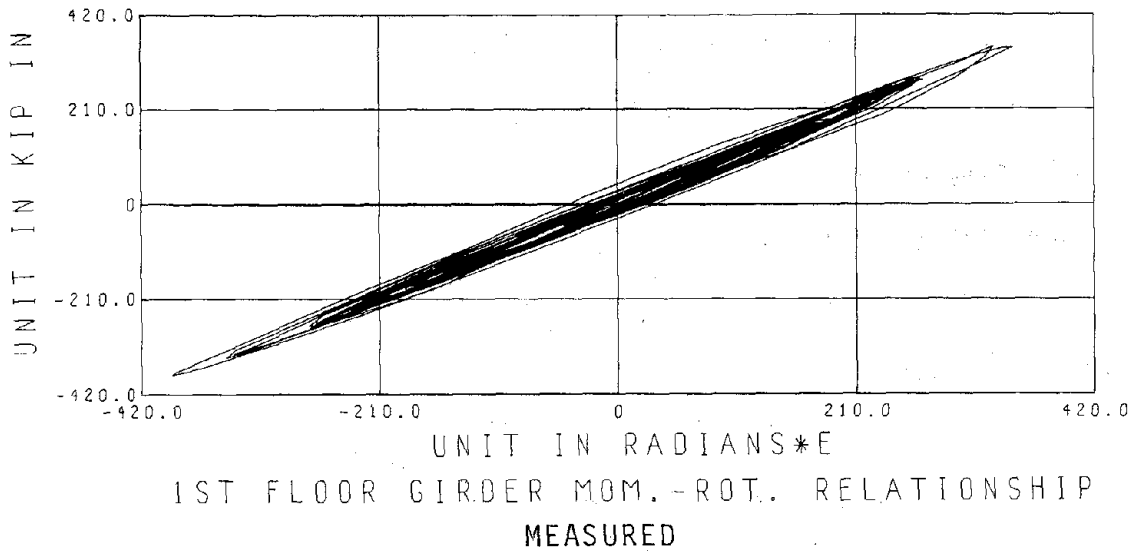


FIGURE 29 MEASURED AND PREDICTED HYSTERETIC BEHAVIORS

CHAPTER 6  
COMMENTS ON THE MODELS

In this chapter we discuss each of the two models, and the value of each in predicting responses. As the form is the same for each model, comments on a model mean comments on the values of the parameters. To keep the study focused, we assemble the final values of the parameters for both models established from the responses to EC-900II and display them in Table 11.

	Model No. 1	Model No. 2
$\beta_1$	1.08	1.08
$\beta_2$	1.03	1.01
$\beta_3$	0.88	0.91
$\beta_4$	1.13	1.10
$\beta_5$	1.06	1.08
$\beta_6$	1.11	1.10
f	2.038	3.857
MA   col.	341.90 k.in	341.90 k.in (const.)
MA   gir.	311.57 k.in	311.57 k.in (const.)
$a_0$	0.134 (const.)	0.428
$a_1$	0.00018 (const.)	0.00022
Error	52078	54535

TABLE 11 FINAL VALUES OF PARAMETERS FOR BOTH MODELS

We first note that the values of the parameters  $\beta_1$  to  $\beta_6$  are almost the same for both models, in fact are within 3% of one another. We could have anticipated this because these parameters represent the effective length factors for the six members of the frame and represent physical quantities that do not change with our change of model. Examination of the individual values in the set leads us to admit, however, that they do not have as physically meaningful values as do the ones in the eight parameter linear model. This comparison was first discussed in Section 3.3. The sets are shown for comparison in Table 12.

	$\beta_1$	$\beta_2$	$\beta_3$	$\beta_4$	$\beta_5$	$\beta_6$
Nonlin. Model 1	1.05	1.06	0.90	1.16	1.09	1.09
Nonlin. Model 2	1.04	1.04	0.93	1.08	1.08	1.08
Linear Model	0.956	0.971	0.891	1.242	1.247	1.322
Linear Model (LVDT)	1.072	1.029	0.917	1.093	1.074	1.128

TABLE 12 COMPARISON OF STIFFNESS PARAMETERS

We explain what we mean when we say that the parameters of the linear model are physically meaningful by repeating the comments made when they were established in Ref. [1]. The parameters  $\beta_1$  to  $\beta_3$  are the effective lengths for the columns and are all less than one, though close to it. The effective lengths for the girders  $\beta_4$  to  $\beta_6$  are all larger than one. We found in the earlier study that these factors are unusually large because they are accounting for the rigid body pitching of the shaking table, and when this pitching is accounted for by its own parameter, the effective lengths of the parameters for the girders have values all larger than one and within 6% of it. As we pointed out in Section 3.3, we feel that whereas the set  $\beta_1$  to  $\beta_6$  will be effective

in helping to predict the nonlinear responses, they are derived from questionable rotations and therefore cannot be used to gain insight into the true effective lengths as can the linear set.

In both of the models the values of the yield moments  $M_A$  of the columns and girders are taken as the same, the values derived from optimization in Model No. 1. These did not change very much during optimization from the "average" yield moments calculated for both the columns and girders and so seem to us to be sensible values.

The major differences between the two models, as we would expect, is revealed in the differences in "f" and the damping coefficients  $a_0$  and  $a_1$ . In Model No. 1 all of the nonlinearity was accounted for by the factor "f", the hysteretic factor reflecting the difference in the elastic and plastic slopes in the bilinear model of the moment-rotation relationships for the members. For this model the value of  $f = 2.038$  corresponds to a ratio of slopes  $p = 0.576$ . We admit that this is larger than we had anticipated, but when we examine the hysteretic behavior created by EC-900II, Fig. 17, we see that it gives a behavior close to the physical. The reason that the value is higher than expected is that the excitation produced only a mildly nonlinear response, a circumstance explained in Chapter 2. Examination of Figs. 14, 15 and 16 shows that Model No. 1 predicts the nonlinear response of the frame extremely well. Not only does it predict the responses accurately for the first six seconds of the response, the duration used in the error function, it predicts them accurately for the full duration of the excitation.

In Model No. 2, accounting for the nonlinear behavior of the frame was shared by the material hysteretic behavior, reflected by "f", and the viscous damping reflected by the factors  $a_0$  and  $a_1$ . The factor  $a_1$ ,



associated with the stiffness matrix, changed little when it was allowed to vary from its value in Model No. 1. The differences between the models is reflected in the differences in the factors "f" and " $a_0$ ". For Model No. 2,  $f = 3.857$  which gives a ratio of slopes  $p = 0.720$  for the hysteretic behavior. This hysteretic behavior is more mildly nonlinear than predicted by Model No. 1 because hysteresis accounts for only part of the nonlinear response. The damping coefficient  $a_0$ , on the other hand, is 0.428 more than three times what it was in Model No. 1. This very large growth in damping is expected because it is well known that damping grows enormously in equivalent linear models that are used to account for nonlinear behavior. When we examine Figs. 22, 23 and 24 we see that the predicted responses are very close for the first six seconds, but the accuracy lessens for the remainder of the excitation.

It is tempting to compare the accuracies of the two models and therefore to interpret whether or not the nonlinear behavior should be shared between the material and viscous damping or should be accounted for entirely by the material. We hesitate here to draw any definite conclusions. We feel that this kind of appraisal can only be made when the two types of models are derived from excitations that inflict significant nonlinear responses in the frame. If the intensity of excitation were increased significantly, the material near the ends of the members would exhibit excursions far into the plastic zone and the amplitudes of the resulting motions might well affect the values of the damping coefficients. As the shaking table will now accommodate this larger intensity, we leave this comparison to a future study.

Finally, if a nonlinear mathematical model truly represents a physical frame, it should be able to predict the responses accurately for a family of seismic disturbances, not just the one used for

formulating the model. Put another way, the mathematical model, if the form is appropriate, should not be sensitive to changes in the seismic disturbance from which values of the parameters are established. To establish the invariance of the two models formulated here, we derive the sets of parameters a second time, this time using a modified El Centro disturbance as opposed to the historical disturbance used for the first two models. The two new sets of parameters are organized the same way as the first and are displayed in Table 13.

	Model No. 1	Model No. 2
$\beta_1$	1.05	1.04
$\beta_2$	1.06	1.04
$\beta_3$	.90	.93
$\beta_4$	1.16	1.15
$\beta_5$	1.09	1.08
$\beta_6$	1.09	1.08
f	1.748	3.244
MA  <sub>col.</sub>	333.78 k.in	333.78 k.in (const.)
MA  <sub>gir.</sub>	323.40 k.in	323.40 k.in (const.)
$a_0$	0.134 (const.)	0.357
$a_1$	0.00018 (const.)	0.00021

TABLE 13 FINAL VALUES OF PARAMETERS FOR BOTH MODELS

If we compare the two sets of parameters in Tables 11 and 13 we find that the parameters, for the same model using different excitations,

differ at most by 3%, though perhaps slightly higher for  $f$  and  $a_0$ .  
The intensities of two different excitations cannot be compared directly,  
so the differences in these parameters can probably be accounted for by  
the difference in intensities of the two disturbances.

REFERENCES

1. Izak Kaya and Hugh D. McNiven, "Investigation of the Elastic Characteristics of a Three-Story Steel Frame Using System Identification," Report No. UCB/EERC-78/24, Earthquake Engineering Research Center, University of California, Berkeley, (1978).
2. Hugh D. McNiven and Vernon C. Matzen, "A Mathematical Model to Predict the Inelastic Response of a Steel Frame: Formulation of the Model," Earthquake Engineering and Structural Dynamics, Vol. 6, 189-202 (1978).
3. M. Menegotto and P. Pinto, "Method of Analysis for Cyclically Loaded Reinforced Concrete Plane Frames Including Changes in Geometry and Nonelastic Behavior of Elements Under Combined Normal Force and Bending," IABSC Symposium on the Resistance and Ultimate Deformability of Structures Acted on by Well-Defined Repeated Loads, Lisbon, (1973).
4. John F. Stanton and Hugh D. McNiven, "The Development of a Mathematical Model to Predict the Flexural Response of Reinforced Concrete Beams to Cyclic Loads, Using System Identification," Report No. UCB/EERC-79/02, Earthquake Engineering Research Center, University of California, Berkeley, (1979).
5. R.W. Clough and D.T. Tang, "Earthquake Simulator Study of a Steel Frame Structure, Vol. I: Experimental Results," Report No. EERC 75-6, Earthquake Engineering Research Center, University of California, Berkeley, (1975).
6. D.T. Tang, "Earthquake Simulator Study of a Steel Frame Structure, Vol. II: Analytical Results," Report No. EERC 75-36, Earthquake Engineering Research Center, University of California, Berkeley, (1975).
7. N. Distefano and B. Peña-Pardo, "System Identification of Frames Under Seismic Loads," Journal of the Engineering Mechanics Division, ASCE, Vol. 102, No. EM2, Proc. Paper 12047, 313-330, (1976).
8. E.L. Wilson and R.W. Clough, "Dynamic, Nonlinear Analysis of Multi-story Frames," Berkeley, California, (July 1963), (not published).
9. N.M. Newmark, "A Method of Computation for Structural Dynamics," ASCE, Engineering Mechanics Division, Journal, V.85, No. EM3, 67-94, (July 1959).
10. M.F. Giberson, "The Response of Nonlinear Multi-Story Structures Subjected to Earthquake Excitation," Report No. 67-503, Earthquake Engineering Research Laboratory, California Institute of Technology, Pasadena, (May 1967).

REFERENCES (cont'd.)

11. D. Rea, R.W. Clough and J.G. Bouwkamp, "Damping Capacity of a Model Steel Structure," Report No. EERC 69-14, Earthquake Engineering Research Center, University of California, Berkeley, (December 1969).



# Preceding page blank

## EARTHQUAKE ENGINEERING RESEARCH CENTER REPORTS

NOTE: Numbers in parenthesis are Accession Numbers assigned by the National Technical Information Service; these are followed by a price code. Copies of the reports may be ordered from the National Technical Information Service, 5285 Port Royal Road, Springfield, Virginia, 22161. Accession Numbers should be quoted on orders for reports (PB --- ---) and remittance must accompany each order. Reports without this information were not available at time of printing. Upon request, EERC will mail inquirers this information when it becomes available.

- EERC 67-1 "Feasibility Study Large-Scale Earthquake Simulator Facility," by J. Penzien, J.G. Bouwkamp, R.W. Clough and D. Rea - 1967 (PB 187 905)A07
- EERC 68-1 Unassigned
- EERC 68-2 "Inelastic Behavior of Beam-to-Column Subassemblages Under Repeated Loading," by V.V. Bertero - 1968 (PB 184 888)A05
- EERC 68-3 "A Graphical Method for Solving the Wave Reflection-Refraction Problem," by H.D. McNiven and Y. Mengi - 1968 (PB 187 943)A03
- EERC 68-4 "Dynamic Properties of McKinley School Buildings," by D. Rea, J.G. Bouwkamp and R.W. Clough - 1968 (PB 187 902)A07
- EERC 68-5 "Characteristics of Rock Motions During Earthquakes," by H.B. Seed, I.M. Idriss and F.W. Kiefer - 1968 (PB 188 338)A03
- EERC 69-1 "Earthquake Engineering Research at Berkeley," - 1969 (PB 187 906)A11
- EERC 69-2 "Nonlinear Seismic Response of Earth Structures," by M. Dibaj and J. Penzien - 1969 (PB 187 904)A08
- EERC 69-3 "Probabilistic Study of the Behavior of Structures During Earthquakes," by R. Ruiz and J. Penzien - 1969 (PB 187 886)A06
- EERC 69-4 "Numerical Solution of Boundary Value Problems in Structural Mechanics by Reduction to an Initial Value Formulation," by N. Distefano and J. Schujman - 1969 (PB 187 942)A02
- EERC 69-5 "Dynamic Programming and the Solution of the Biharmonic Equation," by N. Distefano - 1969 (PB 187 941)A03
- EERC 69-6 "Stochastic Analysis of Offshore Tower Structures," by A.K. Malhotra and J. Penzien - 1969 (PB 187 903)A09
- EERC 69-7 "Rock Motion Accelerograms for High Magnitude Earthquakes," by H.B. Seed and I.M. Idriss - 1969 (PB 187 940)A02
- EERC 69-8 "Structural Dynamics Testing Facilities at the University of California, Berkeley," by R.M. Stephen, J.G. Bouwkamp, R.W. Clough and J. Penzien - 1969 (PB 189 111)A04
- EERC 69-9 "Seismic Response of Soil Deposits Underlain by Sloping Rock Boundaries," by H. Dezfulian and H.B. Seed - 1969 (PB 189 114)A03
- EERC 69-10 "Dynamic Stress Analysis of Axisymmetric Structures Under Arbitrary Loading," by S. Ghosh and E.L. Wilson - 1969 (PB 189 026)A10
- EERC 69-11 "Seismic Behavior of Multistory Frames Designed by Different Philosophies," by J.C. Anderson and V. V. Bertero - 1969 (PB 190 662)A10
- EERC 69-12 "Stiffness Degradation of Reinforcing Concrete Members Subjected to Cyclic Flexural Moments," by V.V. Bertero, E. Bresler and H. Ming Liao - 1969 (PB 202 942)A07
- EERC 69-13 "Response of Non-Uniform Soil Deposits to Travelling Seismic Waves," by H. Dezfulian and H.B. Seed - 1969 (PB 191 023)A03
- EERC 69-14 "Damping Capacity of a Model Steel Structure," by D. Rea, R.W. Clough and J.G. Bouwkamp - 1969 (PB 190 663)A06
- EERC 69-15 "Influence of Local Soil Conditions on Building Damage Potential during Earthquakes," by H.B. Seed and I.M. Idriss - 1969 (PB 191 036)A03
- EERC 69-16 "The Behavior of Sands Under Seismic Loading Conditions," by M.L. Silver and H.B. Seed - 1969 (AD 714 982)A07
- EERC 70-1 "Earthquake Response of Gravity Dams," by A.K. Chopra - 1970 (AD 709 640)A03
- EERC 70-2 "Relationships between Soil Conditions and Building Damage in the Caracas Earthquake of July 29, 1967," by H.B. Seed, I.M. Idriss and H. Dezfulian - 1970 (PB 195 762)A05
- EERC 70-3 "Cyclic Loading of Full Size Steel Connections," by E.P. Popov and R.M. Stephen - 1970 (PB 213 545)A04
- EERC 70-4 "Seismic Analysis of the Charaima Building, Caraballeda, Venezuela," by Subcommittee of the SEAONC Research Committee: V.V. Bertero, P.F. Fratessa, S.A. Mahin, J.H. Sexton, A.C. Scordelis, E.L. Wilson, L.A. Wyllie, H.B. Seed and J. Penzien, Chairman - 1970 (PB 201 455)A06

- EERC 70-5 "A Computer Program for Earthquake Analysis of Dams," by A.K. Chopra and P. Chakrabarti - 1970 (AD 723 994)A05
- EERC 70-6 "The Propagation of Love Waves Across Non-Horizontally Layered Structures," by J. Lysmer and L.A. Drake 1970 (PB 197 896)A03
- EERC 70-7 "Influence of Base Rock Characteristics on Ground Response," by J. Lysmer, H.B. Seed and P.B. Schnabel 1970 (PB 197 897)A03
- EERC 70-8 "Applicability of Laboratory Test Procedures for Measuring Soil Liquefaction Characteristics under Cyclic Loading," by H.B. Seed and W.H. Peacock - 1970 (PB 198 016)A03
- EERC 70-9 "A Simplified Procedure for Evaluating Soil Liquefaction Potential," by H.B. Seed and I.M. Idriss - 1970 (PB 198 009)A03
- EERC 70-10 "Soil Moduli and Damping Factors for Dynamic Response Analysis," by H.B. Seed and I.M. Idriss - 1970 (PB 197 869)A03
- EERC 71-1 "Koyna Earthquake of December 11, 1967 and the Performance of Koyna Dam," by A.K. Chopra and P. Chakrabarti 1971 (AD 731 496)A06
- EERC 71-2 "Preliminary In-Situ Measurements of Anelastic Absorption in Soils Using a Prototype Earthquake Simulator," by R.D. Borcherdt and P.W. Rodgers - 1971 (PB 201 454)A03
- EERC 71-3 "Static and Dynamic Analysis of Inelastic Frame Structures," by F.L. Porter and G.H. Powell - 1971 (PB 210 135)A06
- EERC 71-4 "Research Needs in Limit Design of Reinforced Concrete Structures," by V.V. Bertero - 1971 (PB 202 943)A04
- EERC 71-5 "Dynamic Behavior of a High-Rise Diagonally Braced Steel Building," by D. Rea, A.A. Shah and J.G. Bouwkamp 1971 (PB 203 584)A06
- EERC 71-6 "Dynamic Stress Analysis of Porous Elastic Solids Saturated with Compressible Fluids," by J. Ghaboussi and E. L. Wilson - 1971 (PB 211 396)A06
- EERC 71-7 "Inelastic Behavior of Steel Beam-to-Column Subassemblies," by H. Krawinkler, V.V. Bertero and E.P. Popov 1971 (PB 211 335)A14
- EERC 71-8 "Modification of Seismograph Records for Effects of Local Soil Conditions," by P. Schnabel, H.B. Seed and J. Lysmer - 1971 (PB 214 450)A03
- EERC 72-1 "Static and Earthquake Analysis of Three Dimensional Frame and Shear Wall Buildings," by E.L. Wilson and H.H. Dovey - 1972 (PB 212 904)A05
- EERC 72-2 "Accelerations in Rock for Earthquakes in the Western United States," by P.B. Schnabel and H.B. Seed - 1972 (PB 213 100)A03
- EERC 72-3 "Elastic-Plastic Earthquake Response of Soil-Building Systems," by T. Minami - 1972 (PB 214 868)A08
- EERC 72-4 "Stochastic Inelastic Response of Offshore Towers to Strong Motion Earthquakes," by M.K. Kaul - 1972 (PB 215 713)A05
- EERC 72-5 "Cyclic Behavior of Three Reinforced Concrete Flexural Members with High Shear," by E.P. Popov, V.V. Bertero and H. Krawinkler - 1972 (PB 214 555)A05
- EERC 72-6 "Earthquake Response of Gravity Dams Including Reservoir Interaction Effects," by P. Chakrabarti and A.K. Chopra - 1972 (AD 762 330)A08
- EERC 72-7 "Dynamic Properties of Pine Flat Dam," by D. Rea, C.Y. Liaw and A.K. Chopra - 1972 (AD 763 928)A05
- EERC 72-8 "Three Dimensional Analysis of Building Systems," by E.L. Wilson and H.H. Dovey - 1972 (PB 222 438)A06
- EERC 72-9 "Rate of Loading Effects on Uncracked and Repaired Reinforced Concrete Members," by S. Mahin, V.V. Bertero, D. Rea and M. Atalay - 1972 (PB 224 520)A08
- EERC 72-10 "Computer Program for Static and Dynamic Analysis of Linear Structural Systems," by E.L. Wilson, K.-J. Bathe, J.E. Peterson and H.H. Dovey - 1972 (PB 220 437)A04
- EERC 72-11 "Literature Survey - Seismic Effects on Highway Bridges," by T. Iwasaki, J. Penzien and R.W. Clough - 1972 (PB 215 613)A19
- EERC 72-12 "SHAKE-A Computer Program for Earthquake Response Analysis of Horizontally Layered Sites," by P.B. Schnabel and J. Lysmer - 1972 (PB 220 207)A06
- EERC 73-1 "Optimal Seismic Design of Multistory Frames," by V.V. Bertero and H. Kamil - 1973
- EERC 73-2 "Analysis of the Slides in the San Fernando Dams During the Earthquake of February 9, 1971," by H.B. Seed, K.L. Lee, I.M. Idriss and F. Makdisi - 1973 (PB 223 402)A14



- EERC 73-3 "Computer Aided Ultimate Load Design of Unbraced Multistory Steel Frames," by M.B. El-Hafez and G.H. Powell 1973 (PB 248 315)A09
- EERC 73-4 "Experimental Investigation into the Seismic Behavior of Critical Regions of Reinforced Concrete Components as Influenced by Moment and Shear," by M. Celebi and J. Penzien - 1973 (PB 215 884)A09
- EERC 73-5 "Hysteretic Behavior of Epoxy-Repaired Reinforced Concrete Beams," by M. Celebi and J. Penzien - 1973 (PB 239 568)A03
- EERC 73-6 "General Purpose Computer Program for Inelastic Dynamic Response of Plane Structures," by A. Kanaan and G.H. Powell - 1973 (PB 221 260)A08
- EERC 73-7 "A Computer Program for Earthquake Analysis of Gravity Dams Including Reservoir Interaction," by P. Chakrabarti and A.K. Chopra - 1973 (AD 766 271)A04
- EERC 73-8 "Behavior of Reinforced Concrete Deep Beam-Column Subassemblages Under Cyclic Loads," by O. Küstü and J.G. Bouwkamp - 1973 (PB 246 117)A12
- EERC 73-9 "Earthquake Analysis of Structure-Foundation Systems," by A.K. Vaish and A.K. Chopra - 1973 (AD 766 272)A07
- EERC 73-10 "Deconvolution of Seismic Response for Linear Systems," by R.B. Reimer - 1973 (PB 227 179)A08
- EERC 73-11 "SAP IV: A Structural Analysis Program for Static and Dynamic Response of Linear Systems," by K.-J. Bathe, E.L. Wilson and F.E. Peterson - 1973 (PB 221 967)A09
- EERC 73-12 "Analytical Investigations of the Seismic Response of Long, Multiple Span Highway Bridges," by W.S. Tseng and J. Penzien - 1973 (PB 227 816)A10
- EERC 73-13 "Earthquake Analysis of Multi-Story Buildings Including Foundation Interaction," by A.K. Chopra and J.A. Gutierrez - 1973 (PB 222 970)A03
- EERC 73-14 "ADAP: A Computer Program for Static and Dynamic Analysis of Arch Dams," by R.W. Clough, J.M. Raphael and S. Mojtahedi - 1973 (PB 223 763)A09
- EERC 73-15 "Cyclic Plastic Analysis of Structural Steel Joints," by R.B. Pinkney and R.W. Clough - 1973 (PB 226 843)A08
- EERC 73-16 "QUAD-4: A Computer Program for Evaluating the Seismic Response of Soil Structures by Variable Damping Finite Element Procedures," by T.M. Idriss, J. Lysmer, R. Hwang and H.B. Seed - 1973 (PB 229 424)A05
- EERC 73-17 "Dynamic Behavior of a Multi-Story Pyramid Shaped Building," by R.M. Stephen, J.P. Hollings and J.G. Bouwkamp - 1973 (PB 240 718)A06
- EERC 73-18 "Effect of Different Types of Reinforcing on Seismic Behavior of Short Concrete Columns," by V.V. Bertero, J. Hollings, O. Küstü, R.M. Stephen and J.G. Bouwkamp - 1973
- EERC 73-19 "Olive View Medical Center Materials Studies, Phase I," by B. Bresler and V.V. Bertero - 1973 (PB 235 986)A06
- EERC 73-20 "Linear and Nonlinear Seismic Analysis Computer Programs for Long Multiple-Span Highway Bridges," by W.S. Tseng and J. Penzien - 1973
- EERC 73-21 "Constitutive Models for Cyclic Plastic Deformation of Engineering Materials," by J.M. Kelly and P.P. Gillis 1973 (PB 226 024)A03
- EERC 73-22 "DRAIN - 2D User's Guide," by G.H. Powell - 1973 (PB 227 016)A05
- EERC 73-23 "Earthquake Engineering at Berkeley - 1973," (PB 226 033)A11
- EERC 73-24 Unassigned
- EERC 73-25 "Earthquake Response of Axisymmetric Tower Structures Surrounded by Water," by C.Y. Liaw and A.K. Chopra 1973 (AD 773 052)A09
- EERC 73-26 "Investigation of the Failures of the Olive View Stairtowers During the San Fernando Earthquake and Their Implications on Seismic Design," by V.V. Bertero and R.G. Collins - 1973 (PB 235 106)A13
- EERC 73-27 "Further Studies on Seismic Behavior of Steel Beam-Column Subassemblages," by V.V. Bertero, H. Krawinkler and E.P. Popov - 1973 (PB 234 172)A06
- EERC 74-1 "Seismic Risk Analysis," by C.S. Oliveira - 1974 (PB 235 920)A06
- EERC 74-2 "Settlement and Liquefaction of Sands Under Multi-Directional Shaking," by R. Pyke, C.K. Chan and H.B. Seed 1974
- EERC 74-3 "Optimum Design of Earthquake Resistant Shear Buildings," by D. Ray, K.S. Pister and A.K. Chopra - 1974 (PB 231 172)A06
- EERC 74-4 "LUSH - A Computer Program for Complex Response Analysis of Soil-Structure Systems," by J. Lysmer, T. Udaka, H.B. Seed and R. Hwang - 1974 (PB 236 796)A05

- EERC 74-5 "Sensitivity Analysis for Hysteretic Dynamic Systems: Applications to Earthquake Engineering," by D. Ray 1974 (PB 233 213)A06
- EERC 74-6 "Soil Structure Interaction Analyses for Evaluating Seismic Response," by H.B. Seed, J. Lysmer and R. Hwang 1974 (PB 236 519)A04
- EERC 74-7 Unassigned
- EERC 74-8 "Shaking Table Tests of a Steel Frame - A Progress Report," by R.W. Clough and D. Tang - 1974 (PB 240 869)A03
- EERC 74-9 "Hysteretic Behavior of Reinforced Concrete Flexural Members with Special Web Reinforcement;" by V.V. Bertero, E.P. Popov and T.Y. Wang - 1974 (PB 236 797)A07
- EERC 74-10 "Applications of Reliability-Based, Global Cost Optimization to Design of Earthquake Resistant Structures," by E. Vitiello and K.S. Pister - 1974 (PB 237 231)A06
- EERC 74-11 "Liquefaction of Gravelly Soils Under Cyclic Loading Conditions," by R.T. Wong, H.B. Seed and C.K. Chan 1974 (PB 242 042)A03
- EERC 74-12 "Site-Dependent Spectra for Earthquake-Resistant Design," by H.B. Seed, C. Ugas and J. Lysmer - 1974 (PB 240 953)A03
- EERC 74-13 "Earthquake Simulator Study of a Reinforced Concrete Frame," by P. Hidalgo and R.W. Clough - 1974 (PB 241 944)A13
- EERC 74-14 "Nonlinear Earthquake Response of Concrete Gravity Dams," by N. Pal - 1974 (AD/A 006 583)A06
- EERC 74-15 "Modeling and Identification in Nonlinear Structural Dynamics - I. One Degree of Freedom Models," by N. Distefano and A. Rath - 1974 (PB 241 548)A06
- EERC 75-1 "Determination of Seismic Design Criteria for the Dumbarton Bridge Replacement Structure, Vol. I: Description, Theory and Analytical Modeling of Bridge and Parameters," by F. Baron and S.-H. Pang - 1975 (PB 259 407)A15
- EERC 75-2 "Determination of Seismic Design Criteria for the Dumbarton Bridge Replacement Structure, Vol. II: Numerical Studies and Establishment of Seismic Design Criteria," by F. Baron and S.-H. Pang - 1975 (PB 259 408)A11 (For set of EERC 75-1 and 75-2 (PB 259 406))
- EERC 75-3 "Seismic Risk Analysis for a Site and a Metropolitan Area," by C.S. Oliveira - 1975 (PB 248 134)A09
- EERC 75-4 "Analytical Investigations of Seismic Response of Short, Single or Multiple-Span Highway Bridges," by M.-C. Chen and J. Penzien - 1975 (PB 241 454)A09
- EERC 75-5 "An Evaluation of Some Methods for Predicting Seismic Behavior of Reinforced Concrete Buildings," by S.A. Mahin and V.V. Bertero - 1975 (PB 246 306)A16
- EERC 75-6 "Earthquake Simulator Study of a Steel Frame Structure, Vol. I: Experimental Results," by R.W. Clough and D.T. Tang - 1975 (PB 243 981)A13
- EERC 75-7 "Dynamic Properties of San Bernardino Intake Tower," by D. Rea, C.-Y. Liaw and A.K. Chopra - 1975 (AD/A008 406) A05
- EERC 75-8 "Seismic Studies of the Articulation for the Dumbarton Bridge Replacement Structure, Vol. I: Description, Theory and Analytical Modeling of Bridge Components," by F. Baron and R.E. Hamati - 1975 (PB 251 539)A07
- EERC 75-9 "Seismic Studies of the Articulation for the Dumbarton Bridge Replacement Structure, Vol. 2: Numerical Studies of Steel and Concrete Girder Alternates," by F. Baron and R.E. Hamati - 1975 (PB 251 540)A10
- EERC 75-10 "Static and Dynamic Analysis of Nonlinear Structures," by D.P. Mondkar and G.H. Powell - 1975 (PB 242 434)A08
- EERC 75-11 "Hysteretic Behavior of Steel Columns," by E.P. Popov, V.V. Bertero and S. Chandramouli - 1975 (PB 252 365)A11
- EERC 75-12 "Earthquake Engineering Research Center Library Printed Catalog," - 1975 (PB 243 711)A26
- EERC 75-13 "Three Dimensional Analysis of Building Systems (Extended Version)," by E.L. Wilson, J.P. Hollings and H.H. Dovey - 1975 (PB 243 989)A07
- EERC 75-14 "Determination of Soil Liquefaction Characteristics by Large-Scale Laboratory Tests," by P. De Alba, C.K. Chan and H.B. Seed - 1975 (NUREG 0027)A08
- EERC 75-15 "A Literature Survey - Compressive, Tensile, Bond and Shear Strength of Masonry," by R.L. Mayes and R.W. Clough - 1975 (PB 246 292)A10
- EERC 75-16 "Hysteretic Behavior of Ductile Moment Resisting Reinforced Concrete Frame Components," by V.V. Bertero and E.P. Popov - 1975 (PB 246 388)A05
- EERC 75-17 "Relationships Between Maximum Acceleration, Maximum Velocity, Distance from Source, Local Site Conditions for Moderately Strong Earthquakes," by H.B. Seed, R. Murarka, J. Lysmer and I.M. Idriss - 1975 (PB 248 172)A03
- EERC 75-18 "The Effects of Method of Sample Preparation on the Cyclic Stress-Strain Behavior of Sands," by J. Mulilis, C.K. Chan and H.B. Seed - 1975 (Summarized in EERC 75-28)

- EERC 75-19 "The Seismic Behavior of Critical Regions of Reinforced Concrete Components as Influenced by Moment, Shear and Axial Force," by M.B. Atalay and J. Penzien - 1975 (PB 258 842)A11
- EERC 75-20 "Dynamic Properties of an Eleven Story Masonry Building," by R.M. Stephen, J.P. Hollings, J.G. Bouwkamp and D. Jurukovski - 1975 (PB 246 945)A04
- EERC 75-21 "State-of-the-Art in Seismic Strength of Masonry - An Evaluation and Review," by R.L. Mayes and R.W. Clough 1975 (PB 249 040)A07
- EERC 75-22 "Frequency Dependent Stiffness Matrices for Viscoelastic Half-Plane Foundations," by A.K. Chopra, P. Chakrabarti and G. Dasgupta - 1975 (PB 248 121)A07
- EERC 75-23 "Hysteretic Behavior of Reinforced Concrete Framed Walls," by T.Y. Wong, V.V. Bertero and E.P. Popov - 1975
- EERC 75-24 "Testing Facility for Subassemblages of Frame-Wall Structural Systems," by V.V. Bertero, E.P. Popov and T. Endo - 1975
- EERC 75-25 "Influence of Seismic History on the Liquefaction Characteristics of Sands," by H.B. Seed, K. Mori and C.K. Chan - 1975 (Summarized in EERC 75-28)
- EERC 75-26 "The Generation and Dissipation of Pore Water Pressures during Soil Liquefaction," by H.B. Seed, P.P. Martin and J. Lysmer - 1975 (PB 252 648)A03
- EERC 75-27 "Identification of Research Needs for Improving Aseismic Design of Building Structures," by V.V. Bertero 1975 (PB 248 136)A05
- EERC 75-28 "Evaluation of Soil Liquefaction Potential during Earthquakes," by H.B. Seed, I. Arango and C.K. Chan - 1975 (NUREG 0026)A13
- EERC 75-29 "Representation of Irregular Stress Time Histories by Equivalent Uniform Stress Series in Liquefaction Analyses," by H.B. Seed, I.M. Idriss, F. Makdisi and N. Banerjee - 1975 (PB 252 635)A03
- EERC 75-30 "FLUSH - A Computer Program for Approximate 3-D Analysis of Soil-Structure Interaction Problems," by J. Lysmer, T. Udaka, C.-F. Tsai and H.B. Seed - 1975 (PB 259 332)A07
- EERC 75-31 "ALUSH - A Computer Program for Seismic Response Analysis of Axisymmetric Soil-Structure Systems," by E. Berger, J. Lysmer and H.B. Seed - 1975
- EERC 75-32 "TRIP and TRAVEL - Computer Programs for Soil-Structure Interaction Analysis with Horizontally Travelling Waves," by T. Udaka, J. Lysmer and H.B. Seed - 1975
- EERC 75-33 "Predicting the Performance of Structures in Regions of High Seismicity," by J. Penzien - 1975 (PB 248 130)A03
- EERC 75-34 "Efficient Finite Element Analysis of Seismic Structure - Soil - Direction," by J. Lysmer, H.B. Seed, T. Udaka, R.N. Hwang and C.-F. Tsai - 1975 (PB 253 570)A03
- EERC 75-35 "The Dynamic Behavior of a First Story Girder of a Three-Story Steel Frame Subjected to Earthquake Loading," by R.W. Clough and L.-Y. Li - 1975 (PB 248 841)A05
- EERC 75-36 "Earthquake Simulator Study of a Steel Frame Structure, Volume II - Analytical Results," by D.T. Tang - 1975 (PB 252 926)A10
- EERC 75-37 "ANSR-I General Purpose Computer Program for Analysis of Non-Linear Structural Response," by D.P. Mondkar and G.H. Powell - 1975 (PB 252 386)A08
- EERC 75-38 "Nonlinear Response Spectra for Probabilistic Seismic Design and Damage Assessment of Reinforced Concrete Structures," by M. Murakami and J. Penzien - 1975 (PB 259 530)A05
- EERC 75-39 "Study of a Method of Feasible Directions for Optimal Elastic Design of Frame Structures Subjected to Earthquake Loading," by N.D. Walker and K.S. Pister - 1975 (PB 257 781)A06
- EERC 75-40 "An Alternative Representation of the Elastic-Viscoelastic Analogy," by G. Dasgupta and J.L. Sackman - 1975 (PB 252 173)A03
- EERC 75-41 "Effect of Multi-Directional Shaking on Liquefaction of Sands," by H.B. Seed, R. Pyke and G.R. Martin - 1975 (PB 258 781)A03
- EERC 76-1 "Strength and Ductility Evaluation of Existing Low-Rise Reinforced Concrete Buildings - Screening Method," by T. Okada and B. Bresler - 1976 (PB 257 906)A11
- EERC 76-2 "Experimental and Analytical Studies on the Hysteretic Behavior of Reinforced Concrete Rectangular and T-Beams," by S.-Y.M. Ma, E.P. Popov and V.V. Bertero - 1976 (PB 260 843)A12
- EERC 76-3 "Dynamic Behavior of a Multistory Triangular-Shaped Building," by J. Petrovski, R.M. Stephen, E. Gartenbaum and J.G. Bouwkamp - 1976 (PB 273 279)A07
- EERC 76-4 "Earthquake Induced Deformations of Earth Dams," by N. Serff, H.B. Seed, F.I. Makdisi & C.-Y. Chang - 1976 (PB 292 065)A08

- EERC 76-5 "Analysis and Design of Tube-Type Tall Building Structures," by H. de Clercq and G.H. Powell - 1976 (PB 252 220) A10
- EERC 76-6 "Time and Frequency Domain Analysis of Three-Dimensional Ground Motions, San Fernando Earthquake," by T. Kubo and J. Penzien (PB 260 556)A11
- EERC 76-7 "Expected Performance of Uniform Building Code Design Masonry Structures," by R.L. Mayes, Y. Omote, S.W. Chen and R.W. Clough - 1976 (PB 270 098)A05
- EERC 76-8 "Cyclic Shear Tests of Masonry Piers, Volume 1 - Test Results," by R.L. Mayes, Y. Omote, R.W. Clough - 1976 (PB 264 424)A06
- EERC 76-9 "A Substructure Method for Earthquake Analysis of Structure - Soil Interaction," by J.A. Gutierrez and A.K. Chopra - 1976 (PB 257 783)A08
- EERC 76-10 "Stabilization of Potentially Liquefiable Sand Deposits using Gravel Drain Systems," by H.B. Seed and J.R. Booker - 1976 (PB 258 820)A04
- EERC 76-11 "Influence of Design and Analysis Assumptions on Computed Inelastic Response of Moderately Tall Frames," by G.H. Powell and D.G. Row - 1976 (PB 271 409)A06
- EERC 76-12 "Sensitivity Analysis for Hysteretic Dynamic Systems: Theory and Applications," by D. Ray, K.S. Pister and E. Polak - 1976 (PB 262 859)A04
- EERC 76-13 "Coupled Lateral Torsional Response of Buildings to Ground Shaking," by C.L. Kan and A.K. Chopra - 1976 (PB 257 907)A09
- EERC 76-14 "Seismic Analyses of the Banco de America," by V.V. Bertero, S.A. Mahin and J.A. Hollings - 1976
- EERC 76-15 "Reinforced Concrete Frame 2: Seismic Testing and Analytical Correlation," by R.W. Clough and J. Gidwani - 1976 (PB 261 323)A08
- EERC 76-16 "Cyclic Shear Tests of Masonry Piers, Volume 2 - Analysis of Test Results," by R.L. Mayes, Y. Omote and R.W. Clough - 1976
- EERC 76-17 "Structural Steel Bracing Systems: Behavior Under Cyclic Loading," by E.P. Popov, K. Takanashi and C.W. Roeder - 1976 (PB 260 715)A05
- EERC 76-18 "Experimental Model Studies on Seismic Response of High Curved Overcrossings," by D. Williams and W.G. Godden - 1976 (PB 269 548)A08
- EERC 76-19 "Effects of Non-Uniform Seismic Disturbances on the Dumbarton Bridge Replacement Structure," by F. Baron and R.E. Hamati - 1976 (PB 282 981)A16
- EERC 76-20 "Investigation of the Inelastic Characteristics of a Single Story Steel Structure Using System Identification and Shaking Table Experiments," by V.C. Matzen and H.D. McNiven - 1976 (PB 258 453)A07
- EERC 76-21 "Capacity of Columns with Splice Imperfections," by E.P. Popov, R.M. Stephen and R. Philbrick - 1976 (PB 260 378)A04
- EERC 76-22 "Response of the Olive View Hospital Main Building during the San Fernando Earthquake," by S. A. Mahin, V.V. Bertero, A.K. Chopra and R. Collins - 1976 (PB 271 425)A14
- EERC 76-23 "A Study on the Major Factors Influencing the Strength of Masonry Prisms," by N.M. Mostaghel, R.L. Mayes, R. W. Clough and S.W. Chen - 1976 (Not published)
- EERC 76-24 "GADFLEA - A Computer Program for the Analysis of Pore Pressure Generation and Dissipation during Cyclic or Earthquake Loading," by J.R. Booker, M.S. Rahman and H.B. Seed - 1976 (PB 263 947)A04
- EERC 76-25 "Seismic Safety Evaluation of a R/C School Building," by B. Bresler and J. Axley - 1976
- EERC 76-26 "Correlative Investigations on Theoretical and Experimental Dynamic Behavior of a Model Bridge Structure," by K. Kawashima and J. Penzien - 1976 (PB 263 388)A11
- EERC 76-27 "Earthquake Response of Coupled Shear Wall Buildings," by T. Srichatrapimuk - 1976 (PB 265 157)A07
- EERC 76-28 "Tensile Capacity of Partial Penetration Welds," by E.P. Popov and R.M. Stephen - 1976 (PB 262 899)A03
- EERC 76-29 "Analysis and Design of Numerical Integration Methods in Structural Dynamics," by H.M. Hilber - 1976 (PB 264 410)A06
- EERC 76-30 "Contribution of a Floor System to the Dynamic Characteristics of Reinforced Concrete Buildings," by L.E. Malik and V.V. Bertero - 1976 (PB 272 247)A13
- EERC 76-31 "The Effects of Seismic Disturbances on the Golden Gate Bridge," by F. Baron, M. Arikan and R.E. Hamati - 1976 (PB 272 279)A09
- EERC 76-32 "Infilled Frames in Earthquake Resistant Construction," by R.E. Klingner and V.V. Bertero - 1976 (PB 265 892)A13

- UCB/EERC-77/01 "PLUS - A Computer Program for Probabilistic Finite Element Analysis of Seismic Soil-Structure Interaction," by M.P. Romo Organista, J. Lysmer and H.B. Seed - 1977
- UCB/EERC-77/02 "Soil-Structure Interaction Effects at the Humboldt Bay Power Plant in the Ferndale Earthquake of June 7, 1975," by J.E. Valera, H.B. Seed, C.F. Tsai and J. Lysmer - 1977 (PB 265 795)A04
- UCB/EERC-77/03 "Influence of Sample Disturbance on Sand Response to Cyclic Loading," by K. Mori, H.B. Seed and C.K. Chan - 1977 (PB 267 352)A04
- UCB/EERC-77/04 "Seismological Studies of Strong Motion Records," by J. Shoja-Taheri - 1977 (PB 269 655)A10
- UCB/EERC-77/05 "Testing Facility for Coupled-Shear Walls," by L. Li-Hyung, V.V. Bertero and E.P. Popov - 1977
- UCB/EERC-77/06 "Developing Methodologies for Evaluating the Earthquake Safety of Existing Buildings," by No. 1 - B. Bresler; No. 2 - B. Bresler, T. Okada and D. Zisling; No. 3 - T. Okada and B. Bresler; No. 4 - V.V. Bertero and B. Bresler - 1977 (PB 267 354)A08
- UCB/EERC-77/07 "A Literature Survey - Transverse Strength of Masonry Walls," by Y. Omote, R.L. Mayes, S.W. Chen and R.W. Clough - 1977 (PB 277 933)A07
- UCB/EERC-77/08 "DRAIN-TABS: A Computer Program for Inelastic Earthquake Response of Three Dimensional Buildings," by R. Guendelman-Israel and G.H. Powell - 1977 (PB 270 693)A07
- UCB/EERC-77/09 "SUBWALL: A Special Purpose Finite Element Computer Program for Practical Elastic Analysis and Design of Structural Walls with Substructure Option," by D.Q. Le, H. Peterson and E.P. Popov - 1977 (PB 270 567)A05
- UCB/EERC-77/10 "Experimental Evaluation of Seismic Design Methods for Broad Cylindrical Tanks," by D.P. Clough (PB 272 280)A13
- UCB/EERC-77/11 "Earthquake Engineering Research at Berkeley - 1976," - 1977 (PB 273 507)A09
- UCB/EERC-77/12 "Automated Design of Earthquake Resistant Multistory Steel Building Frames," by N.D. Walker, Jr. - 1977 (PB 276 526)A09
- UCB/EERC-77/13 "Concrete Confined by Rectangular Hoops Subjected to Axial Loads," by J. Vallenias, V.V. Bertero and E.P. Popov - 1977 (PB 275 165)A06
- UCB/EERC-77/14 "Seismic Strain Induced in the Ground During Earthquakes," by Y. Sugimura - 1977 (PB 284 201)A04
- UCB/EERC-77/15 "Bond Deterioration under Generalized Loading," by V.V. Bertero, E.P. Popov and S. Viathanatepa - 1977
- UCB/EERC-77/16 "Computer Aided Optimum Design of Ductile Reinforced Concrete Moment Resisting Frames," by S.W. Zagajski and V.V. Bertero - 1977 (PB 280 137)A07
- UCB/EERC-77/17 "Earthquake Simulation Testing of a Stepping Frame with Energy-Absorbing Devices," by J.M. Kelly and D.F. Tsztoo - 1977 (PB 273 506)A04
- UCB/EERC-77/18 "Inelastic Behavior of Eccentrically Braced Steel Frames under Cyclic Loadings," by C.W. Roeder and E.P. Popov - 1977 (PB 275 526)A15
- UCB/EERC-77/19 "A Simplified Procedure for Estimating Earthquake-Induced Deformations in Dams and Embankments," by F.I. Makdisi and H.B. Seed - 1977 (PB 276 820)A04
- UCB/EERC-77/20 "The Performance of Earth Dams during Earthquakes," by H.B. Seed, F.I. Makdisi and P. de Alba - 1977 (PB 276 821)A04
- UCB/EERC-77/21 "Dynamic Plastic Analysis Using Stress Resultant Finite Element Formulation," by P. Lukkunapvasit and J.M. Kelly - 1977 (PB 275 453)A04
- UCB/EERC-77/22 "Preliminary Experimental Study of Seismic Uplift of a Steel Frame," by R.W. Clough and A.A. Huckelbridge 1977 (PB 278 769)A08
- UCB/EERC-77/23 "Earthquake Simulator Tests of a Nine-Story Steel Frame with Columns Allowed to Uplift," by A.A. Huckelbridge - 1977 (PB 277 944)A09
- UCB/EERC-77/24 "Nonlinear Soil-Structure Interaction of Skew Highway Bridges," by M.-C. Chen and J. Penzien - 1977 (PB 276 176)A07
- UCB/EERC-77/25 "Seismic Analysis of an Offshore Structure Supported on File Foundations," by D.D.-N. Liou and J. Penzien 1977 (PB 283 180)A06
- UCB/EERC-77/26 "Dynamic Stiffness Matrices for Homogeneous Viscoelastic Half-Planes," by G. Dasgupta and A.K. Chopra - 1977 (PB 279 654)A06
- UCB/EERC-77/27 "A Practical Soft Story Earthquake Isolation System," by J.M. Kelly, J.M. Eidinger and C.J. Derham - 1977 (PB 276 814)A07
- UCB/EERC-77/28 "Seismic Safety of Existing Buildings and Incentives for Hazard Mitigation in San Francisco: An Exploratory Study," by A.J. Meltsner - 1977 (PB 281 970)A05
- UCB/EERC-77/29 "Dynamic Analysis of Electrohydraulic Shaking Tables," by D. Rea, S. Abedi-Hayati and Y. Takahashi 1977 (PB 282 569)A04
- UCB/EERC-77/30 "An Approach for Improving Seismic - Resistant Behavior of Reinforced Concrete Interior Joints," by B. Galunic, V.V. Bertero and E.P. Popov - 1977 (PB 290 870)A06

- UCB/EERC-78/01 "The Development of Energy-Absorbing Devices for Aseismic Base Isolation Systems," by J.M. Kelly and D.F. Tsztoo - 1978 (PB 284 978)A04
- UCB/EERC-78/02 "Effect of Tensile Prestrain on the Cyclic Response of Structural Steel Connections, by J.G. Bouwkamp and A. Mukhopadhyay - 1978
- UCB/EERC-78/03 "Experimental Results of an Earthquake Isolation System using Natural Rubber Bearings," by J.M. Eidinger and J.M. Kelly - 1978 (PB 281 686)A04
- UCB/EERC-78/04 "Seismic Behavior of Tall Liquid Storage Tanks," by A. Niwa - 1978 (PB 284 017)A14
- UCB/EERC-78/05 "Hysteretic Behavior of Reinforced Concrete Columns Subjected to High Axial and Cyclic Shear Forces," by S.W. Zagajeski, V.V. Bertero and J.G. Bouwkamp - 1978 (PB 283 858)A13
- UCB/EERC-78/06 "Inelastic Beam-Column Elements for the ANSR-I Program," by A. Riahi, D.G. Row and G.H. Powell - 1978
- UCB/EERC-78/07 "Studies of Structural Response to Earthquake Ground Motion," by O.A. Lopez and A.K. Chopra - 1978 (PB 282 790)A05
- UCB/EERC-78/08 "A Laboratory Study of the Fluid-Structure Interaction of Submerged Tanks and Caissons in Earthquakes," by R.C. Byrd - 1978 (PB 284 957)A08
- UCB/EERC-78/09 "Model for Evaluating Damageability of Structures," by I. Sakamoto and B. Bresler - 1978
- UCB/EERC-78/10 "Seismic Performance of Nonstructural and Secondary Structural Elements," by I. Sakamoto - 1978
- UCB/EERC-78/11 "Mathematical Modelling of Hysteresis Loops for Reinforced Concrete Columns," by S. Nakata, T. Sproul and J. Penzien - 1978
- UCB/EERC-78/12 "Damageability in Existing Buildings," by T. Blejwas and B. Bresler - 1978
- UCB/EERC-78/13 "Dynamic Behavior of a Pedestal Base Multistory Building," by R.M. Stephen, E.L. Wilson, J.G. Bouwkamp and M. Butten - 1978 (PB 286 650)A08
- UCB/EERC-78/14 "Seismic Response of Bridges - Case Studies," by R.A. Imbsen, V. Nutt and J. Penzien - 1978 (PB 286 503)A10
- UCB/EERC-78/15 "A Substructure Technique for Nonlinear Static and Dynamic Analysis," by D.G. Row and G.H. Powell - 1978 (PB 288 077)A10
- UCB/EERC-78/16 "Seismic Risk Studies for San Francisco and for the Greater San Francisco Bay Area," by C.S. Oliveira - 1978
- UCB/EERC-78/17 "Strength of Timber Roof Connections Subjected to Cyclic Loads," by P. Gülkan, R.L. Mayes and R.W. Clough - 1978
- UCB/EERC-78/18 "Response of K-Braced Steel Frame Models to Lateral Loads," by J.G. Bouwkamp, R.M. Stephen and E.P. Popov - 1978
- UCB/EERC-78/19 "Rational Design Methods for Light Equipment in Structures Subjected to Ground Motion," by J.L. Sackman and J.M. Kelly - 1978 (PB 292 357)A04
- UCB/EERC-78/20 "Testing of a Wind Restraint for Aseismic Base Isolation," by J.M. Kelly and D.E. Chitty - 1978 (PB 292 833)A03
- UCB/EERC-78/21 "APOLLO - A Computer Program for the Analysis of Pore Pressure Generation and Dissipation in Horizontal Sand Layers During Cyclic or Earthquake Loading," by P.P. Martin and H.B. Seed - 1978 (PB 292 835)A04
- UCB/EERC-78/22 "Optimal Design of an Earthquake Isolation System," by M.A. Bhatti, K.S. Pister and E. Polak - 1978 (PB 294 735)A06
- UCB/EERC-78/23 "MASH - A Computer Program for the Non-Linear Analysis of Vertically Propagating Shear Waves in Horizontally Layered Deposits," by P.P. Martin and H.B. Seed - 1978 (PB 293 101)A05
- UCB/EERC-78/24 "Investigation of the Elastic Characteristics of a Three Story Steel Frame Using System Identification," by I. Kaya and H.D. McNiven - 1978